THE UNIVERSITY OF MICHIGAN

COLLEGE OF ENGINEERING
DEPARTMENT OF ELECTRICAL ENGINEERING
Radiation Laboratory

SIMPLIFIED MODELING TECHNIQUES FOR

AVIONIC ANTENNA PATTERN SIGNATURES

W. DeHart, J. Ferris and R. Wolford

TABLE OF CONTENTS

ABSTRACT

Under a previous contract, AF33(615)-1964, an investigation was made of measurement techniques to determine antenna radiation characteristics at the fundamental, spurious, and harmonic frequencies. It has been shown that the simplified modeling technique is an effective, low-cost method for obtaining the desired antenna spectrum signature. The investigation of simplified modeling is concluded with the presentation of data for 2 antenna types (a slot and a $\lambda/4$ monopole) mounted on a simplified and a precision aircraft model. The inclusion of the simplified modeling technique in MIL-STD 449 is recommended.

To facilitate prediction of inter-system interference by the Electromagnetic Compatibility Analysis Center, it is desirable to present antenna spectrum signature data to ECAC in digital form. For this reason, an investigation of techniques for digitalizing antenna data was conducted. The digital procedures developed in this study are discussed and the equipment used is shown. Recommendations as to the format of this data for ECAC use is also presented.

The AN/ARC-27 transmitter has been subjected to a closed circuit spurious emission test with the results presented. To further aid in understanding the types of loads into which the transmitter may be operated the characteristic impedance of two antenna types have been measured and are presented.

I. INTRODUCTION

The statement of problem as set forth in the contract which provides for the present investigation is as follows.

The problem is to determine practical methods for obtaining the desired antenna pattern spectrum signatures with minimum cost and complications by the use of simplified aircraft models or mockups and statistical methods for data presentation. The prediction of intersystem electromagnetic compatibility will necessitate a determination of the three dimensional spectral characteristics of all emitters and receptors on the flight vehicle.

To determine realistic pattern spectrum signature, careful consideration must be made of the spectral output of the emitter source, i.e. the typical AF transmitter being used with the antenna as well as the impedance properties of the actual antenna system employed on the vehicle.

The stated objective of the contract is: To make use of 'statistical' or 'digitalized' patterns to experimentally establish the fact that satisfactory antenna signature information can be obtained by the use of crude aircraft models or mockups by comparing with the results of data obtained using precision models. Early attention will be given to the selection of a statistical or digital method of pattern data presentation that would eliminate, if possible, the requirement for numerous antenna patterns. The program will be concerned with investigation, analysis, and experimentation to determine feasible approaches for standardized measurement techniques to become a part of MIL-STD-449B.

The Radio Science Laboratory of the University of Michigan has designed and fabricated a digital converter unit that enables one to record antenna patterns simultaneously in both analog and digital form. The analog-to-digital converter can now be used to record antenna data in digital form.

The present contract is being conducted from the systems aspect rather than the component aspect. In one task, for example, consideration is being given to the determination of the spectrum signature of a typical airborne transmitter (ARC-27). A second task is the determination of the antenna impedance characteristics at the fundamental, spurious and harmonic frequencies; as well as the resulting effect on the transmitter operating characteristics. The principal measurement technique that will be considered during this contract is the determination of the transmitter impedance characteristics at the fundamental, spurious, and harmonic frequencies. This information will be of value in helping to predict the expected level of interfering signals.

II. SIMPLIFIED MODELING

During the initial period of the present contract, the investigation of sim-
plified modeling was continued using a unilobe antenna structure (slot antenna).
Interim Report 7274-1-T presented a small amount of data for the slot antenna at
the scale fundamental frequency, 8 GHz, and approximately the fourth harmonic
frequency, 33 GHz. In this report, the study of simplified modeling is concluded
with the presentation of a complete set of data for the slot antenna recorded at the
fundamental frequency and the second, third, fourth, and fifth harmonic frequen-
cies. Also included is a three-dimensional set of antenna patterns for the $\lambda/4$
monopole at its scale fundamental frequency. Some $\lambda/4$ monopole data has been
previously presented for a principle plane cut at 5 frequencies.

2.1 Slot Antenna

Principle plane radiation patterns of the slot antenna (open-ended section of
X-band waveguide) have been recorded at 8, 16, 24, 32 and 40 GHz. These patterns
were obtained with the slot located in the underside of the fuselage midway between
the wings as shown in Fig. 1 for the precision T-33 model and in Fig. 2 for the
simplified T-33 model. Tapered transitions were used in the waveguide system
between frequency bands to minimize the generation of higher order modes. Good
pattern agreement is exhibited between the precision and simplified models at all
frequencies as is shown in Figs. 3 through 12 for the transverse elevation cut[+]
(ϕ = 90° and 270°; θ variable) and in Figs. 13 through 22 for the longitudinal eleva-
tion cut (ϕ = 0° and 180°; θ variable). The above pattern data, when reduced to
statistical data in the form of cumulative gain distributions, again exhibits favor-
able agreement over the full range of interest as may be seen in Fig. 23 through
27 for the transverse cut and Figs. 28 through 32 for the longitudinal cut. The
measurements were performed with a system dynamic range of 60 db rather than
the usual 40 db range.

[+]In all plots of antenna data shown on SA 128-60 charts in this report, the lower
angle scale ($\pm$ 180°) is to be used.

·2.2 $\lambda/4$ Monopole Antenna

A three-dimensional set of patterns has been recorded for the $\lambda/4$ monopole antenna at the scale fundamental frequency of 2.4 GHz. The antenna was mounted on the underside of the nose of the precision and simplified T-33 models as shown in Figs. 33 and 34. These patterns, which were also recorded with the 60 db system, were obtained to compare the two models at cuts other than the principle plane cuts which have been presented in a previous report. The three-dimensional patterns were obtained by varying ϕ in 10° increments from 0° to 90°, and at each of these increments a θ cut was recorded of the antenna characteristics. These patterns are shown in Figs. 35 through 54 with the odd numbers for the precision model and even numbered figures for the simplified model. The cumulative gain distributions for the above data are shown in Figs. 55 - 64.

The U of M analog-to-digital converter was employed in all of the above antenna measurements to simultaneously record the data in digital form on magnetic tape as the analog pattern was being plotted on chart paper. This digitized data was later automatically processed, reduced, and plotted in the form of cumulative gain distributions by the procedures to be discussed later in this report.

The cumulative gain distributions presented in this report illustrate the agreement that can be achieved between a simplified and a precision model. It is felt that the degree of accuracy obtainable is adequate to demonstrate the feasibility of the simplified modeling technique for obtaining spectrum signature data. Therefore, no further study of simplified modeling is planned for this contract.

2.3 Degree of Simplification

There are, however, several variations of simplification that one might consider for investigation. For example, it may be feasible to use a simplified model that is formed from one flat plate. The outline of the flat plate would be the shadow of the aircraft as seen from a plan view. This form of simplified modeling might well suffice for the measurement of an antenna which was located on the fuselage belly between the wings of the aircraft such as the slot antenna studied

above. However, this may not be adequate for those antennas that may be mounted on the side of the aircraft.

It is to be recalled that, for the simplified model used in the present study, the wings and tail structure were formed from aluminum plates. However, the fuselage was represented by a metallic cylinder whose diameter was approximately equal to the mean diameter of the aerodynamically shaped fuselage of the precision model. The length of the cylindrical section was approximately equal to the overall length of the precision model's fuselage. The data presented for the $\lambda/4$ monopole antenna is felt to demonstrate the necessity of a cylindrical fuselage, since this antenna was located in an area of the aircraft which is aerodynamically contoured. The cumulative gains distributions for the $\lambda/4$ monopole antenna (Figs 55 - 64) indicate the excellent results achieved with the cylindrical fuselage for all the θ cuts recorded for the antenna.

2.4 Need for MIL-STD 449 Requirements

As a result of the simplified modeling study, it is now felt that recommendations should be made to incorporate the simplified modeling technique into MIL-STD-449. The technique must consider how the model is to be fabricated, what materials are to be used in the fabrication, and how the model is to be used to obtain the spectrum signature patterns that are required. Items that must be considered in the fabrication of the model are: 1) the dimensions of the fuselage, 2) the shape of the fuselage (i.e. whether cones, cylinders or flat plates are to be employed), 3) the need to model the wings and tail structure (if they are modeled - the degree of simplfication), and 4) the need to model items out-lying on the wings, such as engines, fuel tanks, etc. It is felt the simplified modeling technique must consider the description and fabrication of all these items.

III DATA RECORDING AND REDUCTION TECHNIQUES

A second aspect of the present contract has been an investigation of data handling techniques and procedures for presenting the data obtained by the Air Force or other service to ECAC. To ensure that recommendations resulting from the techniques and procedures developed by The University of Michigan are compatible with both ECAC and the Air Force, close liaison has been maintained with these organizations.

3.1 ECAC Data Format

During recent discussions with ECAC personnel, it was learned that they prefer antenna pattern data to be in the form of "number pairs". A number pair consists of the antenna gain value and the associated angle (azimuth or elevation) for a given data point. It is felt by ECAC that it is less complicated to write the various programs required for interference prediction for the data assembled in the number pair format. This format relieves a program of the burden of having to search the input data to match a given gain value with its correct angle if data is accidentally placed in the computer in the wrong sequence. Also, if this one data format is adhered to by Air Force or other service, format variations are eliminated and the computer program may perform calculations for statistical analysis of the data much more readily.

ECAC considers cards to be a more desirable form of data storage than magnetic taps, since they are less susceptible to deterioration and damage and, even if partially damaged, may be repunched without difficulty. It is recommended by ECAC that antenna gain values be represented by 4 digits, thus enabling amplitudes to be recorded to .5 db, which is typical of microwave measurement accuracy and is compatible with the resolution of the Michigan data recording system. It is suggested that the angle associated with the antenna gain value also be represented by 4 digits, allowing an increment of 0.1° to be recorded. This is desirable when measuring a nigh-gain narrow-beam antenna, whereas when measuring a low-gain wide-beam antenna, an angle increment of 1.0° will suffice.

Considering the above data format, it follows that the card format will consist of 8 columns per number pair. Thus 9 data points are placed on each card, consuming 72 columns. The remaining 8 columns may be used for identification purposes. A total of 40 cards are thus required for each antenna pattern, which appears feasible to both ECAC and Michigan. Also it will be necessary for each set of data forwarded to ECAC to be accompanied with a data sheet describing the card content, i.e. antenna model and type, etc. This data sheet may be a punched card.

3.2 Automatic Digital Recording Procedure

An automatic digital recording technique has been developed by the University of Michigan. Figure 65 is a block diagram of the Michigan system. A high-gain receiver is employed to measure the antenna radiation characteristic and an antenna pattern recorder plots this characteristic in analog form on standard chart paper. Simultaneously, the analog waveform is sampled at one-degree intervals (for 360° coverage) by an analog-to-digital converter and the magnitude of the sample values are recorded on a general purpose tape recorder in the form of binary coded numbers. Figure 66 shows the wide-range, high-gain receiving system which incorporates the analog chart recorder and the analog-to-digital converter. Figure 67 is a closeup view of the U of M analog-to-digital converter. The basic operation of the analog-to-digital converter has been discussed in the previous interim report 7274-1-T. Figure 68 shows the general purpose tape recorder which places the digital data on 1/4" magnetic tape.

Upon completion of the antenna measurements the general purpose tape recorder is carried to a University facility on the North Campus. There the 1/4" magnetic tape is played back into a converter unit, which transfers the data onto 1" magnetic tape in a format which is compatible with the University of Michigan IBM 7090 computer. The equipment used to affect this data transfer is shown in Fig. 69. A Raytheon analog-to-digital converter is seen in the center of the photo with logic racks at the left and an IBM tape recorder rack at the right.

The antenna data now on tape is subsequently transferred to the punched card form by employing IBM processing equipment located at a University facility at Willow Run. A computer program, which is required to direct the processing, is read into an IBM 1401 processing unit along with the antenna data on magnetic tape. The digital data is processed and automatically punched onto IBM cards for storage or shipment to ECAC. The IBM 1401 processing unit is seen at the left in Fig. 70 with IBM tape recorder racks at the center. The 1401 processing unit is again shown in Fig. 71 with its associated IBM 1402 card punching unit.

Although the above procedure may appear lengthy and cumbersome, it was developed to demonstrate the feasibility of recording antenna patterns.in both analog and digital form simultaneously with subsequent transferal of the digital data to punched cards for storage. In spite of the complexity of the procedure, it was found to provide a high degree of accuracy. This accuracy is illustrated by Figs. 72 and 73 which are typical analog antenna patterns selected at random from the pattern sets. Plotted on these analog patterns are the digital data as read from the punched IBM cards after completion of the digitalizing procedure (only 60 of the total 360 values sampled by the digital converter are shown on each pattern to avoid the clutter of too many points.) .

Consideration is presently being given to procedures which will reduce the amount of equipment and time required to place the digital data in card form. For example, if the antenna data could be recorded initially on 1" magnetic tape in the appropriate data format (by combining digitalizing, programming, and recording circuity into one package) it would be necessary only to play back the tape through a processing and punching unit to obtain the punched cards that would be forwarded to and ultimately analyzed by ECAC. Nevertheless, the above system developed by the University of Michigan is a completely automated system, i. e. one in which no human judgement errors can enter into the digitalizing of the data. Only the common problems encountered by electronic equipment would need to be handled.

3.3 Semi-Automatic Digital Recording Procedure

An alternate procedure has been investigated by Michigan for placing digital data onto cards as suggested by ECAC. This procedure is semi-automatic in that it requires manual sampling of an analog antenna pattern. An operator manipulates a pair of cursors on a machine on which the antenna pattern is placed. This machine, labelled "Oscar" by the Benson-Lehner Company, is manually directed to sample the analog waveform at any selected point and supply the magnitude of the sampled value to an analog-to-digital converter unit. The converter unit digitalizes the data and feeds a card punching unit which automatically punches the data onto cards. Figure 74 shows the equipment used in this procedure. The analog-to-digital converter unit is seen at the left of the photo, the "Oscar" machine in the center, and the card punch unit on the right. This semi-automatic procedure has several drawbacks not found in the completely automatic procedure described in the preceeding section. First, it is doubtful whether this system can conveniently punch the digitalized data onto IBM cards in the format suggested by ECAC. Secondly, the analog waveform must be sampled manually by a human operator. Our investigation has shown that when the equipment is operated by a person who is unfamiliar with antenna problems, there is a high probability of erros appearing in the digital data. These errors are usually very difficult to locate and very costly to correct. Thirdly, the curve sampling procedure is very tiring to the eyes of the operator and this also increases the probability of errors in the data.

It is felt that our investigation has uncovered the severe limitations of this technique of data conversion. Such would be the result of work placed with commercial analog-to-digital converter facilities unless the facility was completely automated. The errors introduced into the data by the human operator, if not discovered, would render the data essentially meaningless to ECAC. Therefore, if it is necessary to use the semi-automatic procedure, it is suggested that only

trained antenna personnel be used as the machine operators. The results obtained at Michigan using antenna trained personnel to handle the manual aspects of this procedure have been quite rewarding, but this was not the case when using untrained antenna personnel. However, the optimum procedure for converting antenna data to digital form is to employ the fully automatic system that was discussed in the previous section.

3.4 Automatic Data Reduction Procedure

To justify the simplified modeling technique, it will be recalled that most of our data was presented in cumulative gain distributions and a small amount of data in sliding-sector curves. To reduce the data into these statistical forms by hand was found to be very time consuming and costly. Therefore, an automatic data reduction procedure was developed by the University of Michigan. A block diagram of this system is shown in Fig. 75. The antenna data, previously placed on cards, is read into the IBM 1401 processing unit along with one or more computer programs. All the information is placed on magnetic tape in the appropriate format by the 1401 unit. The information then enters the IBM 7090 digital computer via magnetic tape, is reduced to the desired statistical forms, and is again placed on magnetic tape by the computer. A partial view of the IBM 7090 digital computer is seen in Fig. 76. The reduced data is punched onto cards by the IBM 1401 and 1402 unit. These cards are interpreted by a Benson-Lehner electroplotter which automatically plots the desired cumulative gain distributions, sliding sector curves, etc. on paper. Figure 77 shows the Benson-Lehner electroplotter with its associated card reading unit on the right.

It is not felt that the above procedure and equipment is particularly pertinent to the operations conducted by ECAC. The statistical data produced was of value to Michigan only in the justification of the simplified modeling technique and has provided an inexpensive and rapid means for presenting the data used in this report.

9

3.5 Report of Data Techniques

As a conclusion to the data techniques investigation, it is recommended that a technical report be prepared outlining the various techniques that may be employed to place data in a format that would be acceptable to both the service and ECAC. It is recommended that this report consist of several chapters, conceivably eight. The suggested titles of the eight chapters are as follows:

Chapter 1 Summary of Findings
Chapter 2 U of M Analog to Digital Converter
Chapter 3 U of M Magnetic Tape Transfer
Chapter 4 U of M Magnetic Tape to Card Transfer
Chapter 5 Semi-Automatic Digital Recording Procedure
Chapter 6 Other Digital Recording Techniques
Chapter 7 ECAC Requirements
Chapter 8 Recommendations

The preceeding is a suggested outline and is subject to change in the final version of the report. Of the eight chapters noted above, Chapter 6 is the most important since it will describe the other digital techniques that might be employed to place antenna data in digital form. It is suggested that a study be conducted to determine the merits of the other techniques available. If these are not felt to be applicable, the present Michigan recording technique would be modified to rapidly produce pattern data in digital form rather than the lengthy process that is presently employed. A preliminary investigation into the feasibility of condensing the Michigan recording procedure has been started and it is felt that these improvements would be applicable to the spectrum signature program.

IV. SYSTEM ASPECT

A third aspect of the present contract is the consideration of the overall system. In considering the overall system, one desires to know what information is to be collected by the service and supplied to ECAC for interference predictions. Since there are many types of systems in use today, we must confine ourselves initially to one of the more popular systems. As our knowledge of this system increases, we will be able to apply it to more complicated systems. For example, the system that we have chosen to consider first is a communications system that functions in the VHF-UHF frequency region. This system employs coaxial cables as transmission lines, thus limiting the scope of the investigation. A waveguide system is far more complicated and will require further study after knowledge is gained from the coaxial transmission line investigation.

4. 1 Power Transfer Considerations

In the previous Interim (7274-1-T) power transfer considerations of a transmitter through a length of coaxial transmission line to an antenna were presented. In this analysis, a rather complicated equation (Equation 26) was derived. Since the derivation of this equation, a simplified equation has been developed. The derivation is shown in the Appendix and the resulting equation is

$$\frac{P}{P_{max}} = \frac{1}{\alpha^2 \cos^2 kd_a + \sin^2 kd_a}$$

Fig. 78 is a set of universal curves calculated from the above equation showing the variation of power delivered to the antenna as a function of the transmission line length, d_a . From these curves, it is a simple matter to determine the probability that, with a particular transmitter and antenna, the power radiated by the antenna will exceed some arbitrary power level when the exact length of the transmission line is not known. This information may be obtained from three measurements; 1) the antenna standing wave ratio, 2) the transmitter standing wave ratio, and 3) the maximum power available from the transmitter. These three

11

measurements should be made at a point on the transmission line near the antenna to minimize the effects of transmission line losses. Techniques for the first and third measurements are relatively simple, but the measurement of the transmitter standing wave ratio is not well understood. Therefore, a technique for obtaining this data must be developed. It is felt that this procedure must be simple to be readily usable by untrained personnel.

To initiate the development of this technique, it will be necessary to obtain data from a typical transmitter used by the service. The initial set of data will be the spurious response of the transmitter. The initial data will be obtained with the transmitter operating into a 50 ohm dummy load (closed system).

4.2   Typical Transmitter - Radio Set AN/ARC-27

A 28 volt, 20 amp power supply was designed and built to power the ARC-27 received from WPAFB. Initial use of the power supply indicated that its filtering action was inadequate. An improved filtering system has been added to the power supply to provide an output voltage that contains less than 1 percent ripple. It is felt this filtering is adequate and typical of actual aircraft operation. The power supply and filter section are seen at the left in Fig. 79, which also shows the ARC-27 and its control boxes.

The preliminary operational check of the ARC-27 was conducted at the Michigan Air National Guard to take advantage of their special test facilities. The transmitter was found to be inoperative in the UHF range (300-399 MHz) and below specifications in the VHF range (225-300 MHz). The UHF output was sub-sequently restored by the replacement of a damaged filter choke and numerous weak vacuum tubes. Ulilizing the power supply built at the U of M, partial align-ment of the transmitter has been achieved as indicated by the power levels shown in Fig. 80, which is a plot of the transmitter output power vs. frequency.

A Polarad spectrum analyzer was initially employed to determine the spur-ious emissions of the ARC-27. For the purposes of this test the transmitter was tuned to a fundamental frequency of 300 MHz and loaded with a medium power

50 ohm termination (closed circuit test). The spurious signals observed, through the third harmonic, are listed in Fig. 81. Several of the signals were observed to have an "unknown" origin. These signals may be due to the spectral characteristics of the spectrum analyzer rather than the transmitter. Therefore, further tests will be conducted employing standard RFI measuring instrumentation to clarify the question of signal origin.

Figure 82 illustrates the impedance characteristics of the modified monopole antenna plotted in 100 MHz increments from 300 through 1500 MHz. The antenna in question is an operational model (pick-ax) obtained from the Michigan Air National Guard. This antenna previously served as the model for the 1/8 scale modified monopole antenna used in the investigation of simplified modeling. Fig. 83 illustrates the impedance characteristics of a second antenna (model AT-256A/ARC) which was measured at the frequencies noted above. This antenna is also an operational model and was obtained from WPAFB. Both of the above antennas are typical of those used by the service with radio set AN/ARC-27. The impedance data of Figs. 82 and 83 illustrate the wide range of loads into which the AN/ARC-27 must operate at the fundamental, spurious and harmonic frequencies.

4.3 <u>Conclusions and Recommendations</u>

In view of the wide range of loads (Figures 82 and 83) into which the AN/ARC 27 transmitter may be operated further tests are required. Future tests will be performed with the transmitter operating into each of the antennas noted in 4.2 above (open field tests). The purpose of these tests will be to obtain an understanding of the affects of load variation at the spurious and harmonic frequencies. Further, it will be desirable to vary the length of transmission line between the transmitter and load to obtain an understanding of its affect at the above frequencies. Test procedures are being prepared so that the output impedance characteristics of the transmitter may be determined at the fundamental and harmonic frequencies.

Fig. 2. Slot Antenna on Simplified Model T-33
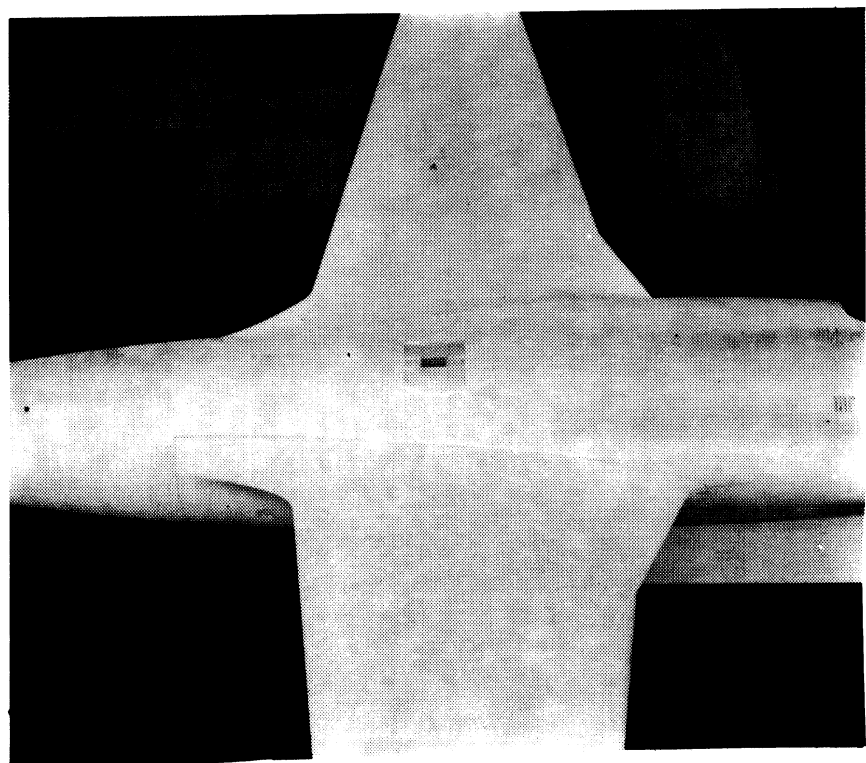
Fig. 1. Slot Antenna on Precision Model T-33

FIG: 3

X-Band Slot
8.0 Gc
Precision T-33
Transverse Cut

RELATIVE POWER ONE WAY (db)

ANGLE θ

CHART NO. 128-60   PRINTED IN U.S.A.   SCIENTIFIC-ATLANTA, INC., ATLANTA, GEORGIA

15
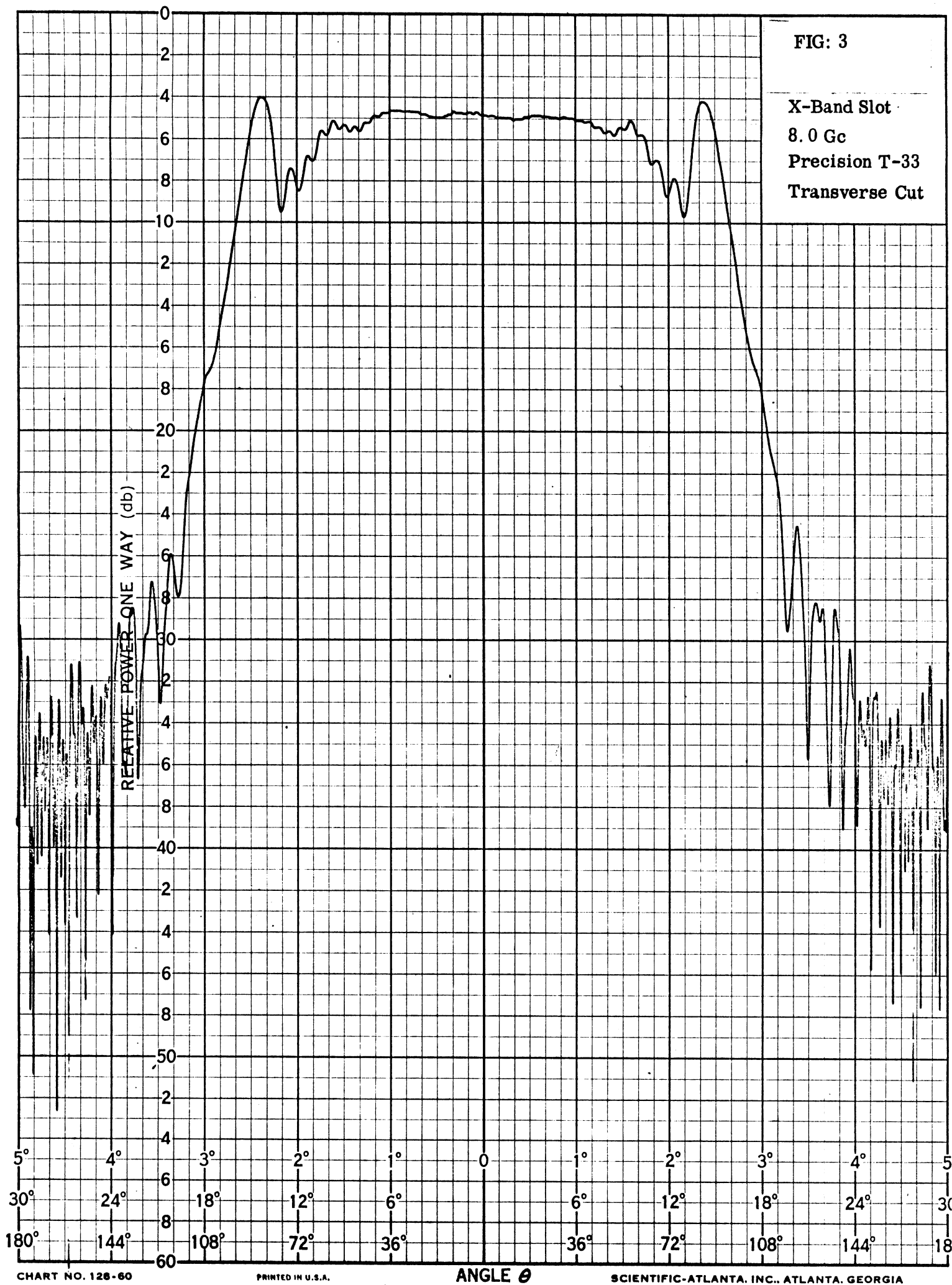
FIG. 4

X-Band Slot
8.0 Gc
Simplified T-33
Transverse Cut

FIG. 5

X-Band Slot
16.0 Gc
Precision T-33
Transverse Cut

RELATIVE POWER ONE WAY (db)

ANGLE θ

CHART NO. 128-60   PRINTED IN U.S.A.   SCIENTIFIC-ATLANTA, INC., ATLANTA, GEORGIA

17
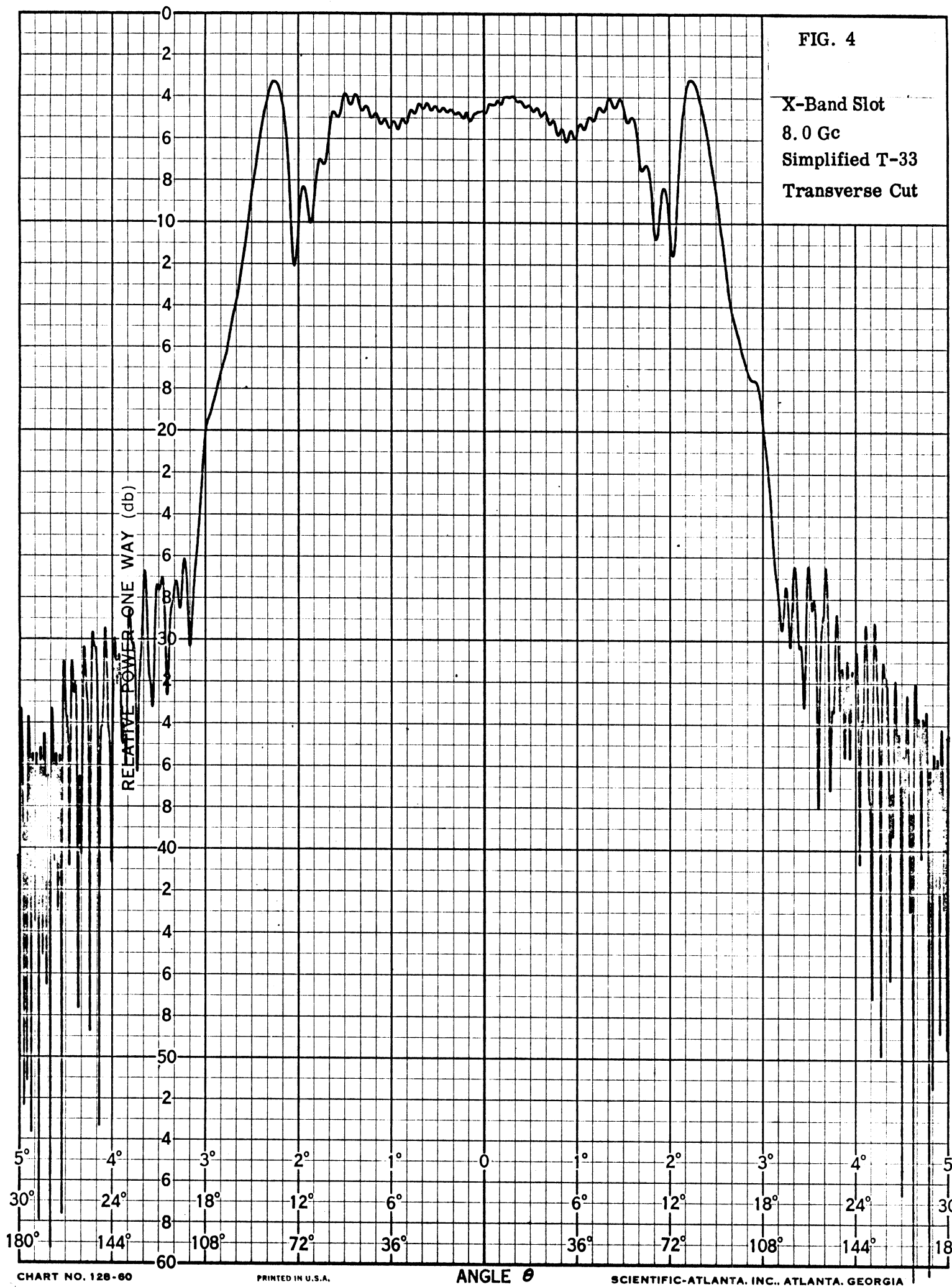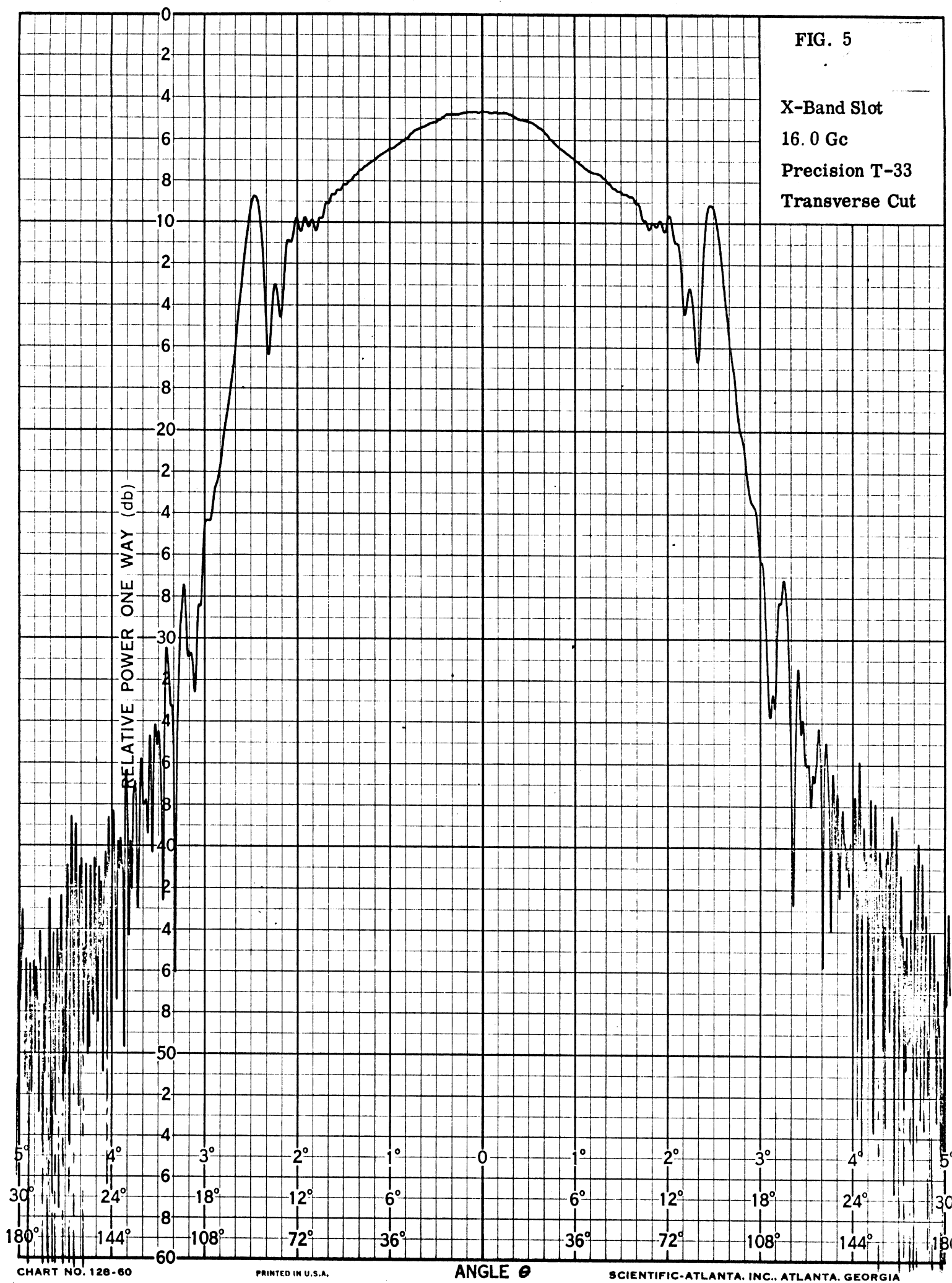
FIG. 6

X-Band Slot
16.0 Gc
Transverse Cut
Simplified T-33

RELATIVE POWER ONE WAY (db)

ANGLE θ

CHART NO. 128-60 · PRINTED IN U.S.A. · SCIENTIFIC-ATLANTA, INC., ATLANTA, GEORGIA

18

FIG. 7

X-Band Slot
24.0 Gc
Precision T-33
Transverse Cut

RELATIVE POWER ONE WAY (db)

ANGLE θ
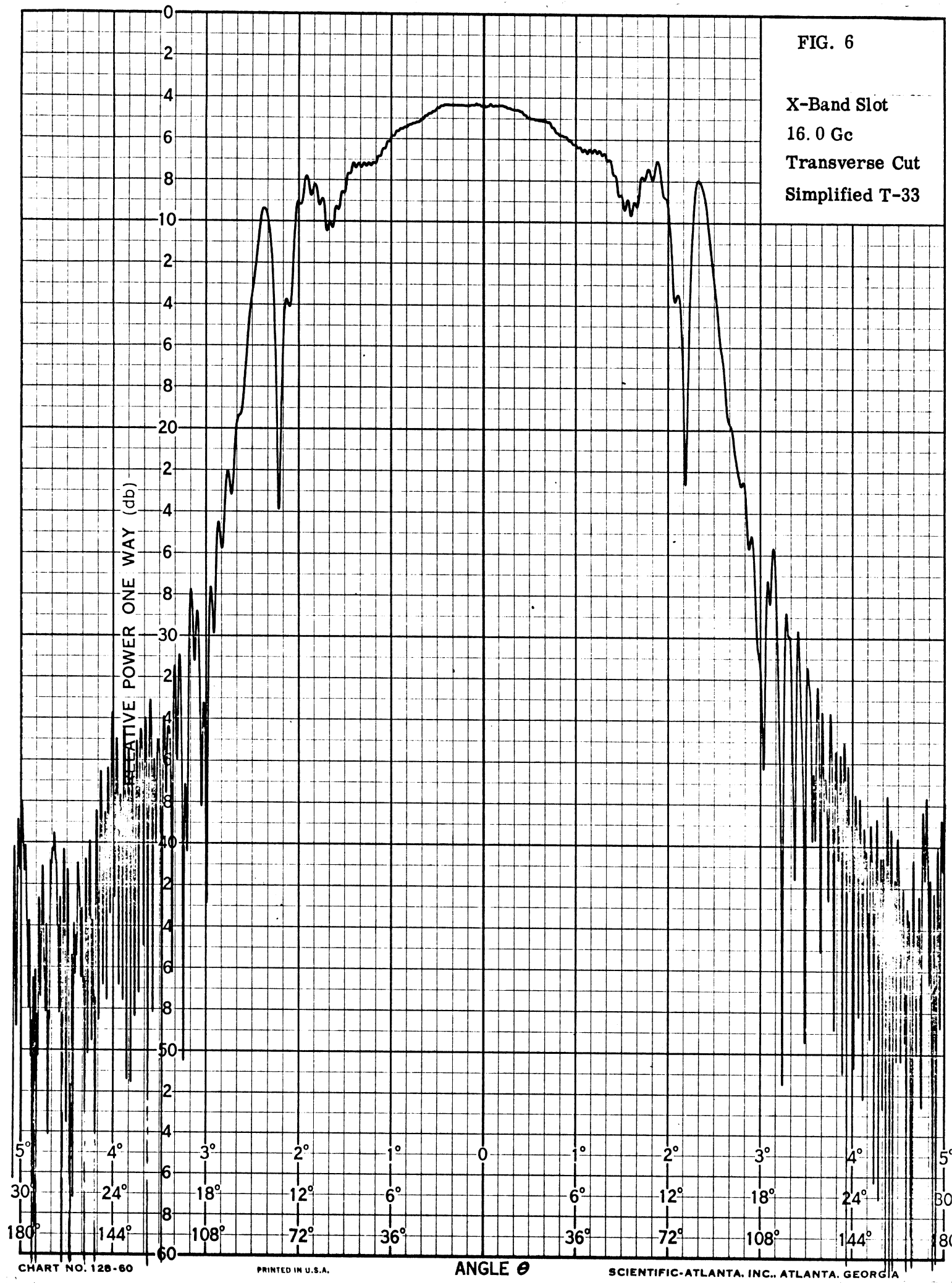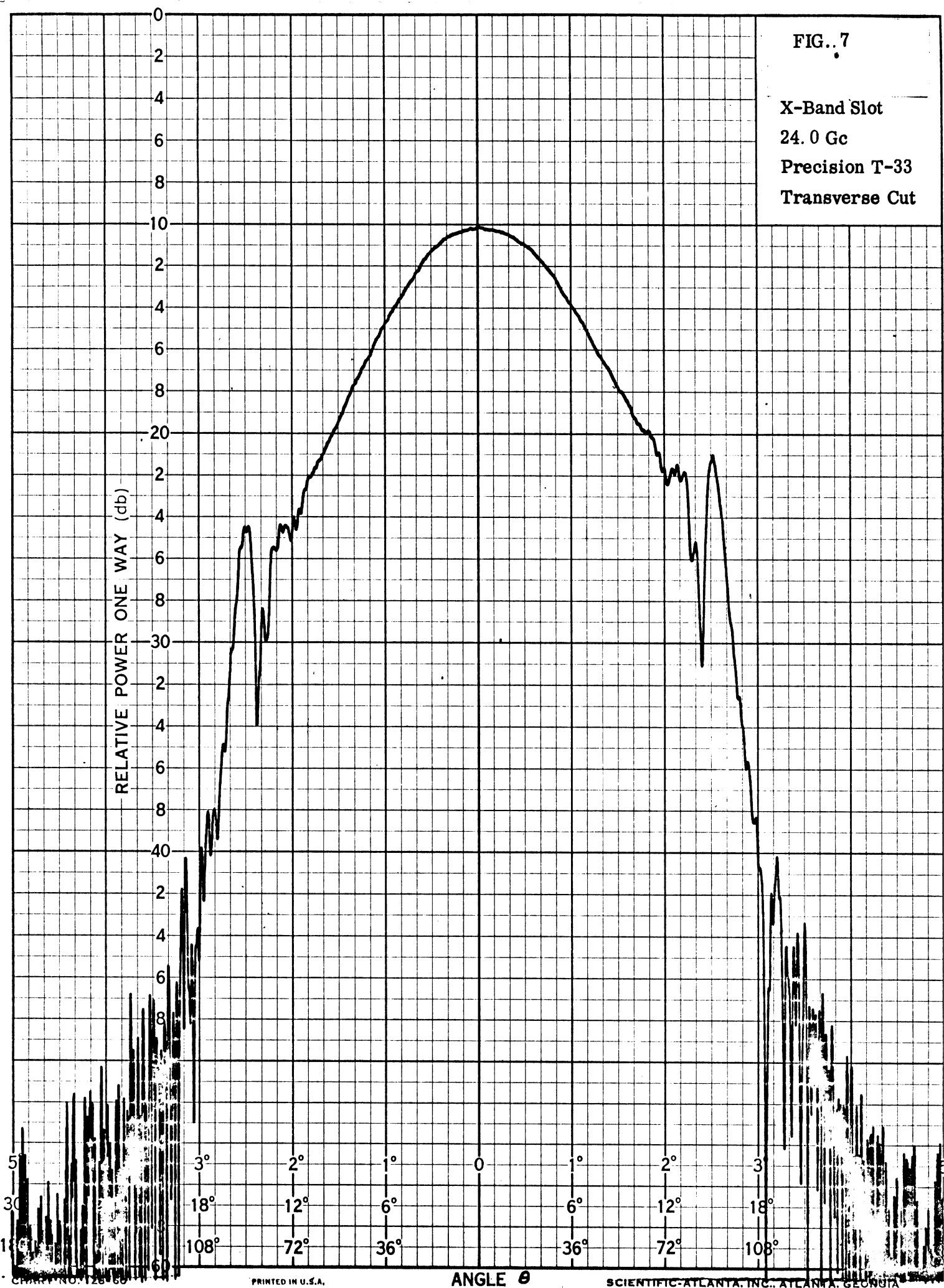
FIG. 8

X-Band Slot
24. 0 Gc
Simplified T-33
Transverse Cut
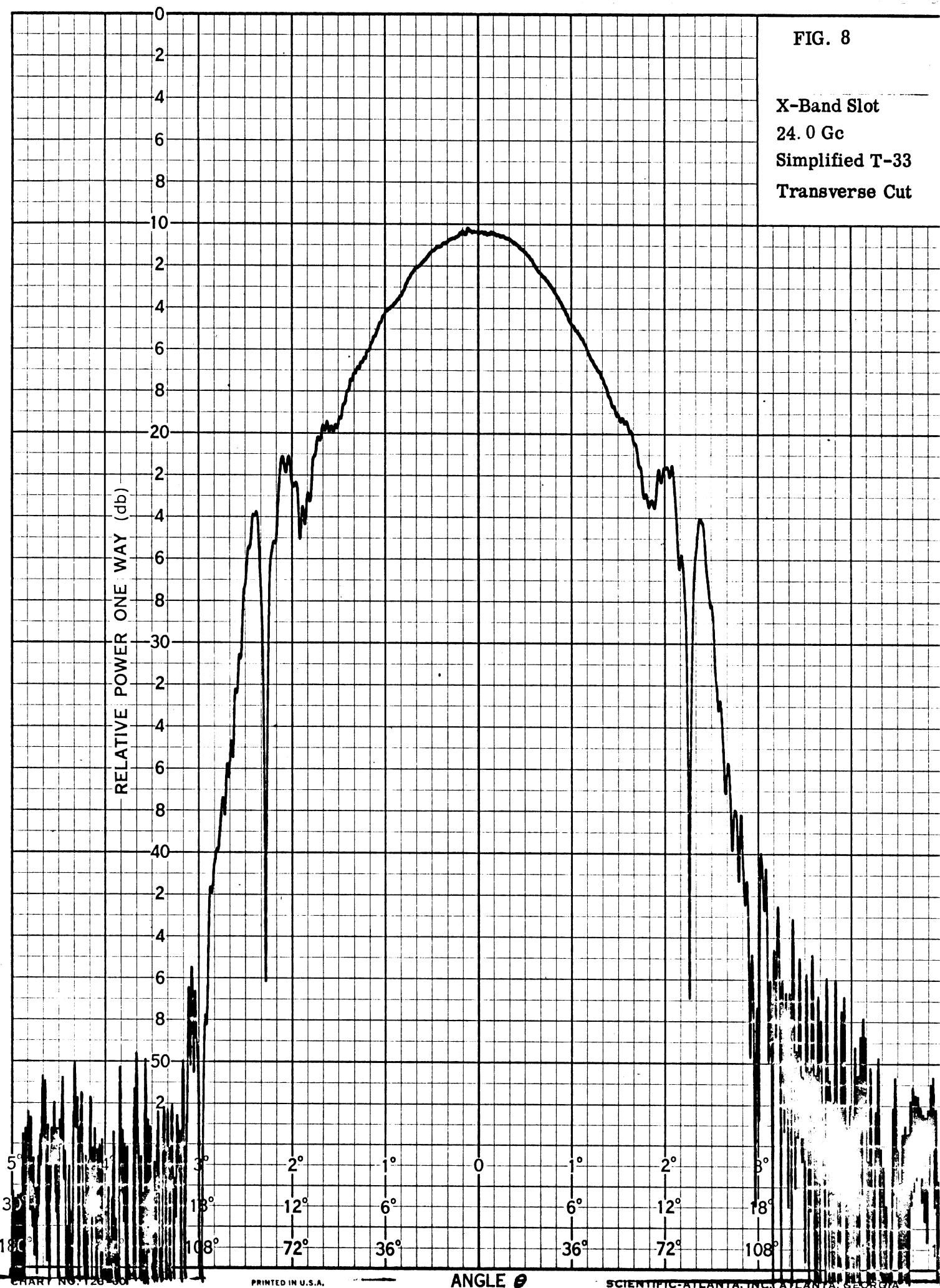
FIG. 9

X-Band Slot
32.0 Gc
Precision T-33
Transverse Cut

FIG. 10

X-Band Slot
32.0 Gc
Simplified T-33
Transverse Cut

RELATIVE POWER ONE WAY (db)

ANGLE θ

CHART NO. 128-60   PRINTED IN U.S.A.   SCIENTIFIC-ATLANTA, INC., ATLANTA, GEORGIA
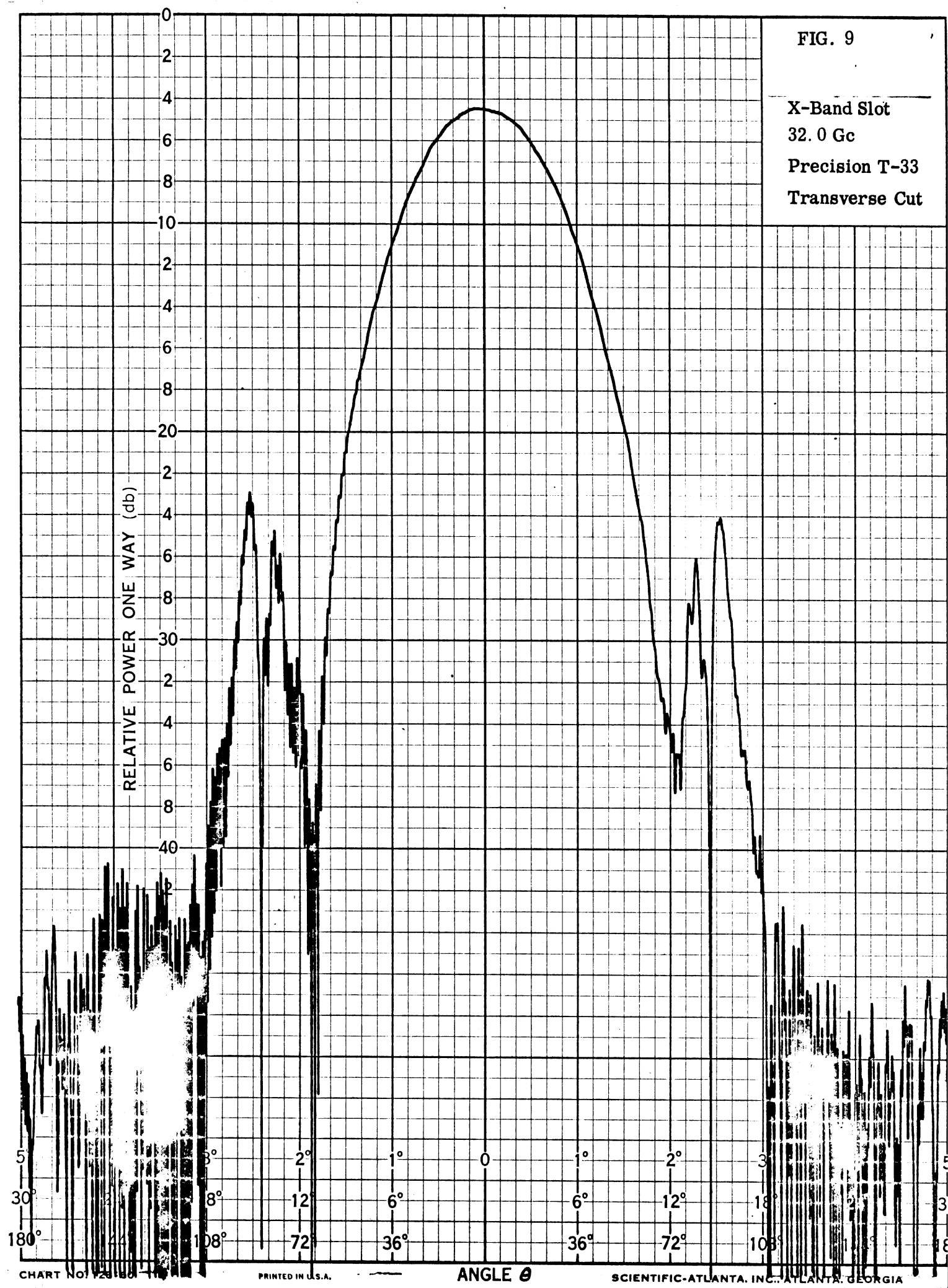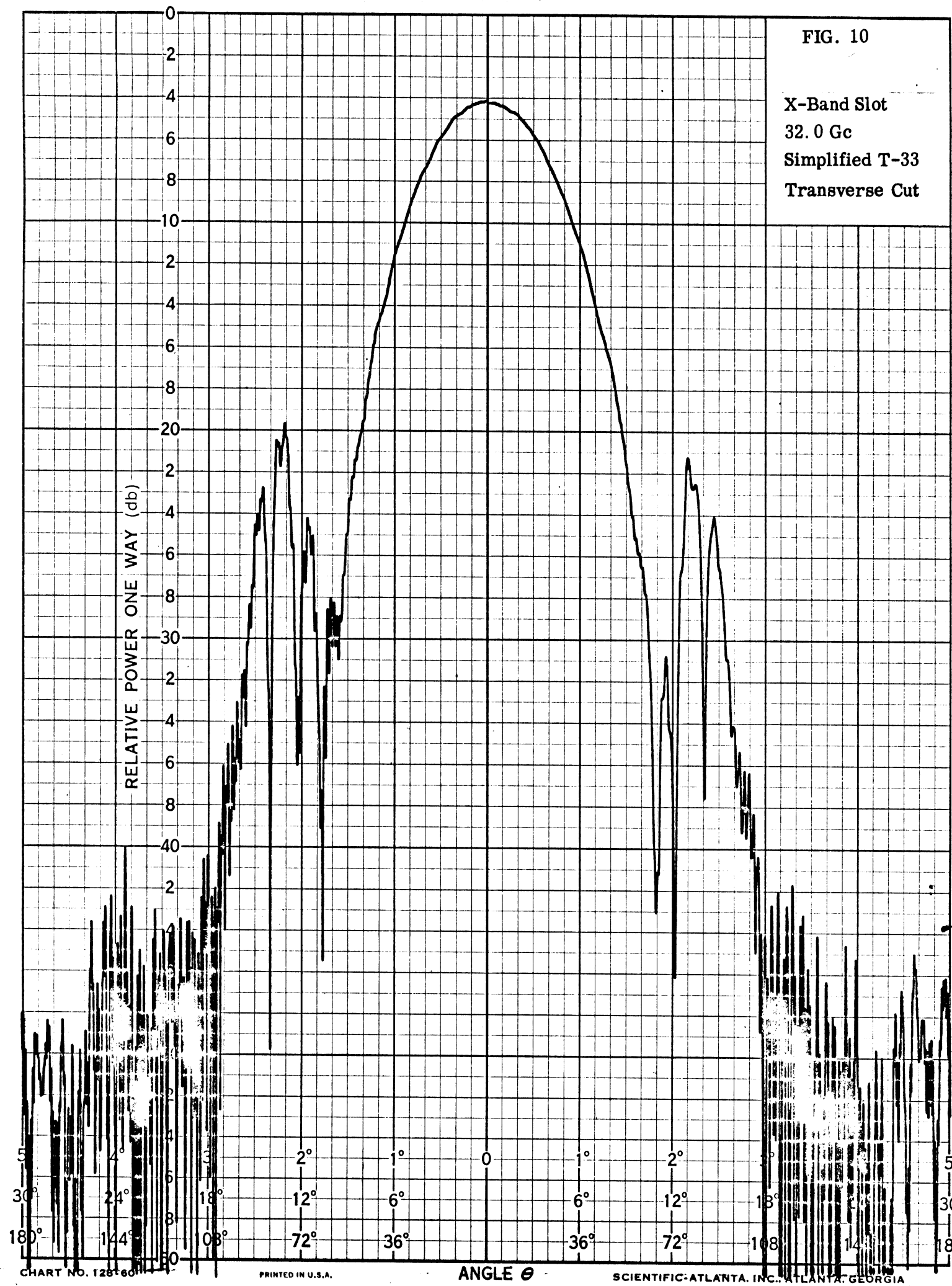
FIG. 11

X-Band Slot
40.0 Gc
Precision T-33
Transverse Cut
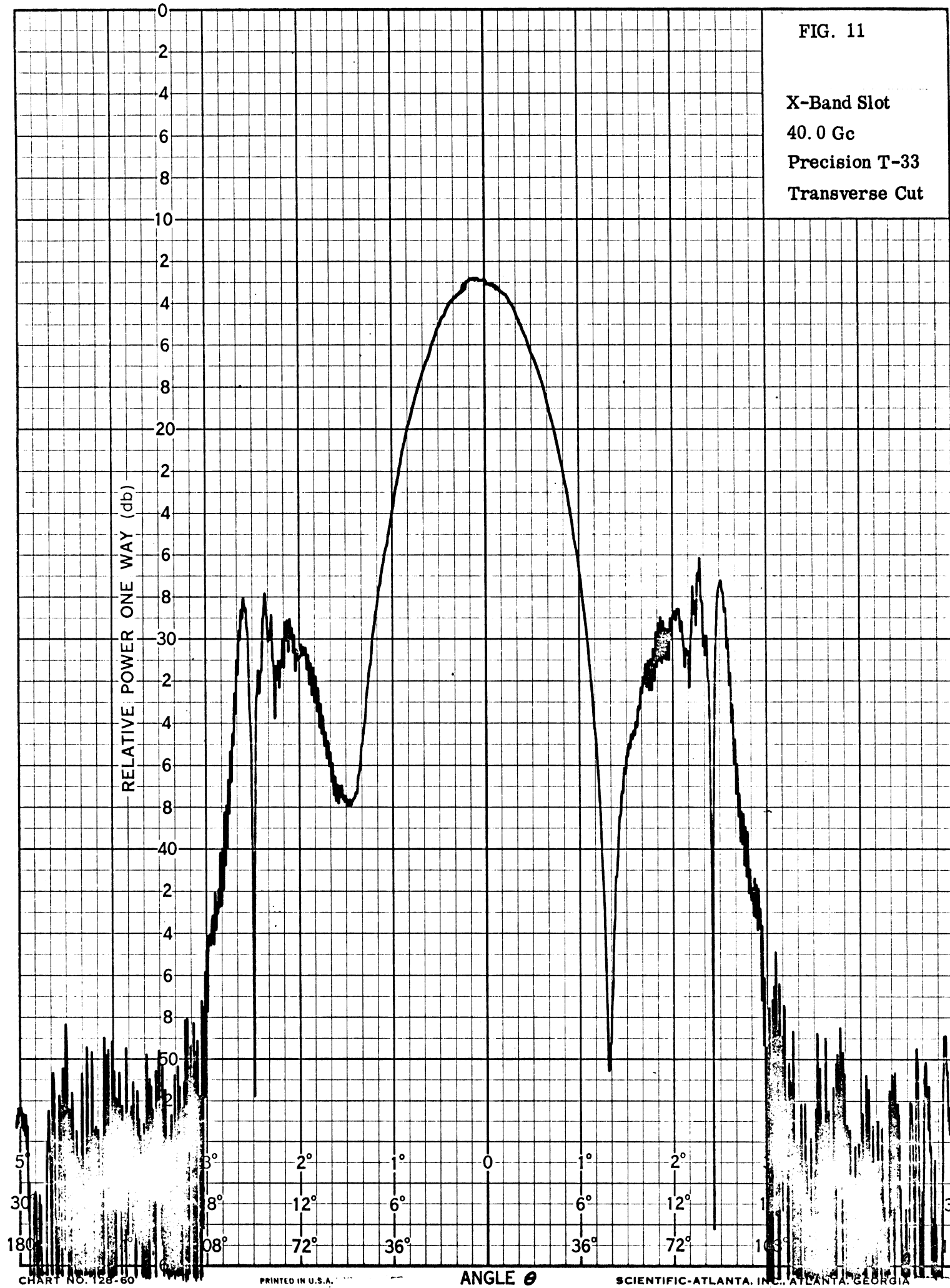
FIG. 12

X-Band Slot
40.0 Gc
Simplified T-33
Transverse Cut
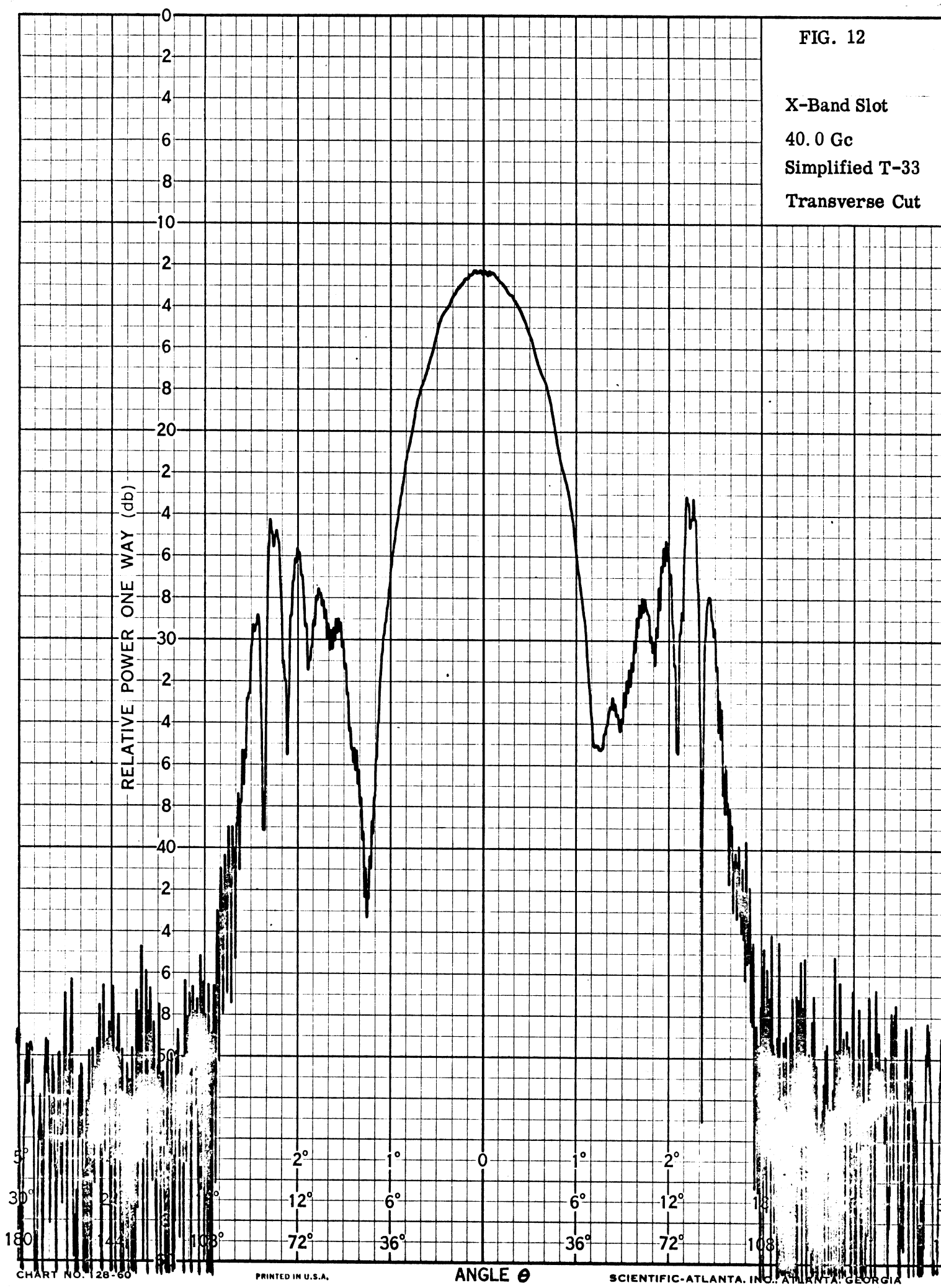
FIG. 13

X-Band Slot
8.0 Gc
Precision T-33
Longitudinal Cut
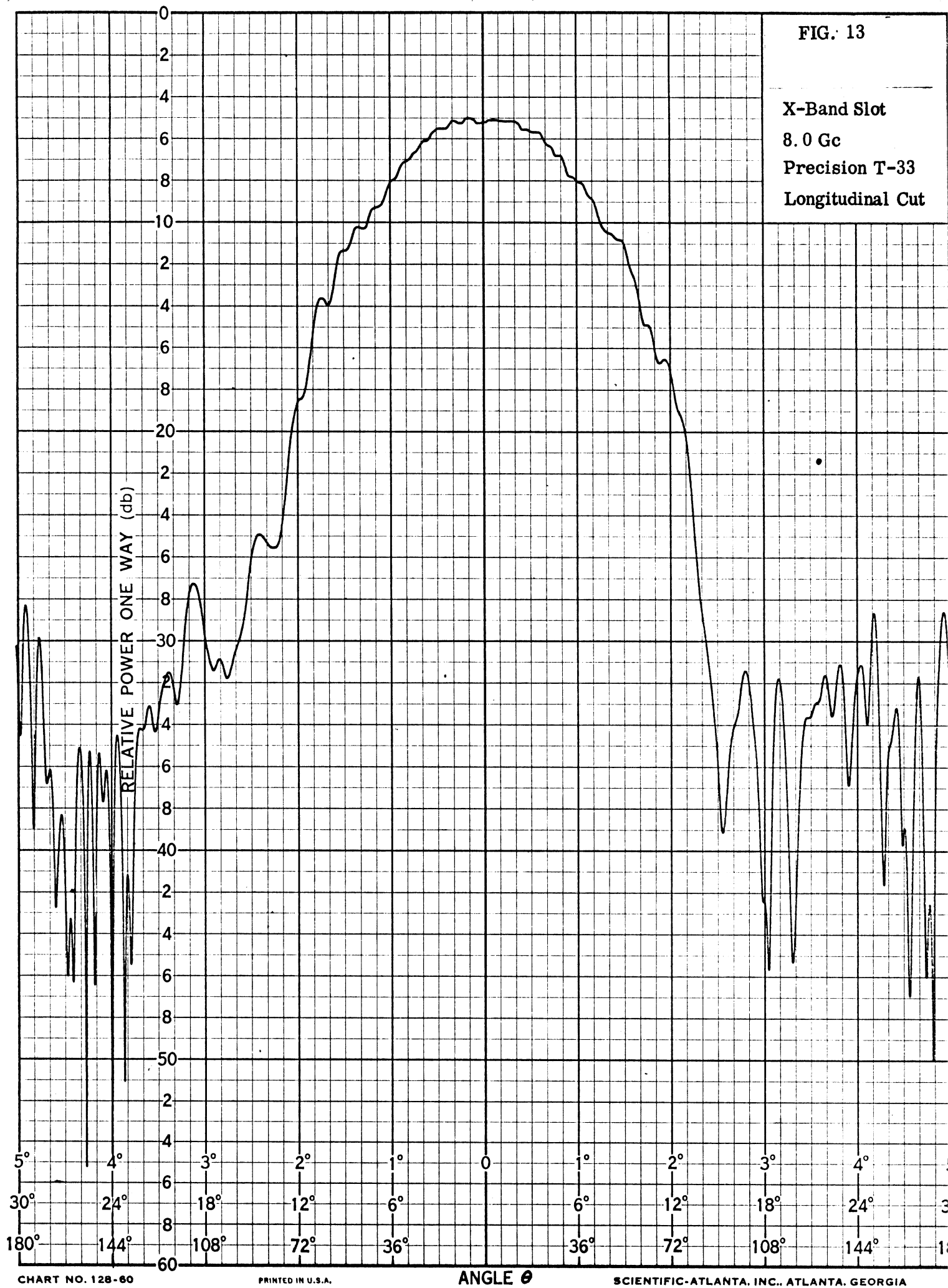
RELATIVE POWER ONE WAY (db)

ANGLE θ

CHART NO. 128-60   PRINTED IN U.S.A.   SCIENTIFIC-ATLANTA, INC., ATLANTA, GEORGIA

25

FIG. 14

X-Band Slot
8.0 Gc
Simplified T-33
Longitudinal Cut

RELATIVE POWER ONE WAY (db)

ANGLE θ

CHART NO. 128-60   PRINTED IN U.S.A.   SCIENTIFIC-ATLANTA, INC., ATLANTA, GEORGIA

FIG. 15

X-Band Slot
16. 0 Gc
Precision T-33
Longitudinal Cut

RELATIVE POWER ONE WAY (db)

ANGLE θ

CHART NO. 128-60   PRINTED IN U.S.A.   SCIENTIFIC-ATLANTA, INC., ATLANTA, GEORGIA
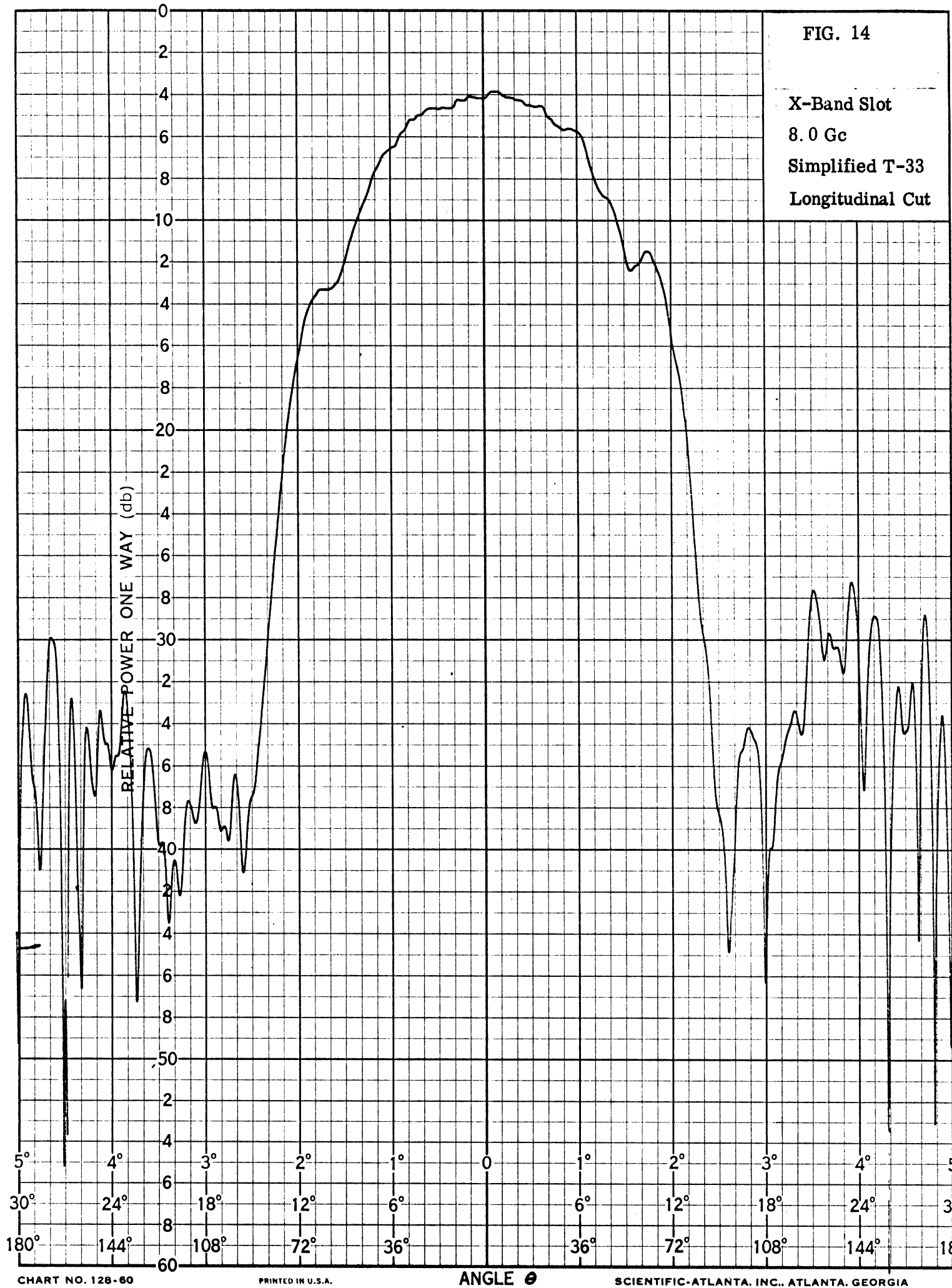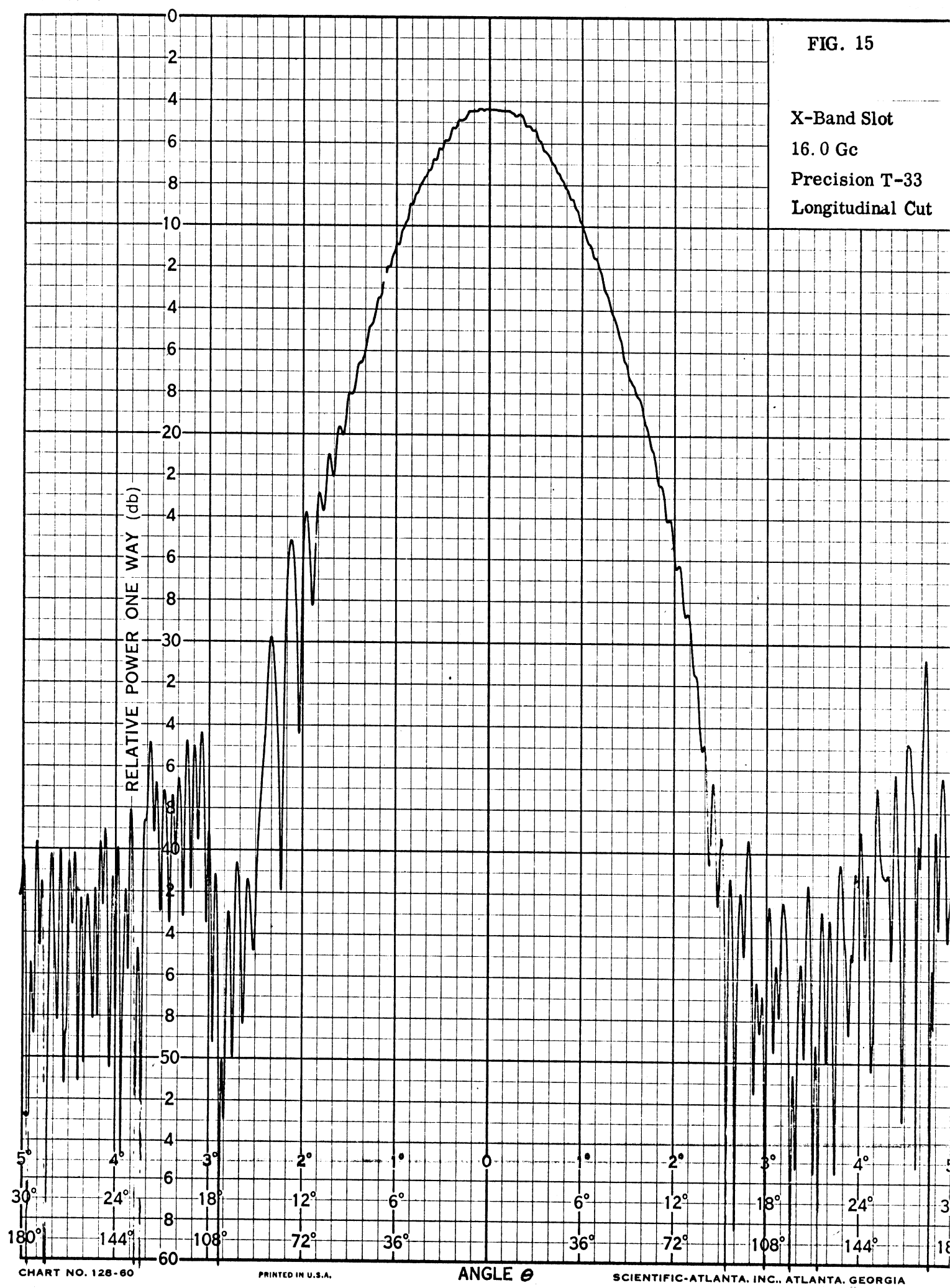
FIG. 16

X-Band Slot
16.0 Gc
Simplified T-33
Longitudinal Cut

RELATIVE POWER ONE WAY (db)

ANGLE θ

CHART NO. 128-60   PRINTED IN U.S.A.   SCIENTIFIC-ATLANTA, INC., ATLANTA, GEORGIA

28
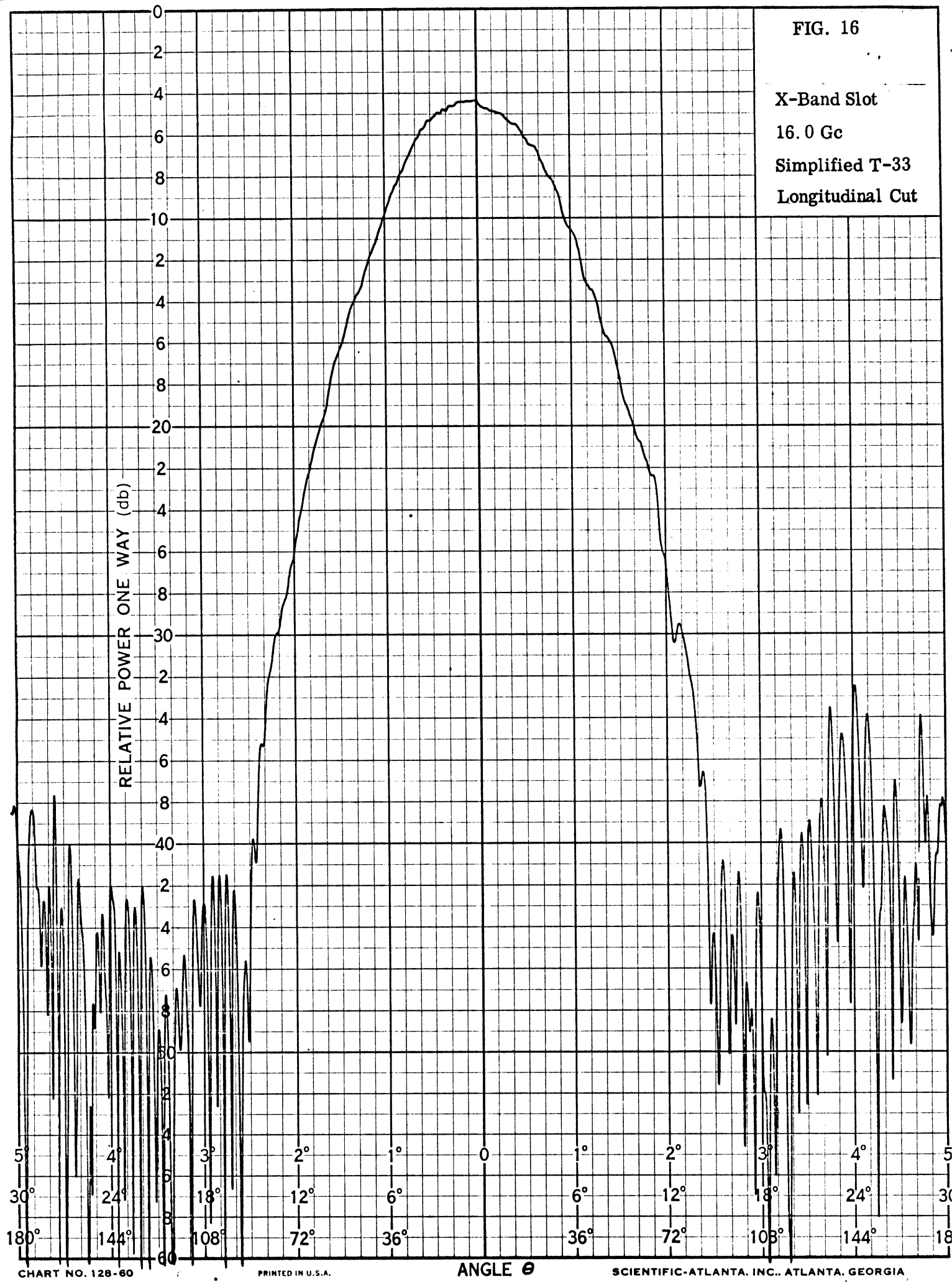
FIG. 17

X-Band Slot
24.0 Gc
Precision T-33
Longitudinal Cut
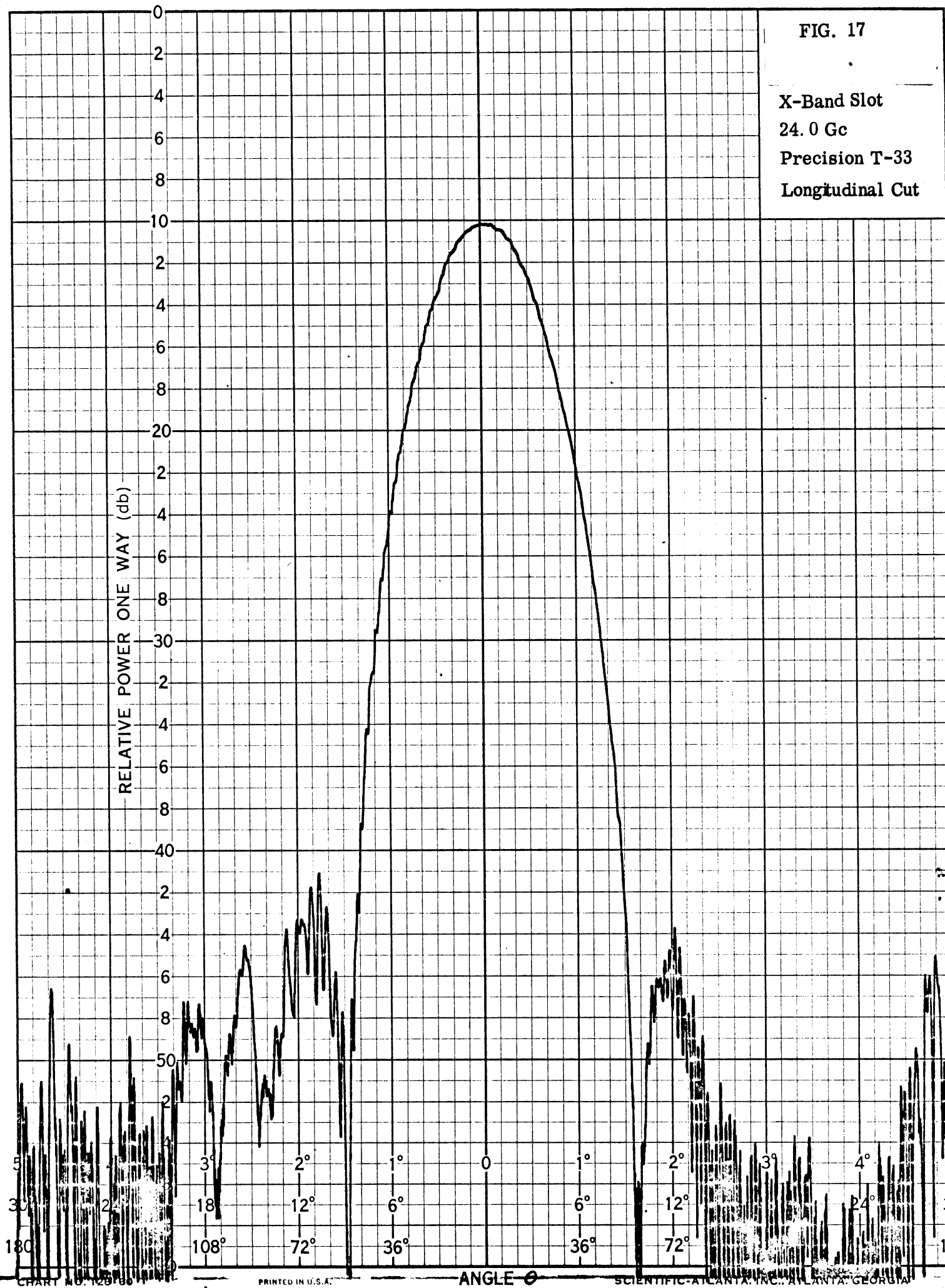
FIG. 18

X-Band Slot
24.0 Gc
Simplified T-33
Longitudinal Cut
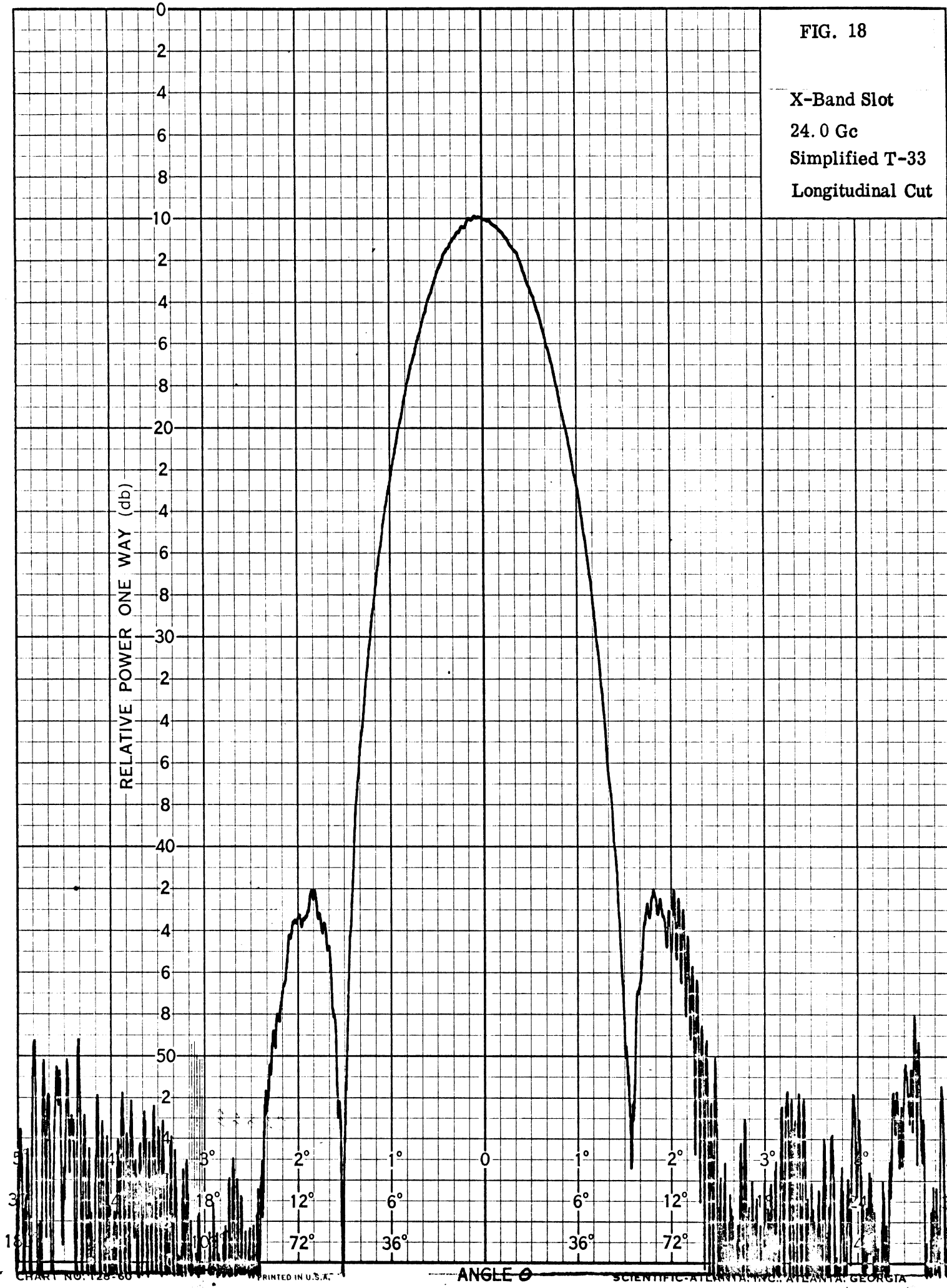
FIG. 19

X-Band Slot
32.0 Gc
Precision T-33
Longitudinal Cut
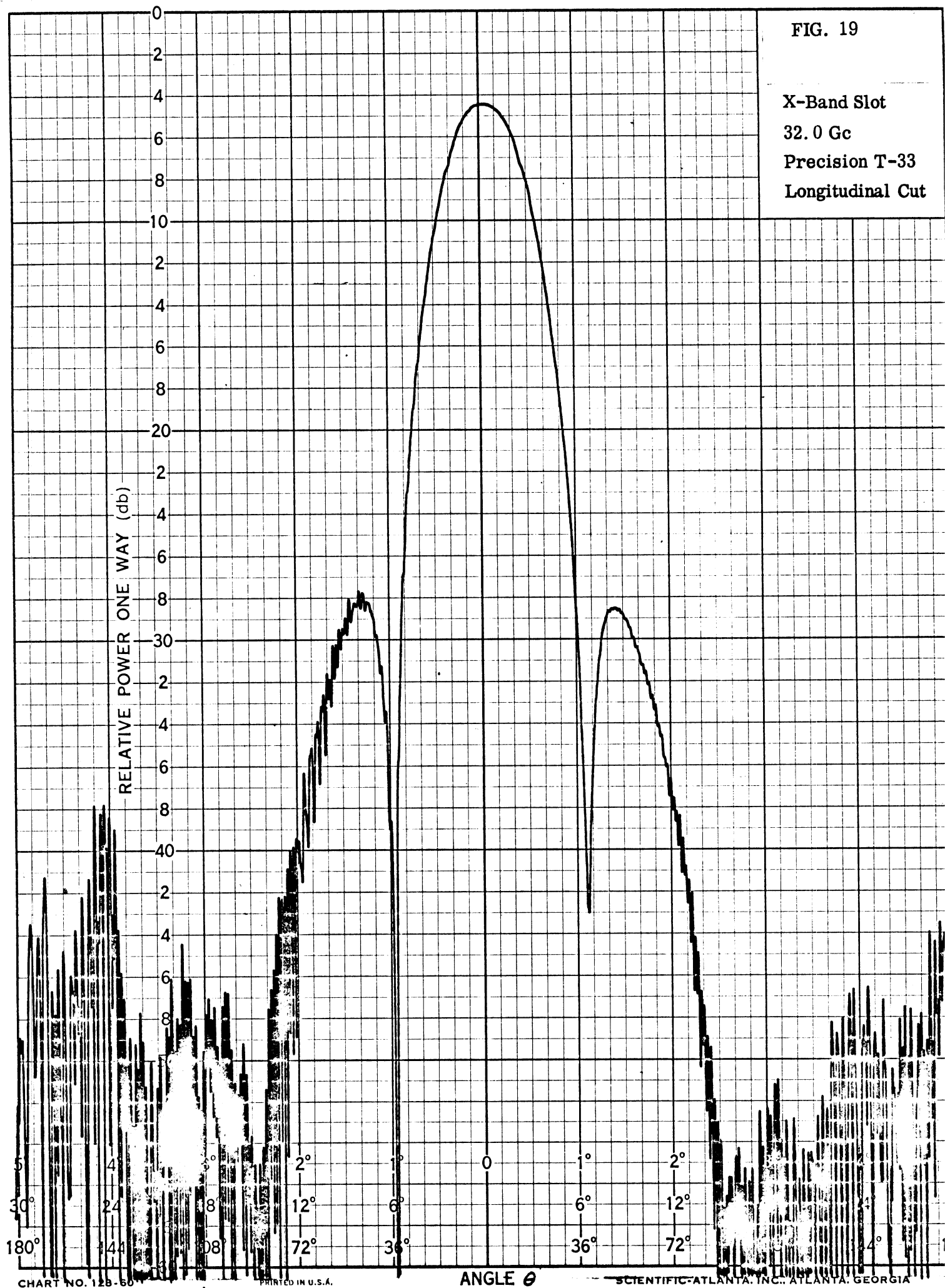
FIG. 20

X-Band Slot
32.0 Gc
Simplified T-33
Longitudinal Cut

RELATIVE POWER ONE WAY (db)

0
2
4
6
8
10
2
4
6
8
20
2
4
6
8
30
2
4
6
8
40
2
4
6
8
5

ANGLE θ

2°   1°   0   1°   2°   3°
12°   6°   6°   12°
72°   36°   36°   72°   144°

6°
30°
180°   14°

CHART NO. 128-60   PRINTED IN U.S.A.   SCIENTIFIC-ATLANTA, INC., ATLANTA, GEORGIA

32
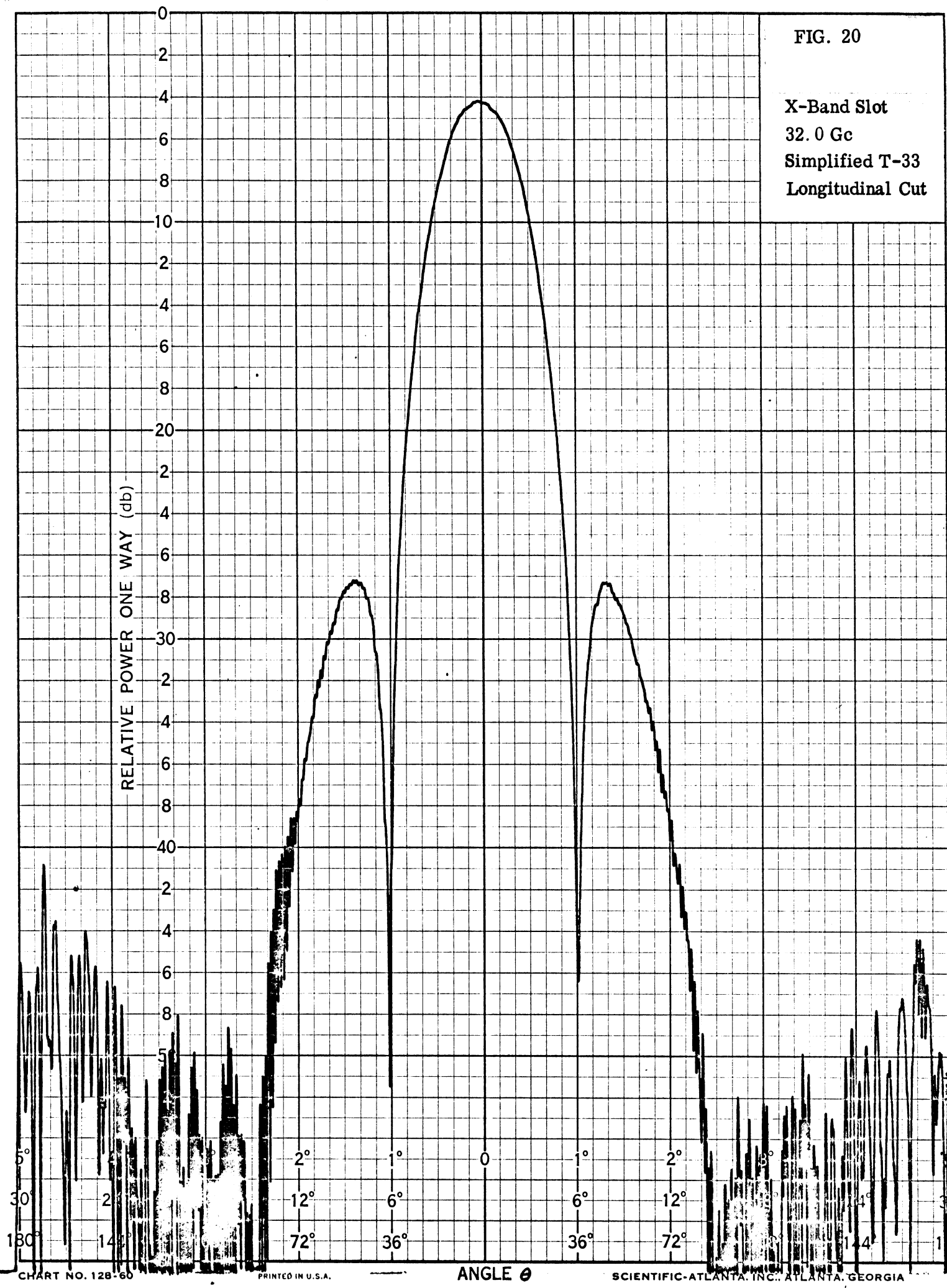
FIG. 21

X-Band Slot
40.0 Gc
Precision T-33
Longitudinal Cut
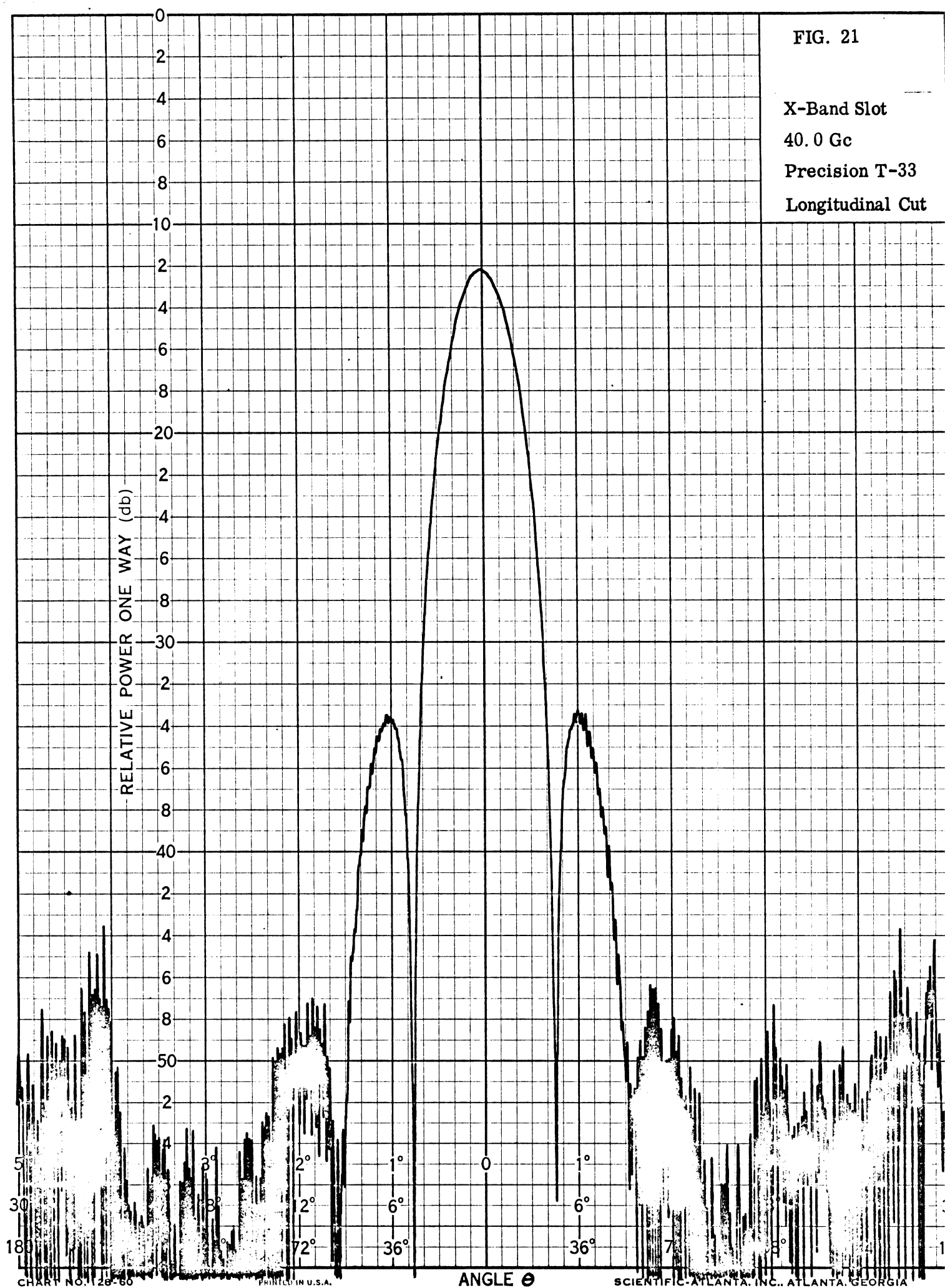
FIG. 22

X-Band Slot
40.0 Gc
Simplified T-33
Longitudinal Cut

ANGLE Θ

34
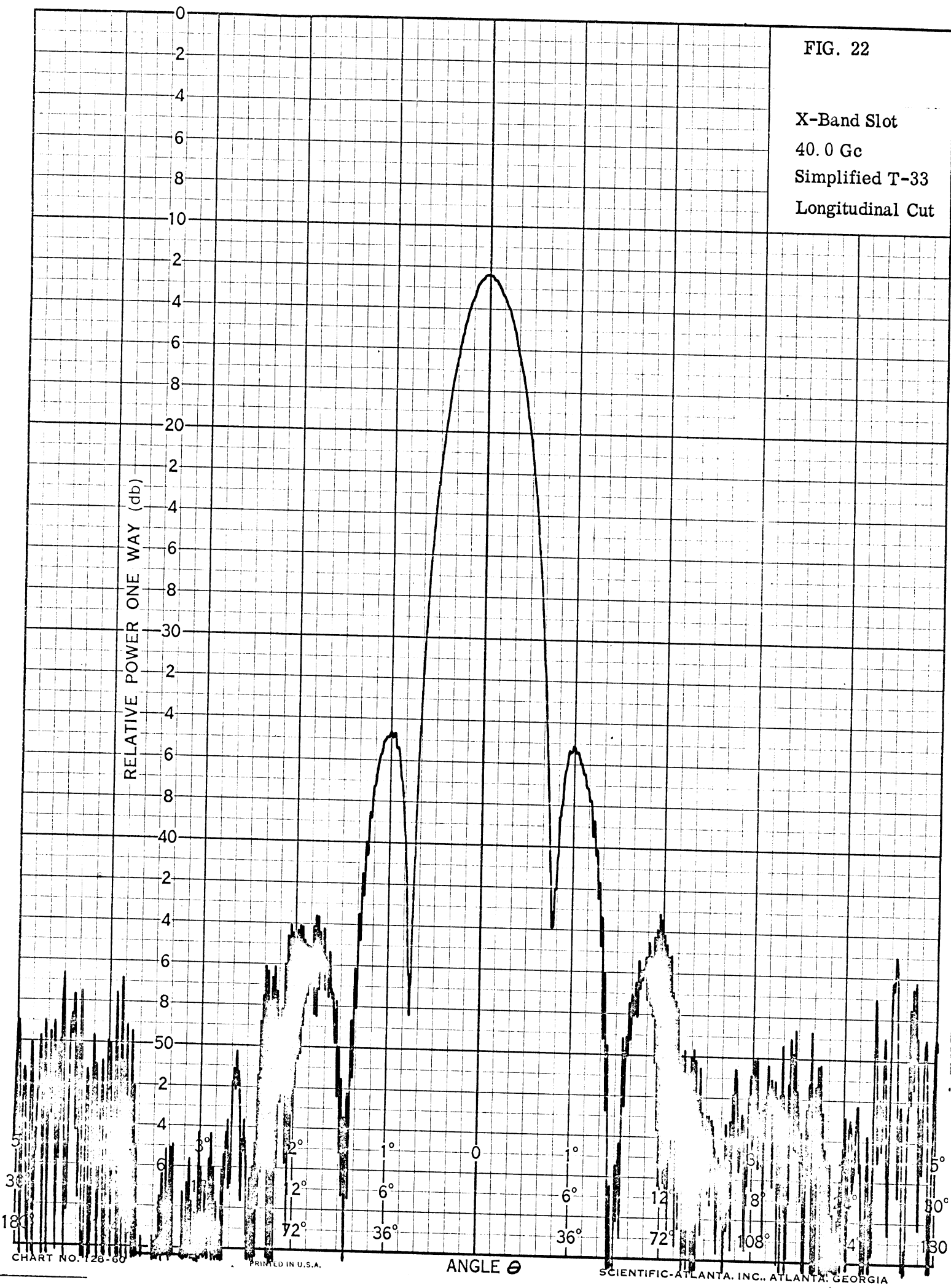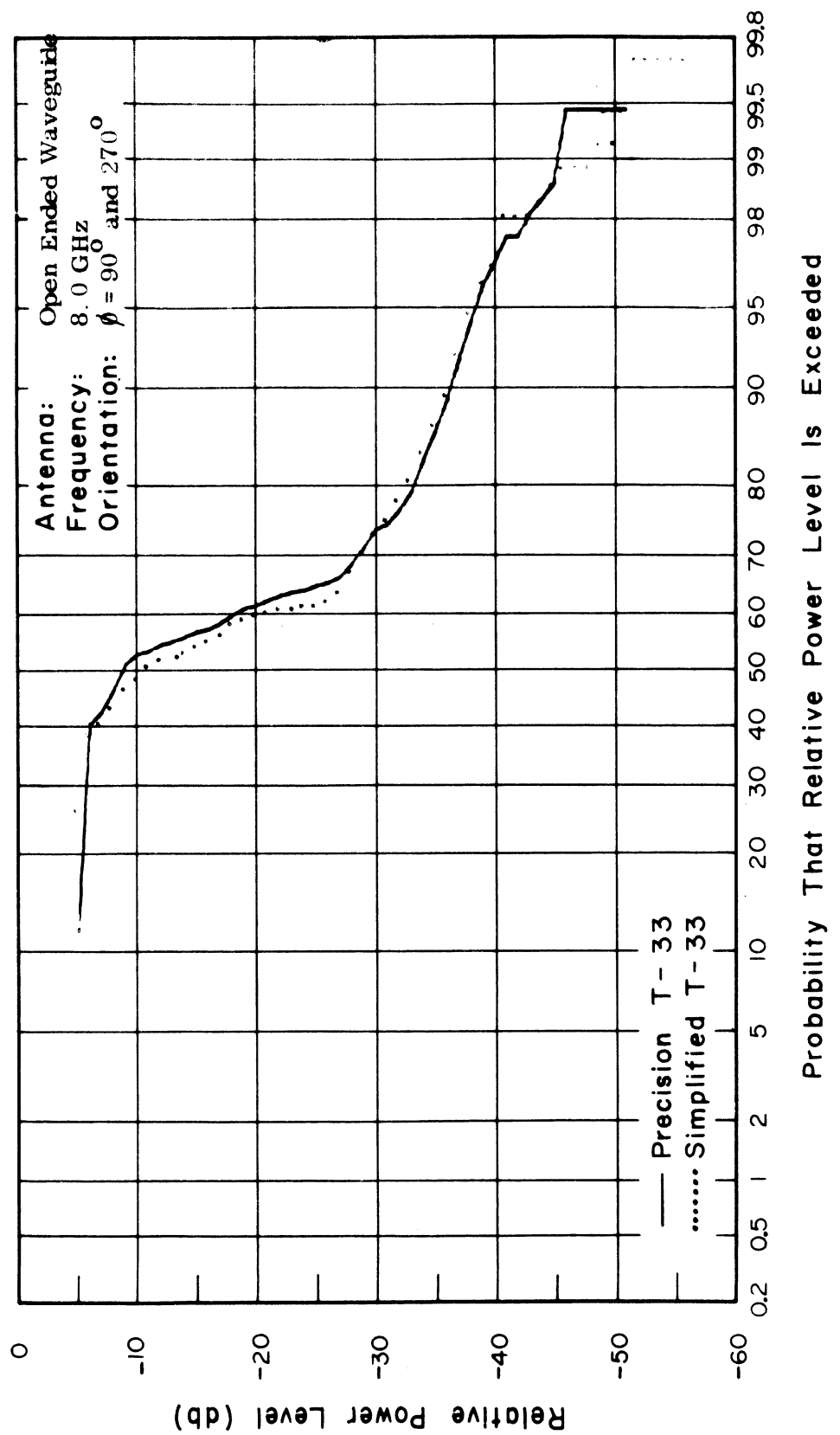
Fig. 23. Cumulative Gain Distributions of Precision and Simplified Models.
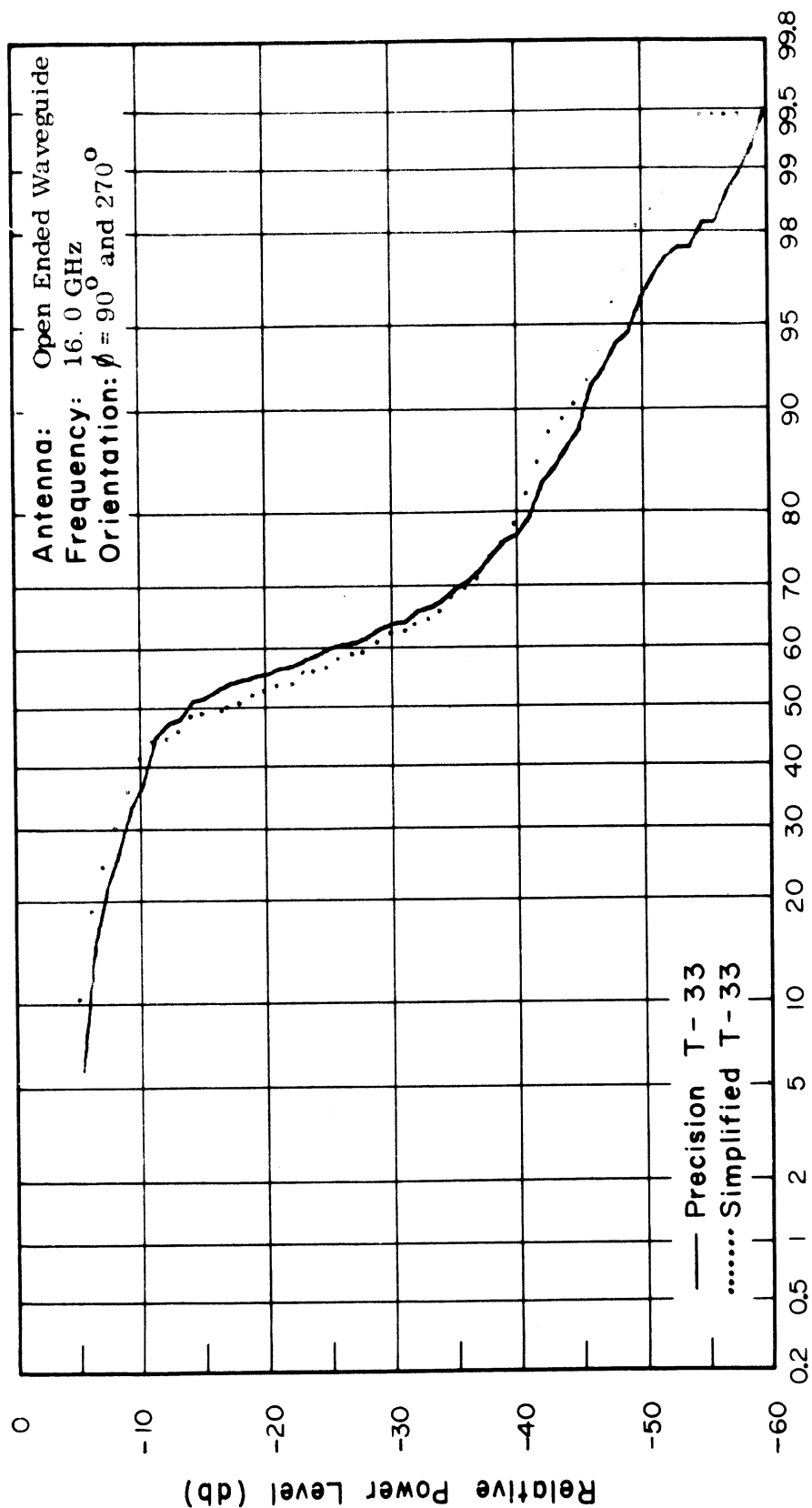
Fig. 24. Cumulative Gain Distributions of Precision and Simplified Models.

Antenna: Open Ended Waveguide
Frequency: 16.0 GHz
Orientation: $\phi = 90^{\circ}$ and 270°

—— Precision T-33
······ Simplified T-33

Probability That Relative Power Level Is Exceeded

Relative Power Level (db)
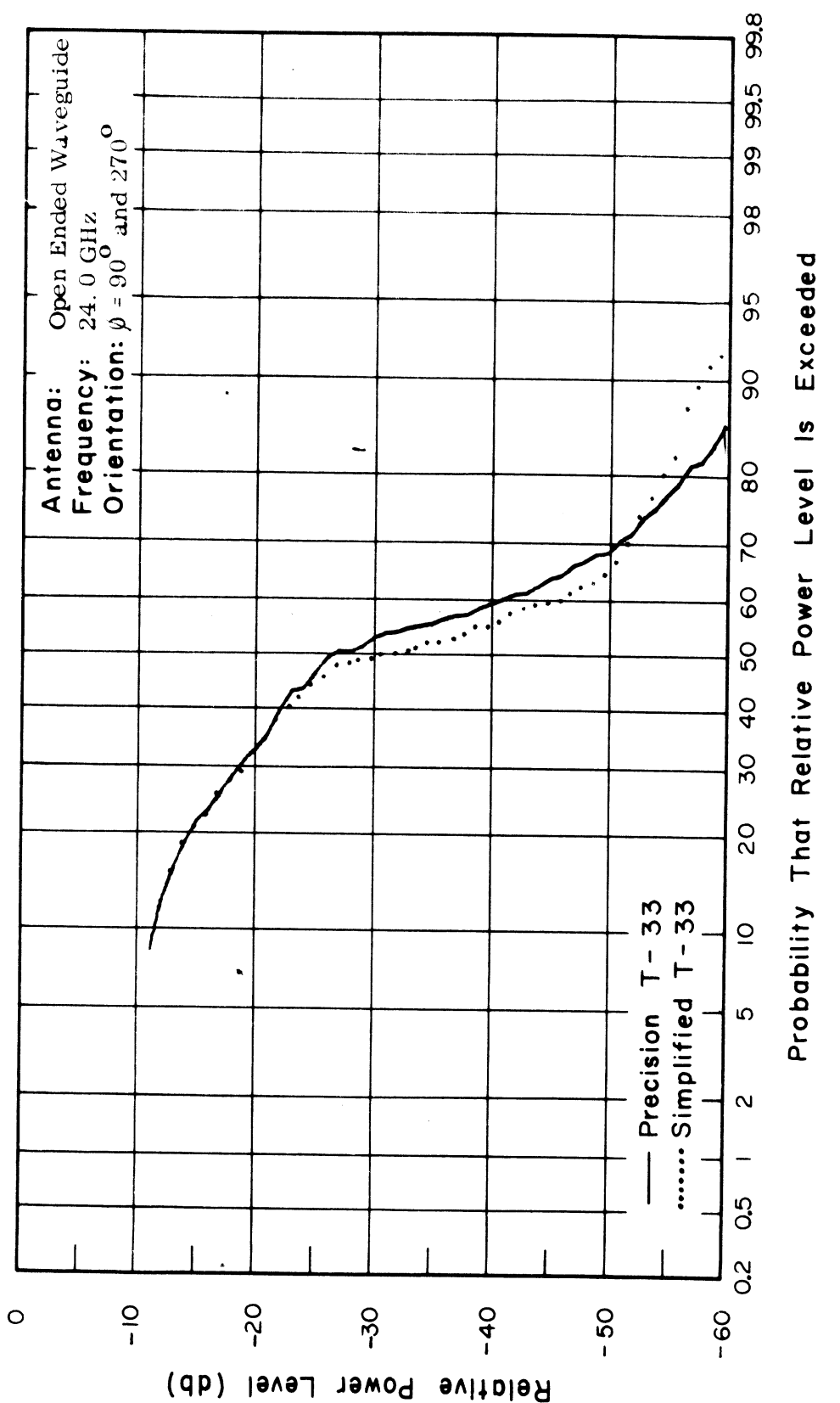
Fig. 25. Cumulative Gain Distributions of Precision and Simplified Models.
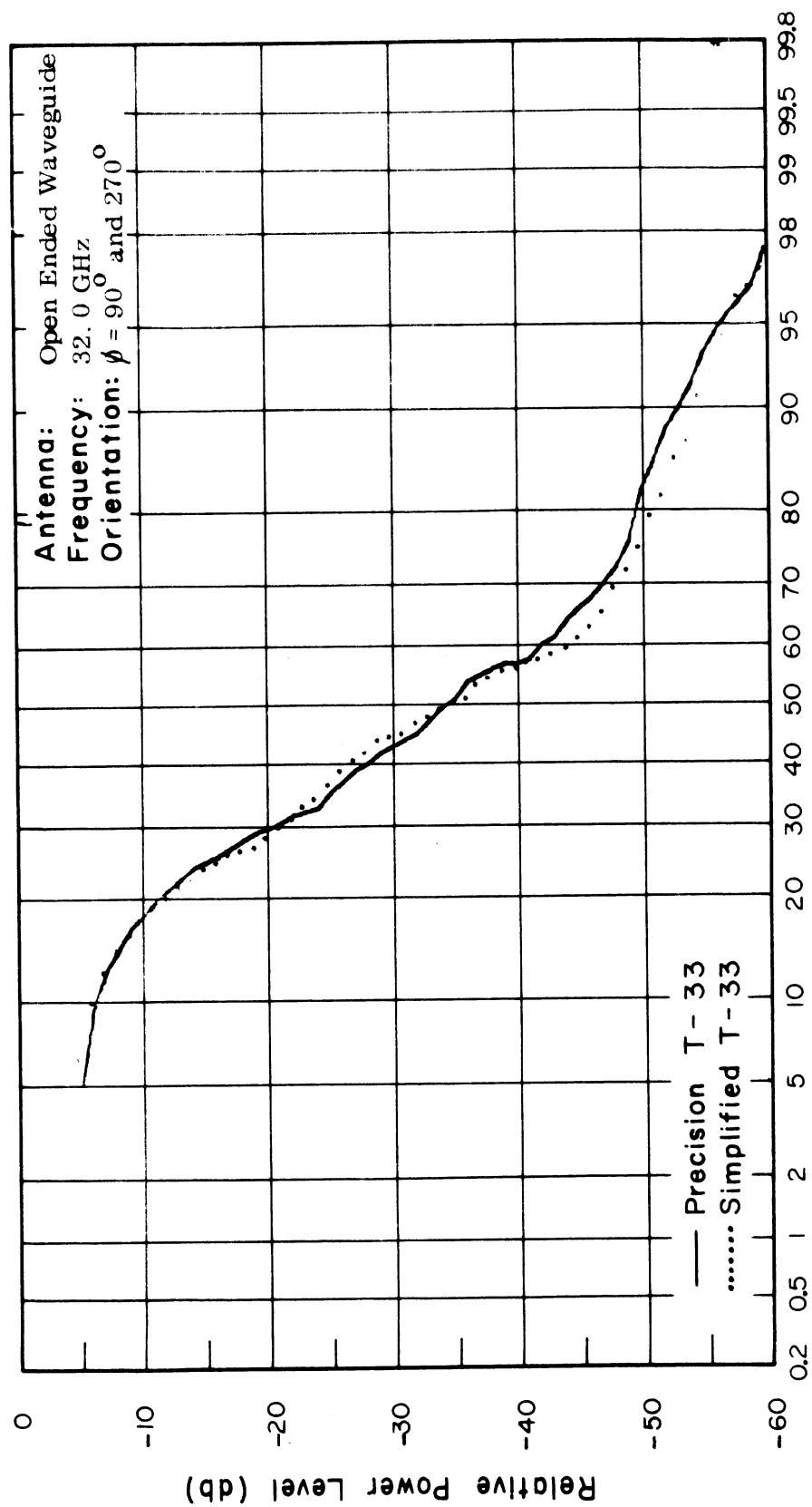
Fig. 26.   Cumulative Gain Distributions of Precision and Simplified   Models.
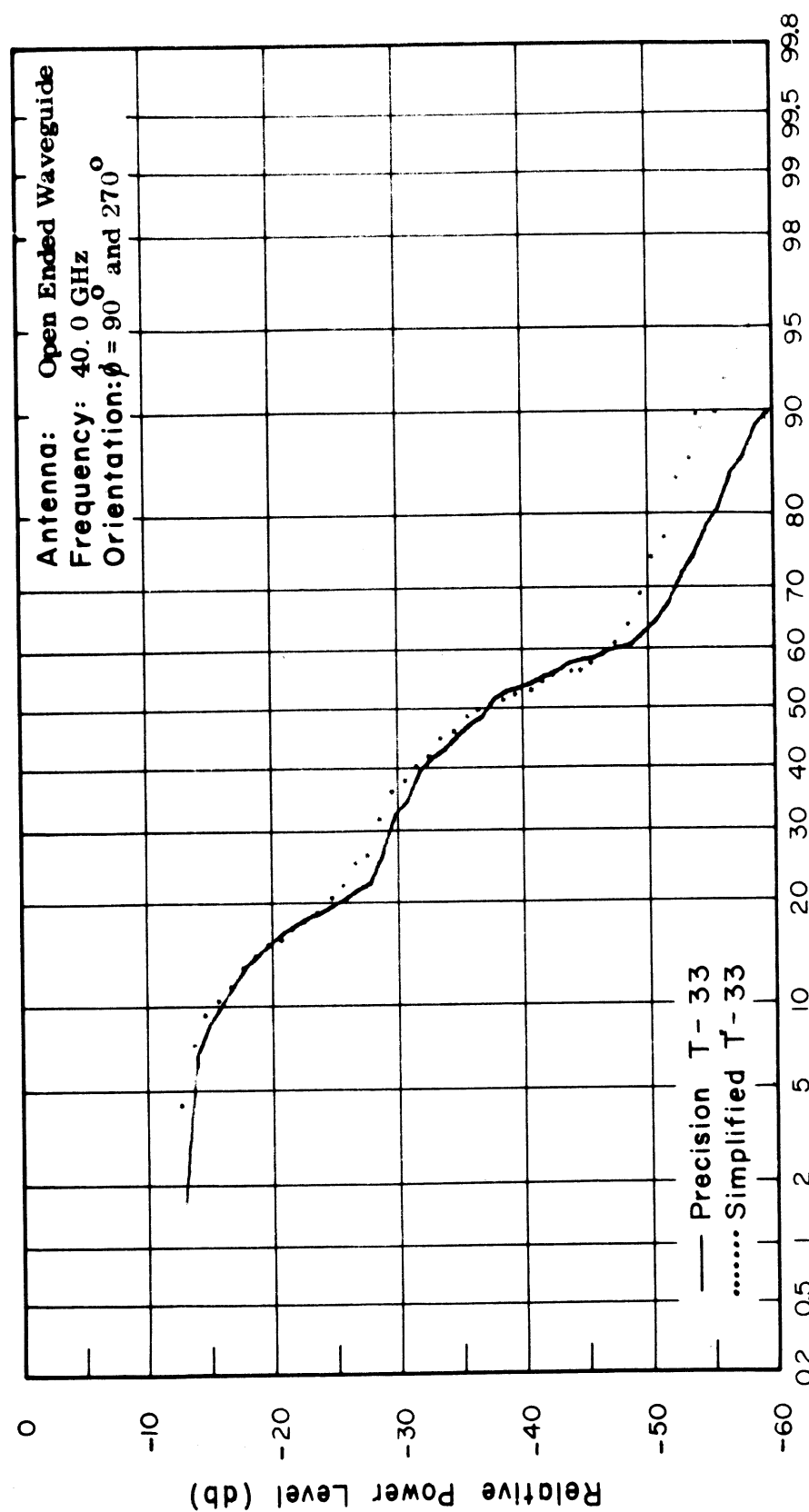
Fig. 27. Cumulative Gain Distributions of Precision and Simplified Models.

Antenna: Open Ended Waveguide
Frequency: 8.0 GHz
Orientation: $\phi = 0^\circ$ and 180°

—— Precision T-33
······ Simplified T-33

Probability That Relative Power Level Is Exceeded

Relative Power Level (db)
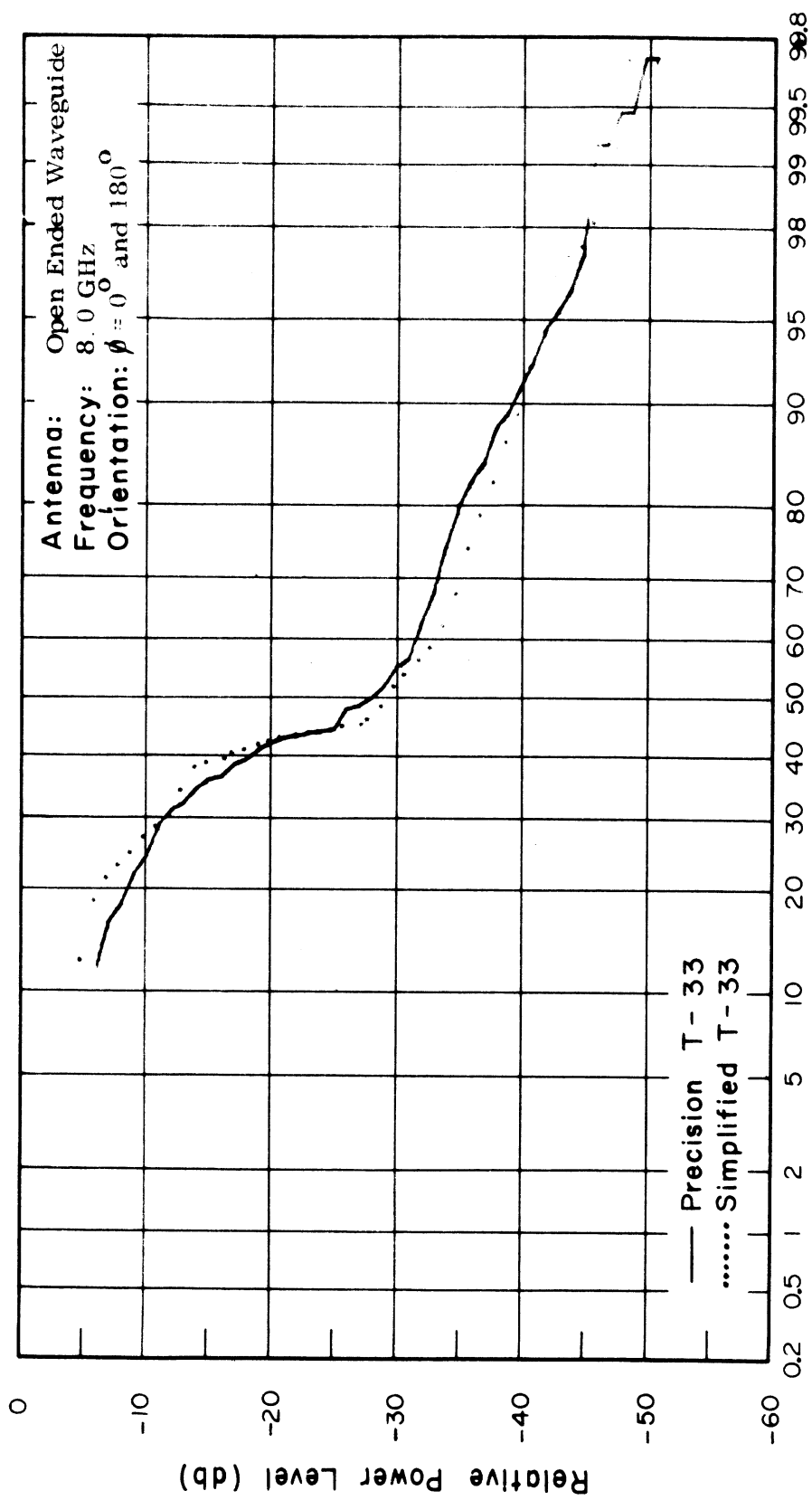
Fig. 28. Cumulative Gain Distributions of Precision and Simplified Models.

40
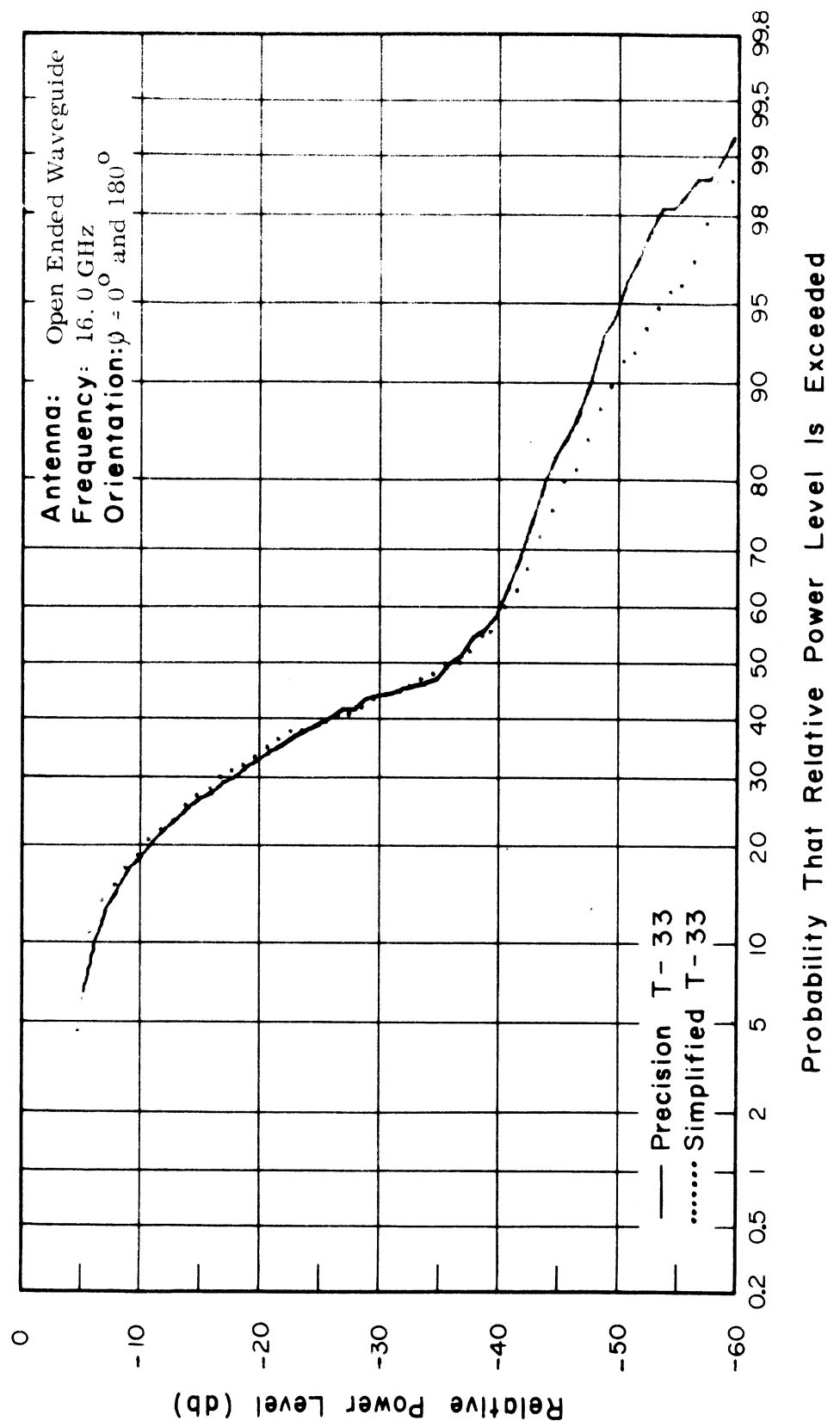
Fig. 29. Cumulative Gain Distributions of Precision and Simplified Models.
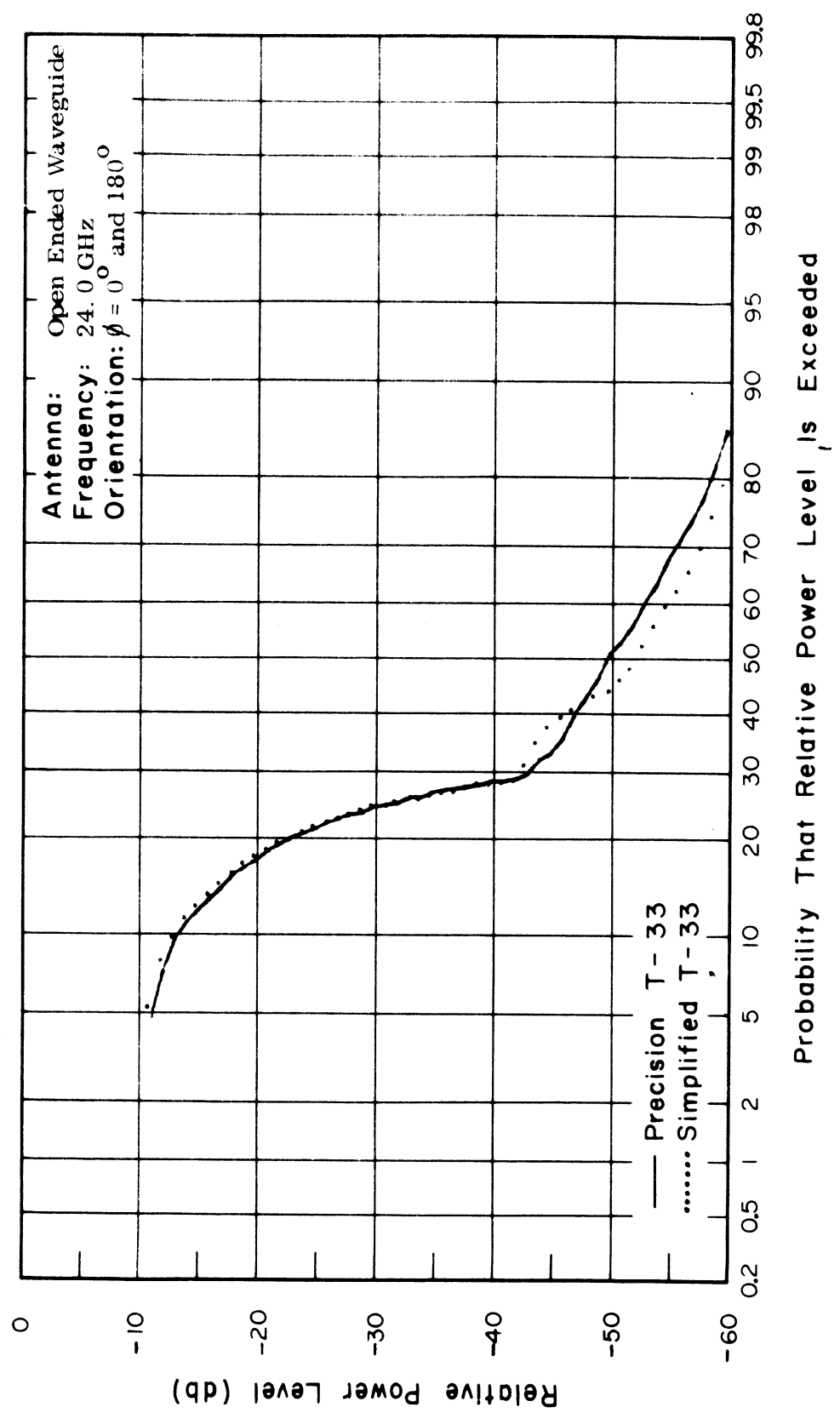
Fig. 30. Cumulative Gain Distributions of Precision and Simplified Models.
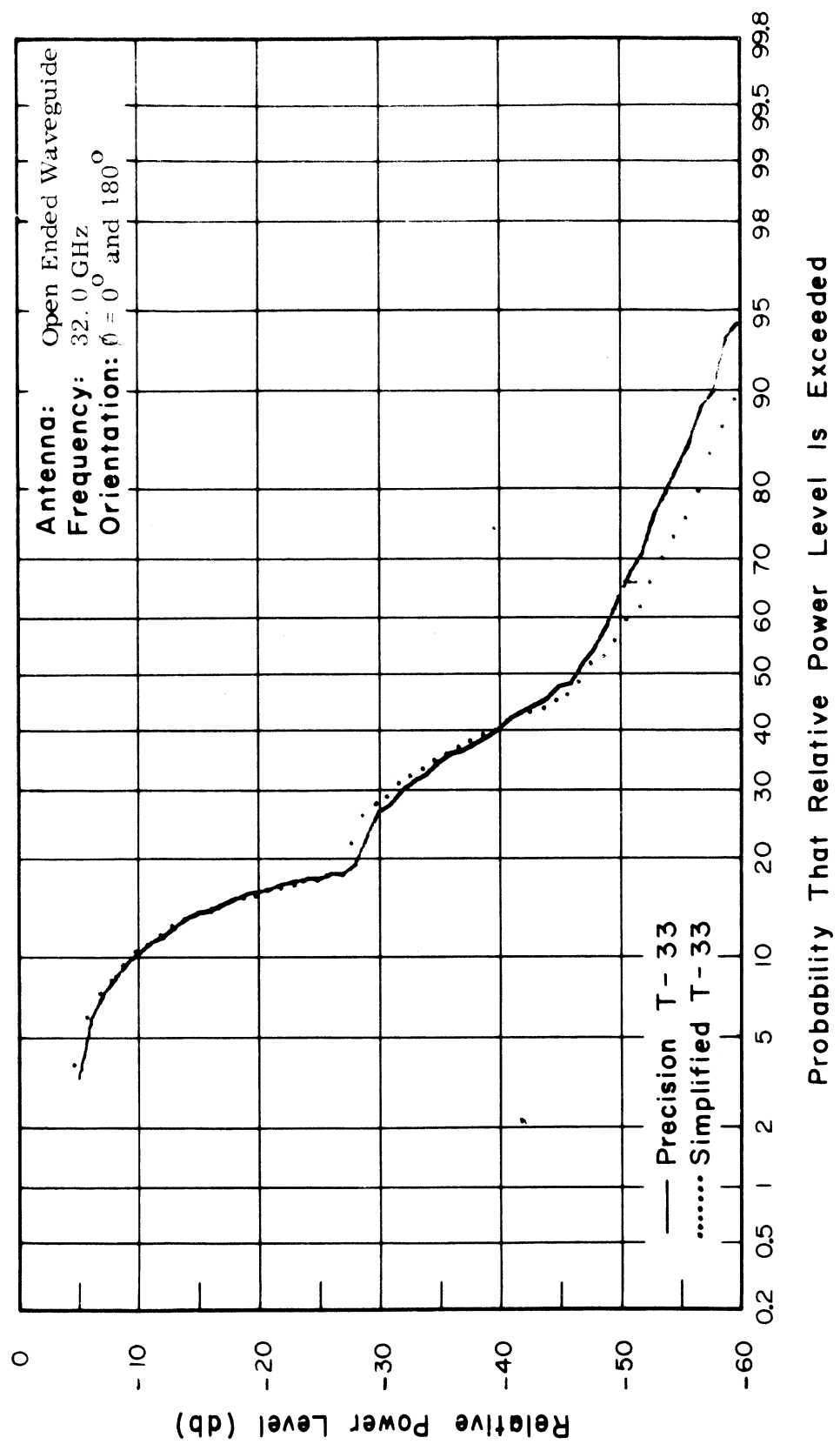
Fig. 31. Cumulative Gain Distributions of Precision and Simplified Models.
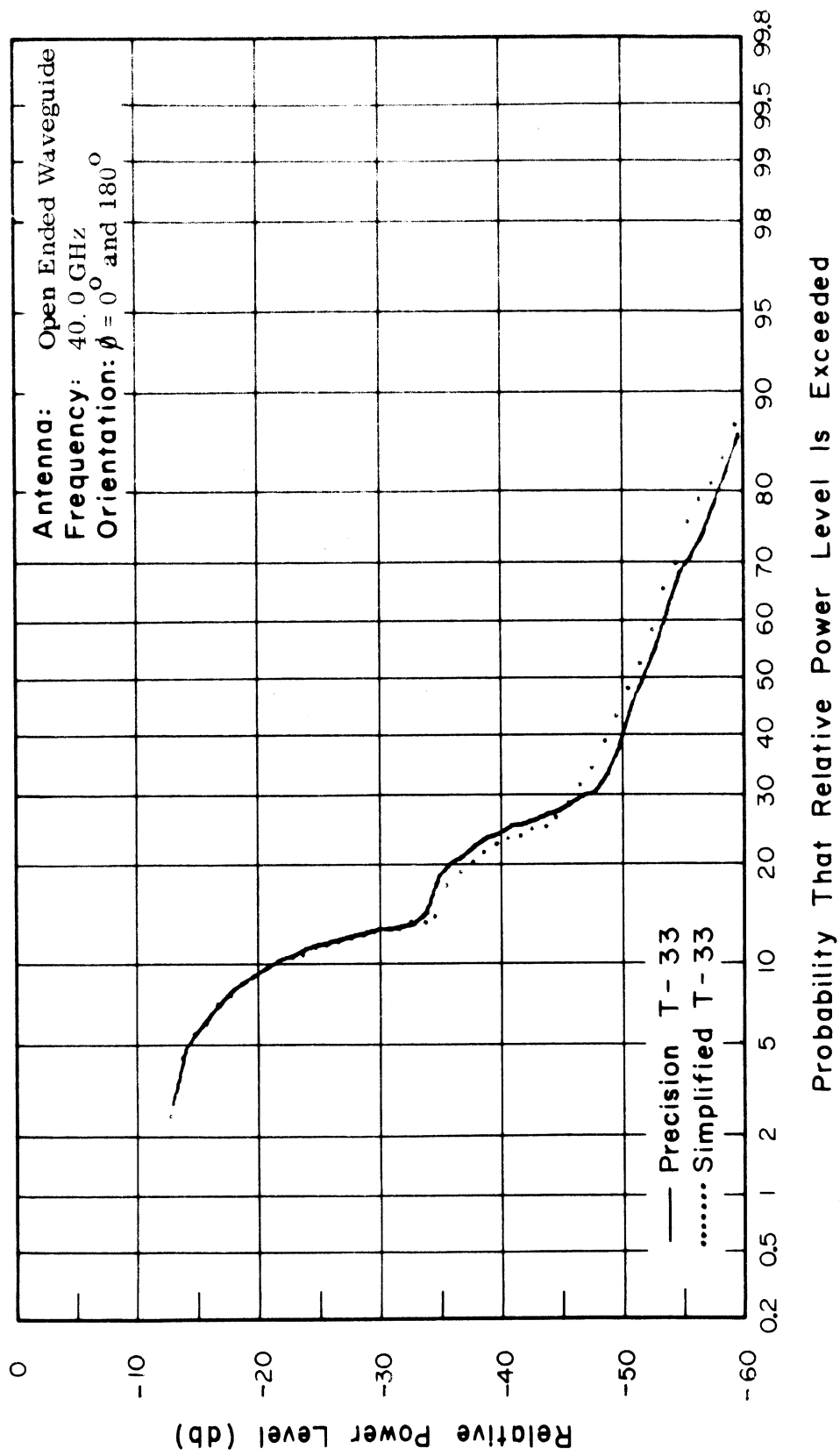
Fig. 32. Cumulative Gain Distributions of Precision and Simplified Models.

Fig. 34. $\lambda/4$ Monopole Antenna on Simplified Model T-33.
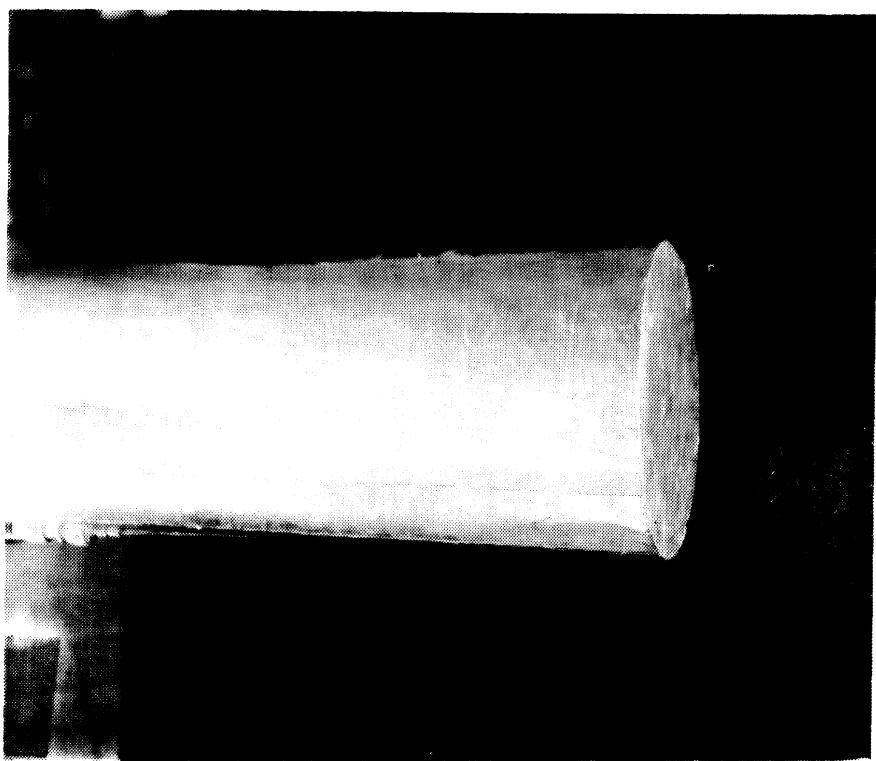
Fig. 33. $\lambda/4$ Monopole Antenna on Precision Model T-33.

45

FIG. 35

λ/4 Monopole
2.4 Gc
Precision T-33
Transverse Cut
∅=90° and 270°

RELATIVE POWER ONE WAY (db)

ANGLE Θ

CHART NO. 128-60   PRINTED IN U.S.A.   SCIENTIFIC-ATLANTA. INC.. ATLANTA. GEORGIA

46

FIG. 36

λ/4 Monopole
2.4 Gc
Simplified T-33
Transverse Cut
φ = 90° and 270°

RELATIVE POWER ONE WAY (db)

ANGLE θ

CHART NO. 128-60   PRINTED IN U.S.A.   SCIENTIFIC-ATLANTA. INC.. ATLANTA. GEORGIA

47
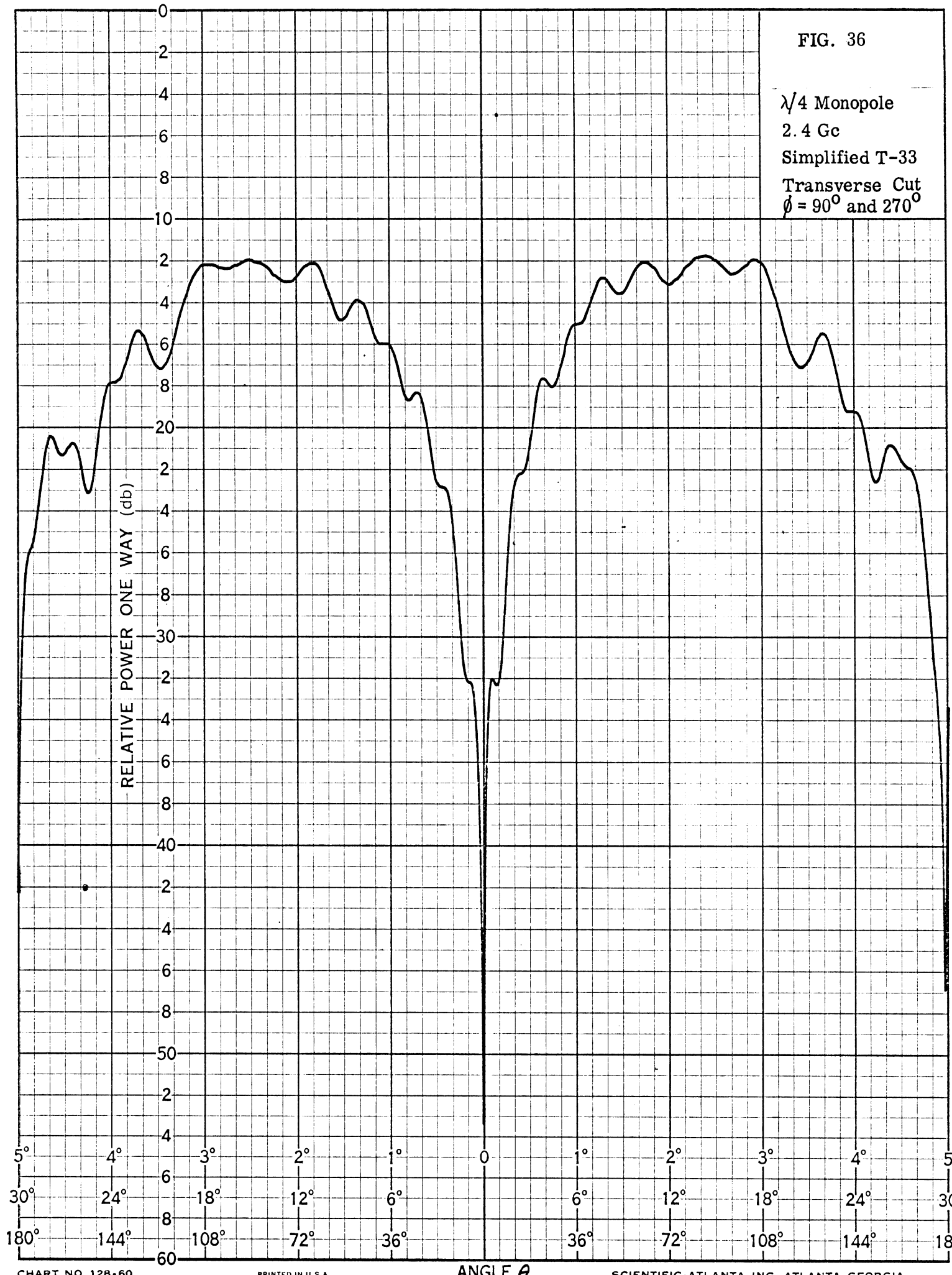
FIG. 37

λ/4 Monopole
2.4 Gc
Precision T-33
$\phi = 80^{\circ}$ and 260°

RELATIVE POWER ONE WAY (db)

ANGLE θ
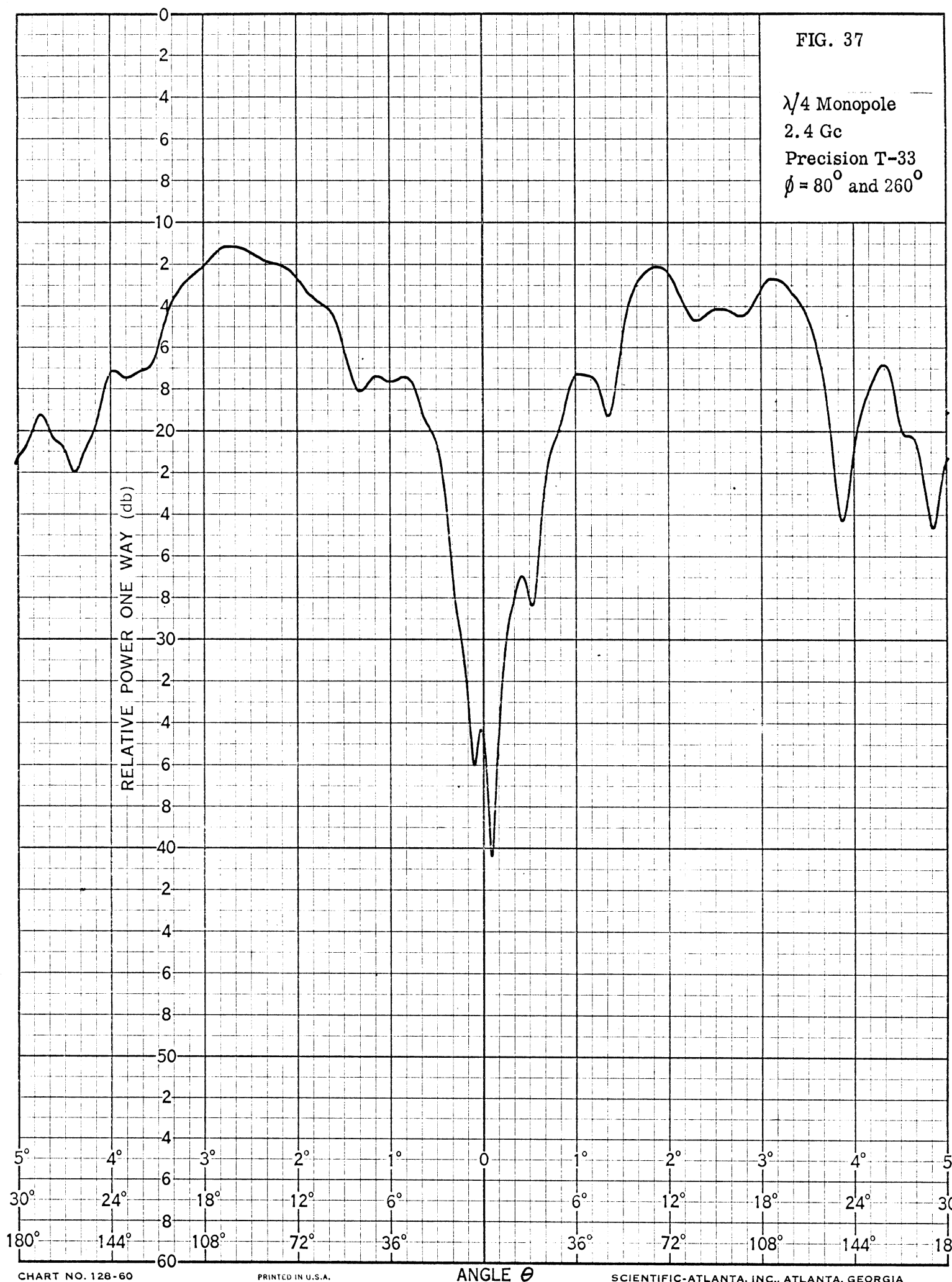
FIG. 38

λ/4 Monopole
2.4 Gc
Simplified T-33
∅ = 80° and 260°

RELATIVE POWER ONE WAY (db)

ANGLE θ

CHART NO. 128-60   PRINTED IN U.S.A.   SCIENTIFIC-ATLANTA. INC., ATLANTA. GEORGIA

FIG. 39

λ/4 Monopole
2.4 Gc
Precision T-33
$\phi = 70^{o}$ and 250°

RELATIVE POWER ONE WAY (db)

ANGLE θ

CHART NO. 128-60   PRINTED IN U.S.A.   SCIENTIFIC-ATLANTA, INC., ATLANTA, GEORGIA
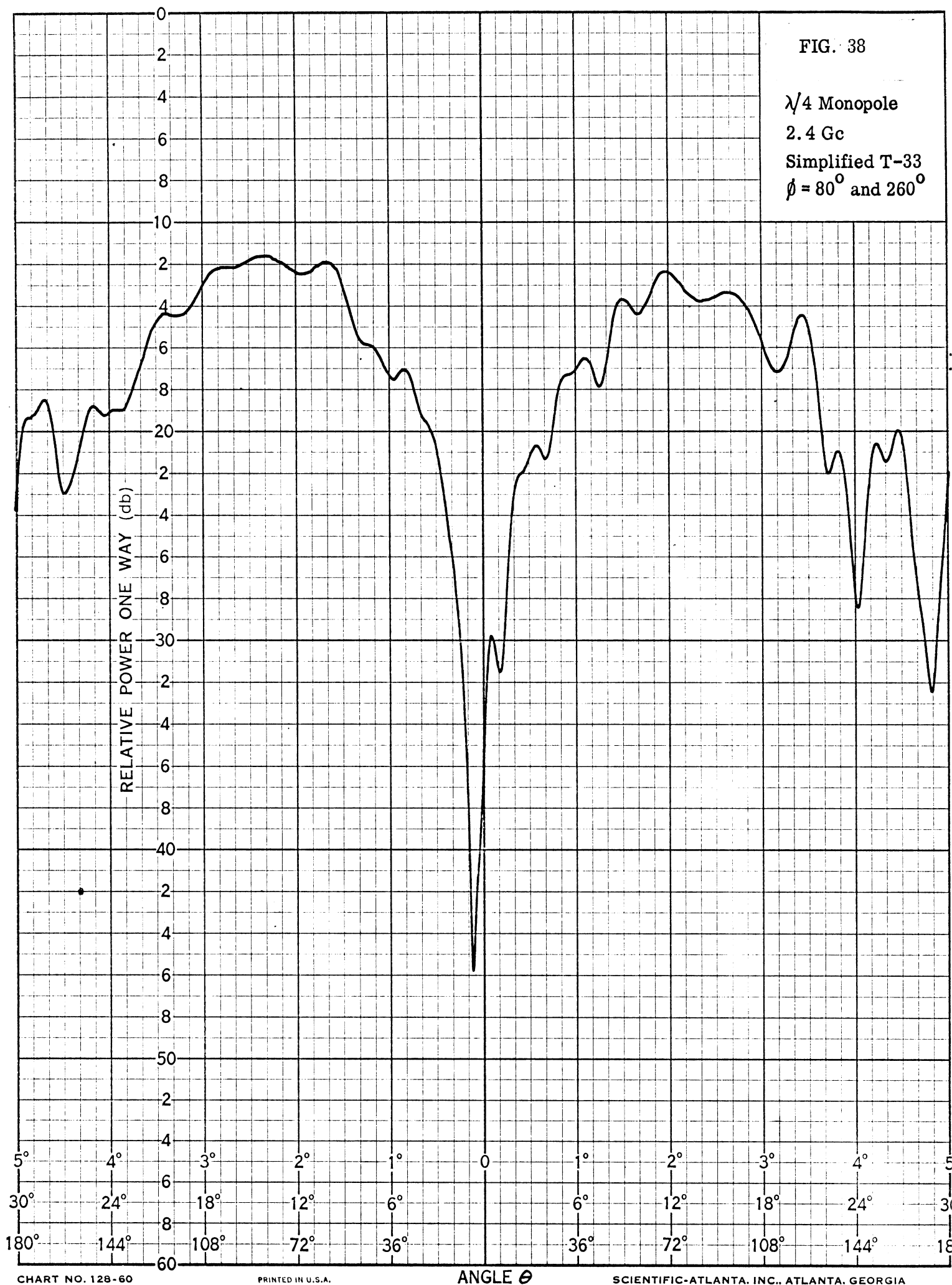
50
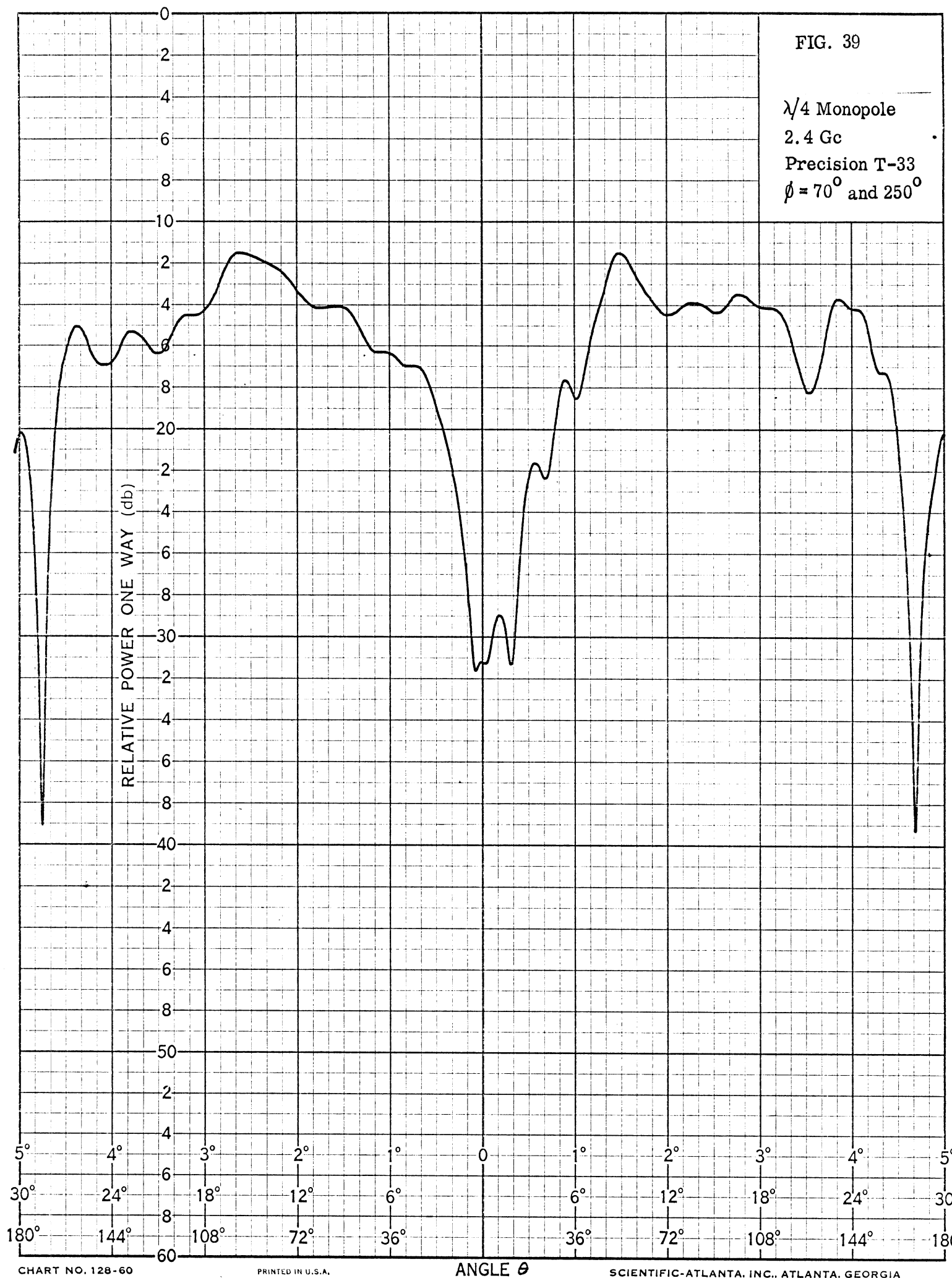
FIG. 40

$\lambda/4$ Monopole
2.4 Gc
Simplified T-33
$\phi = 70°$ and $250°$

RELATIVE POWER ONE WAY (db)

ANGLE θ
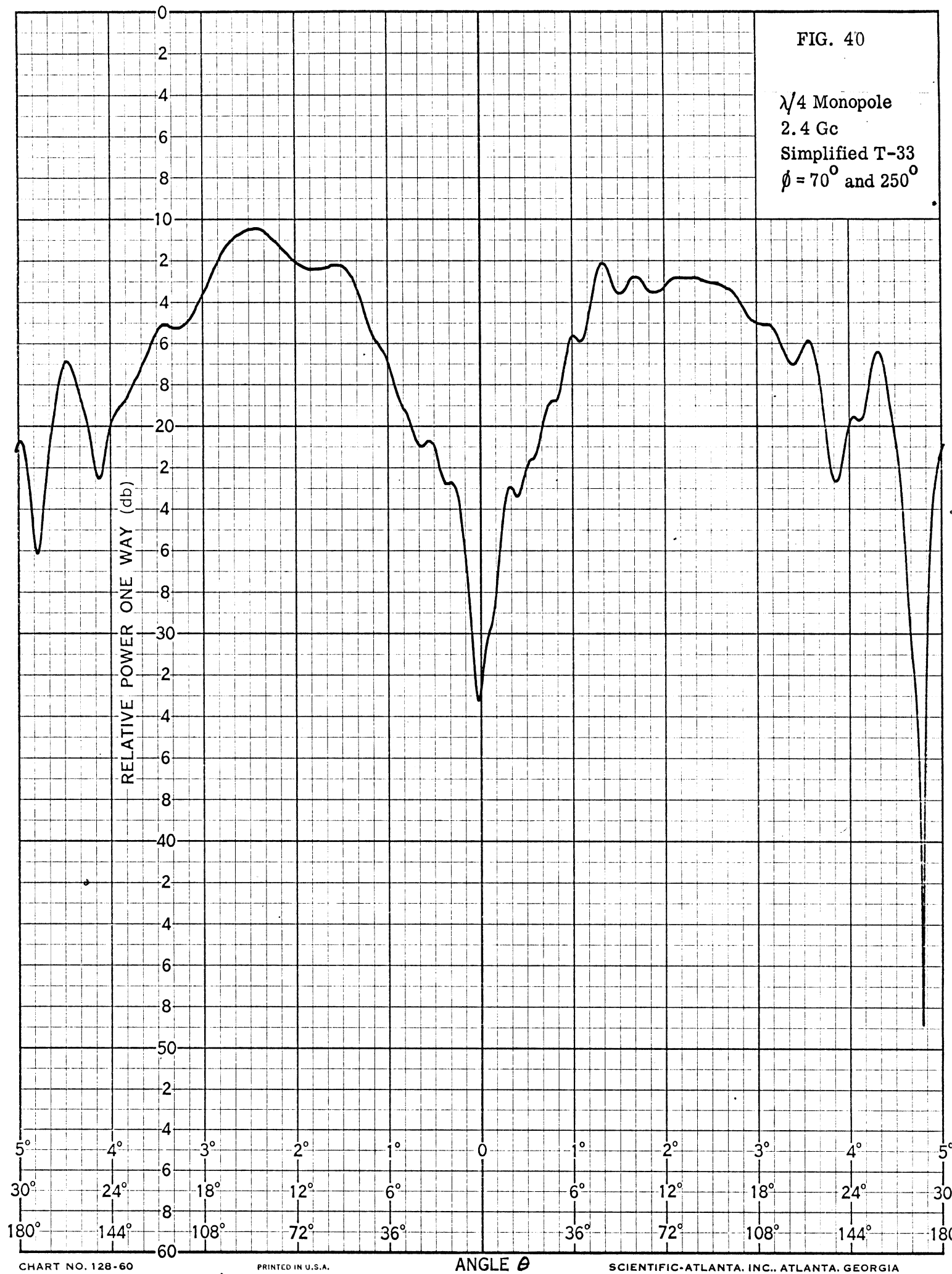
FIG. 41

λ/4 Monopole
2.4 Gc
Precision T-33
∅ = 60° and 240°

RELATIVE POWER ONE WAY (db)

ANGLE θ

FIG. 42

λ/4 Monopole
2.4 Gc
Simplified T-33
φ = 60° and 240°

RELATIVE POWER ONE WAY (db)

ANGLE θ

CHART NO. 128-60   PRINTED IN U.S.A.   SCIENTIFIC-ATLANTA, INC., ATLANTA, GEORGIA
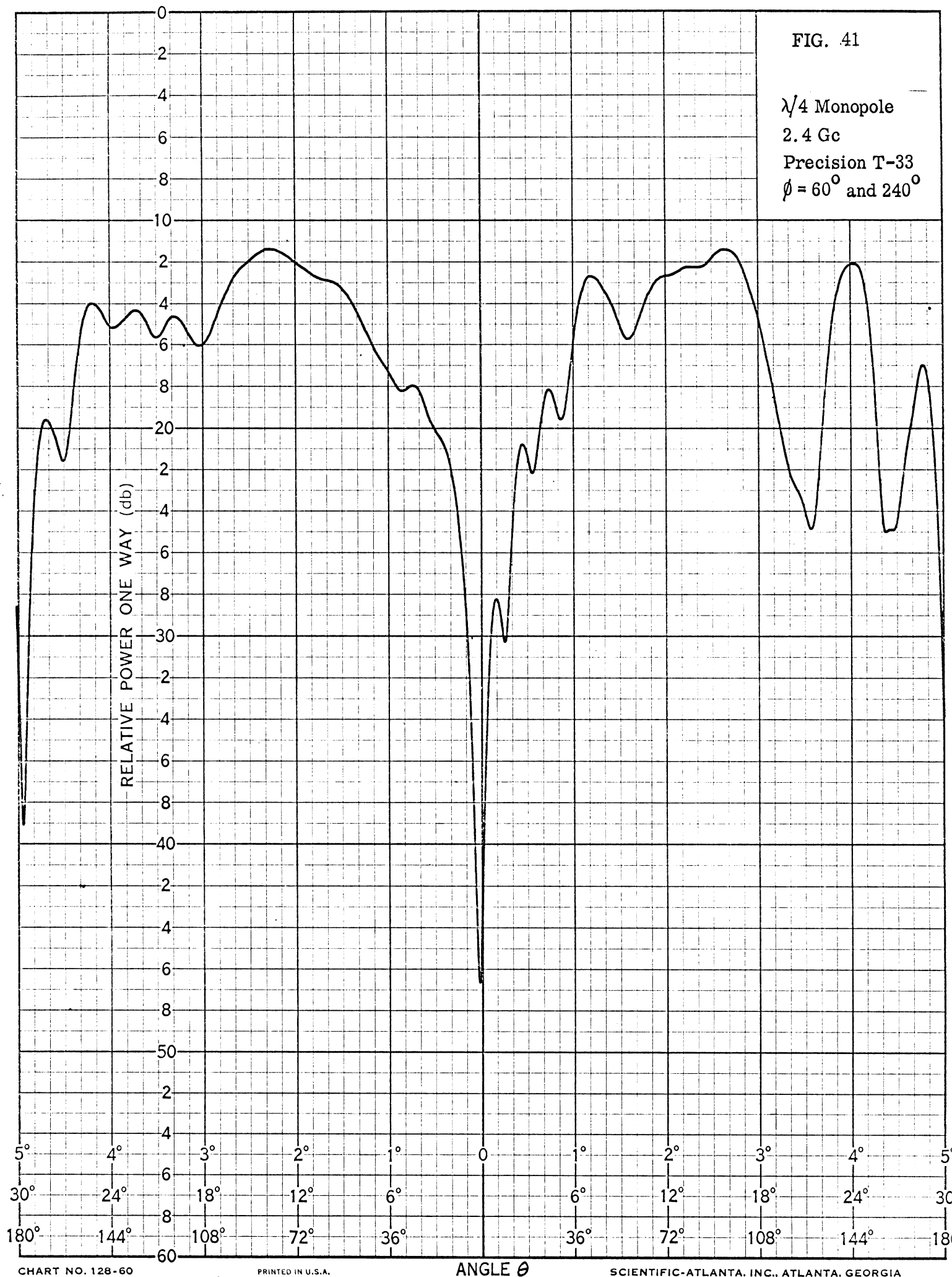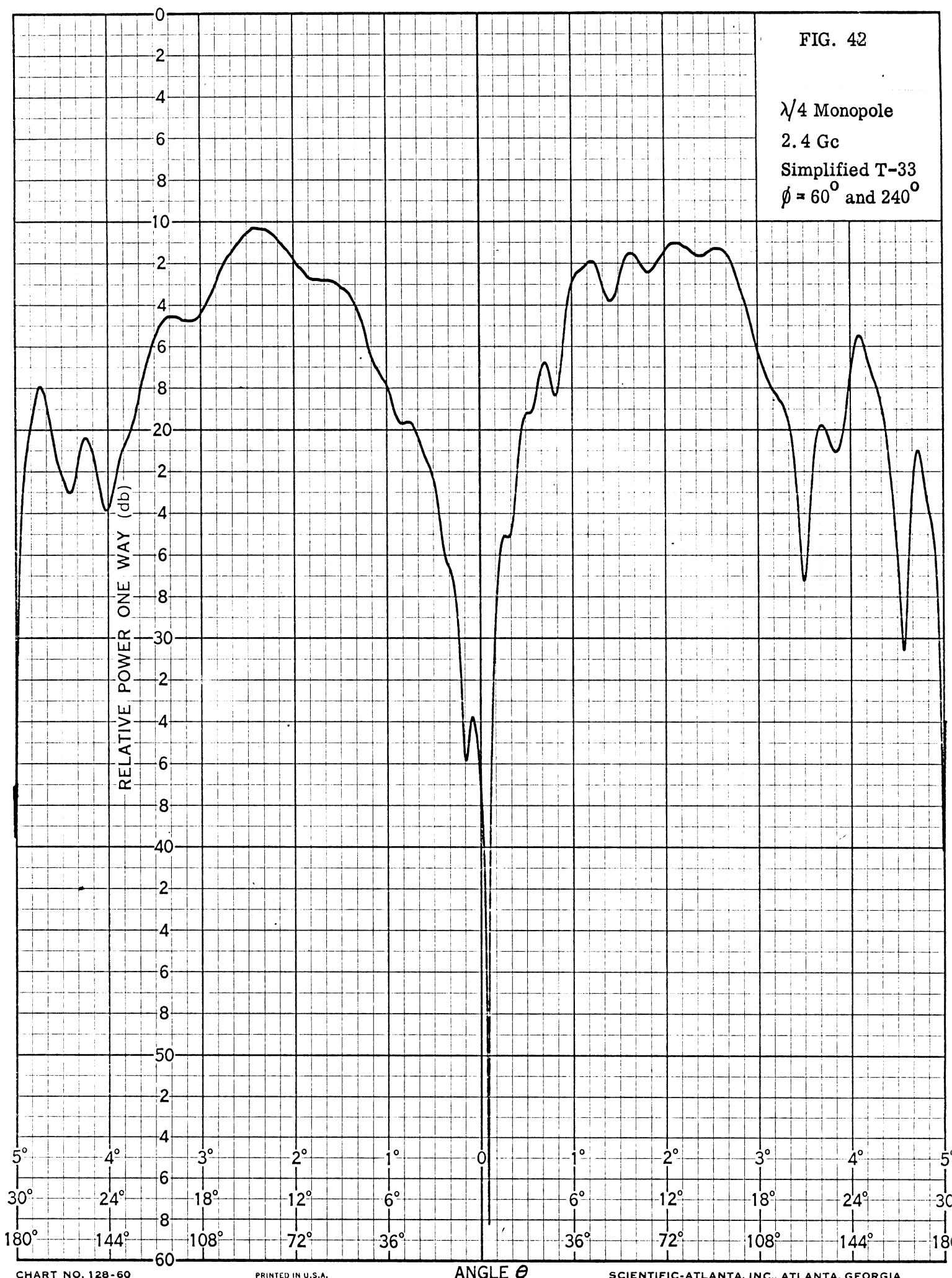
FIG. 43

λ/4 Monopole

2.4 Gc

Precision T-33

$\phi = 50^{\circ}$ and 230°

RELATIVE POWER ONE WAY (db)

ANGLE θ

CHART NO. 128-60   PRINTED IN U.S.A.   SCIENTIFIC-ATLANTA. INC.. ATLANTA. GEORGIA
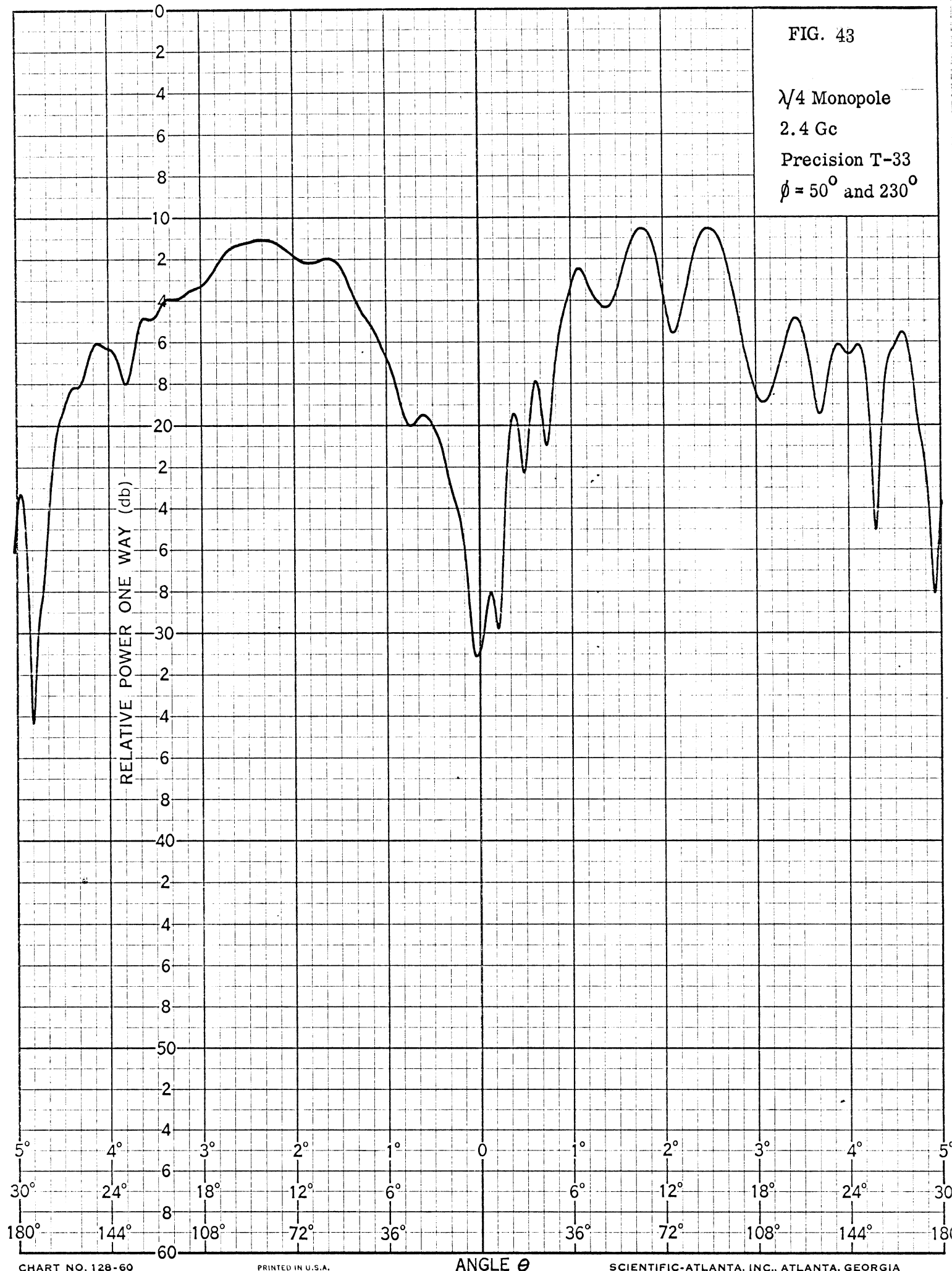
FIG. 44

λ/4 Monopole
2.4 Gc
Simplified T-33
$\phi = 50^{\circ}$ and 230°
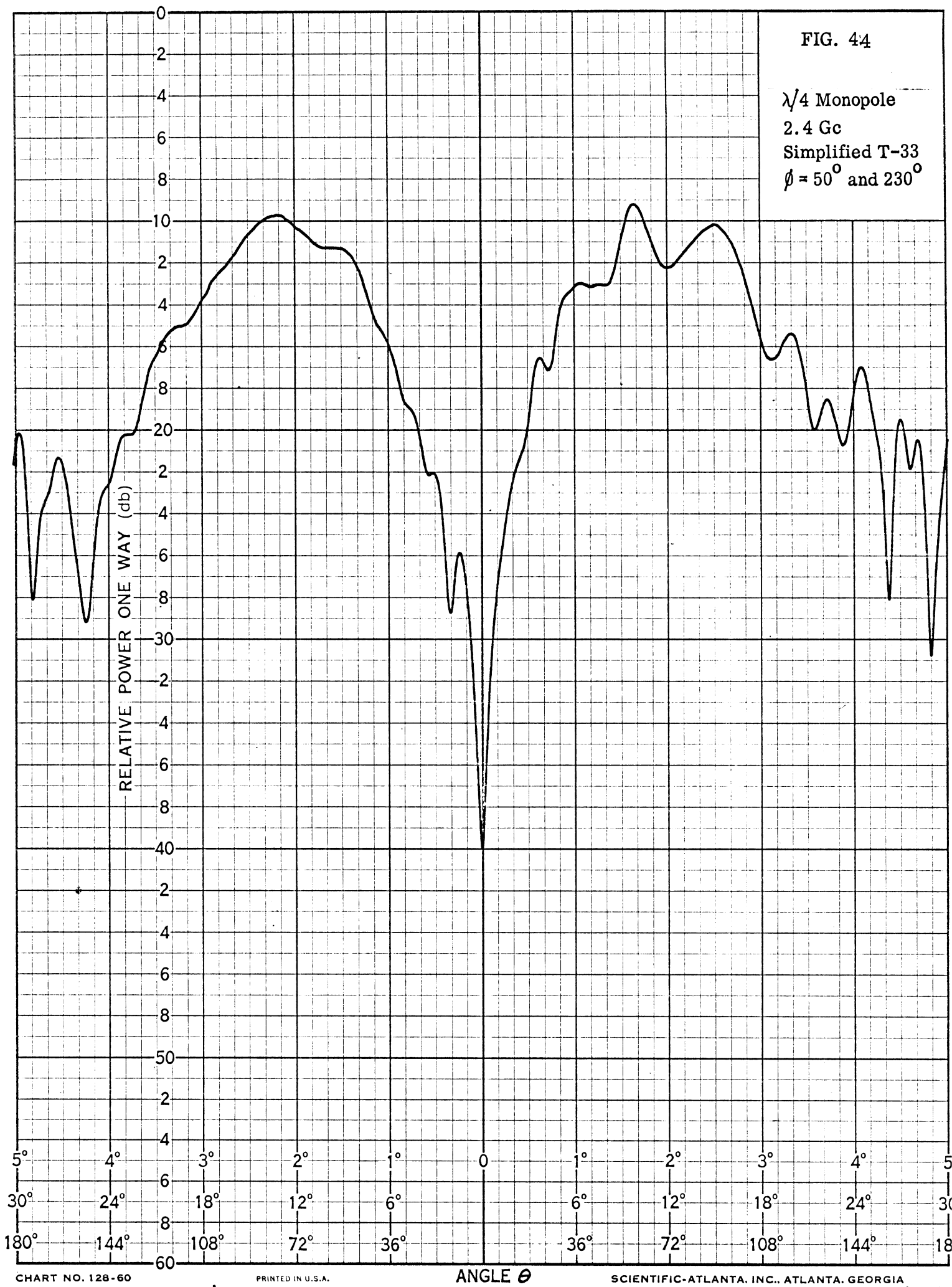
RELATIVE POWER ONE WAY (db)

ANGLE θ

FIG. 45

λ/4 Monopole
2.4 Gc
Precision T-33
ϕ=40° and 220°

RELATIVE POWER ONE WAY (db)

ANGLE θ

CHART NO. 128-60   PRINTED IN U.S.A.   SCIENTIFIC-ATLANTA. INC., ATLANTA. GEORGIA

56

FIG. 46

λ/4 Monopole
2.4 Gc
Simplified T-33
ϕ=40° and 220°

RELATIVE POWER ONE WAY (db)
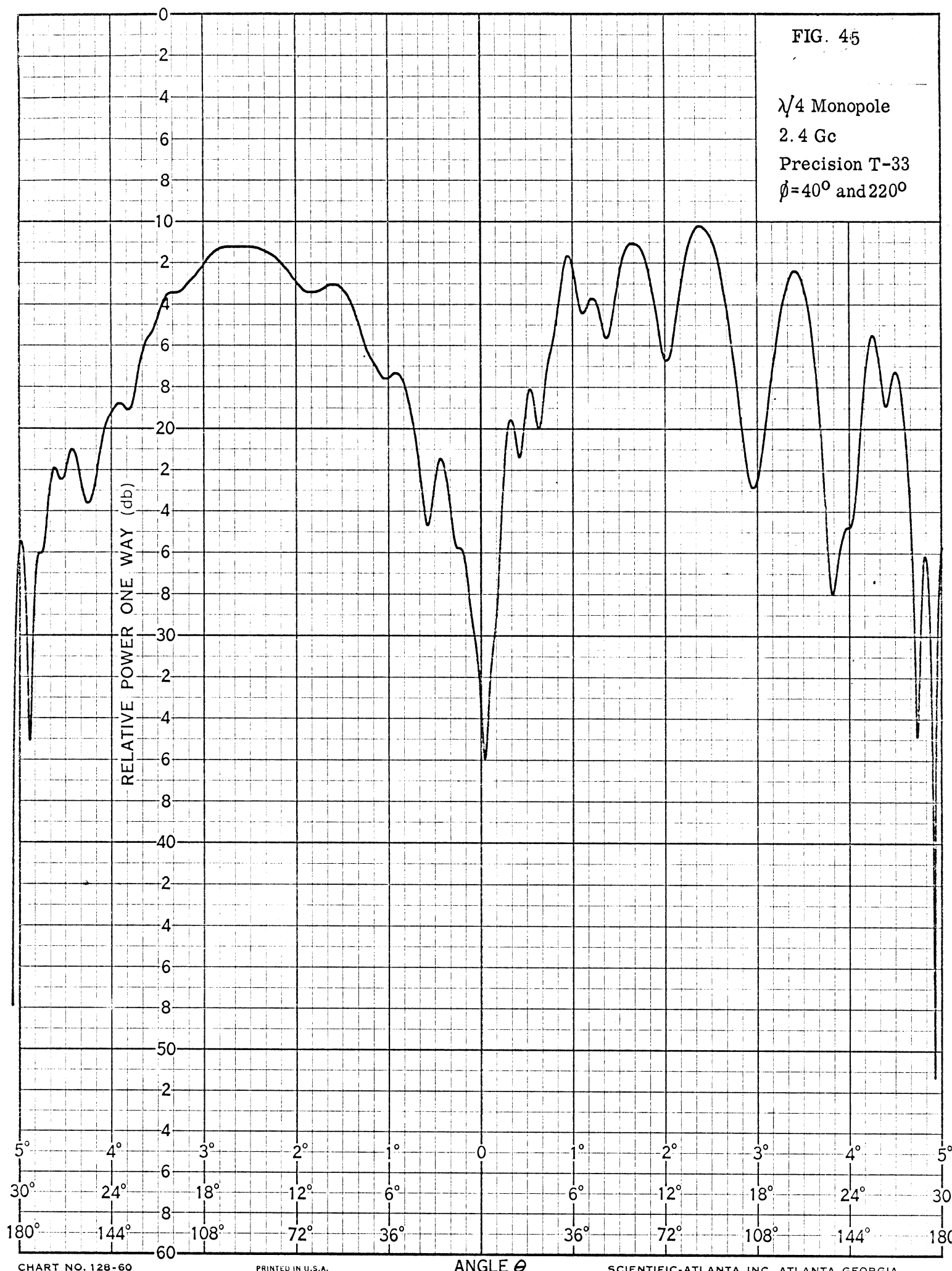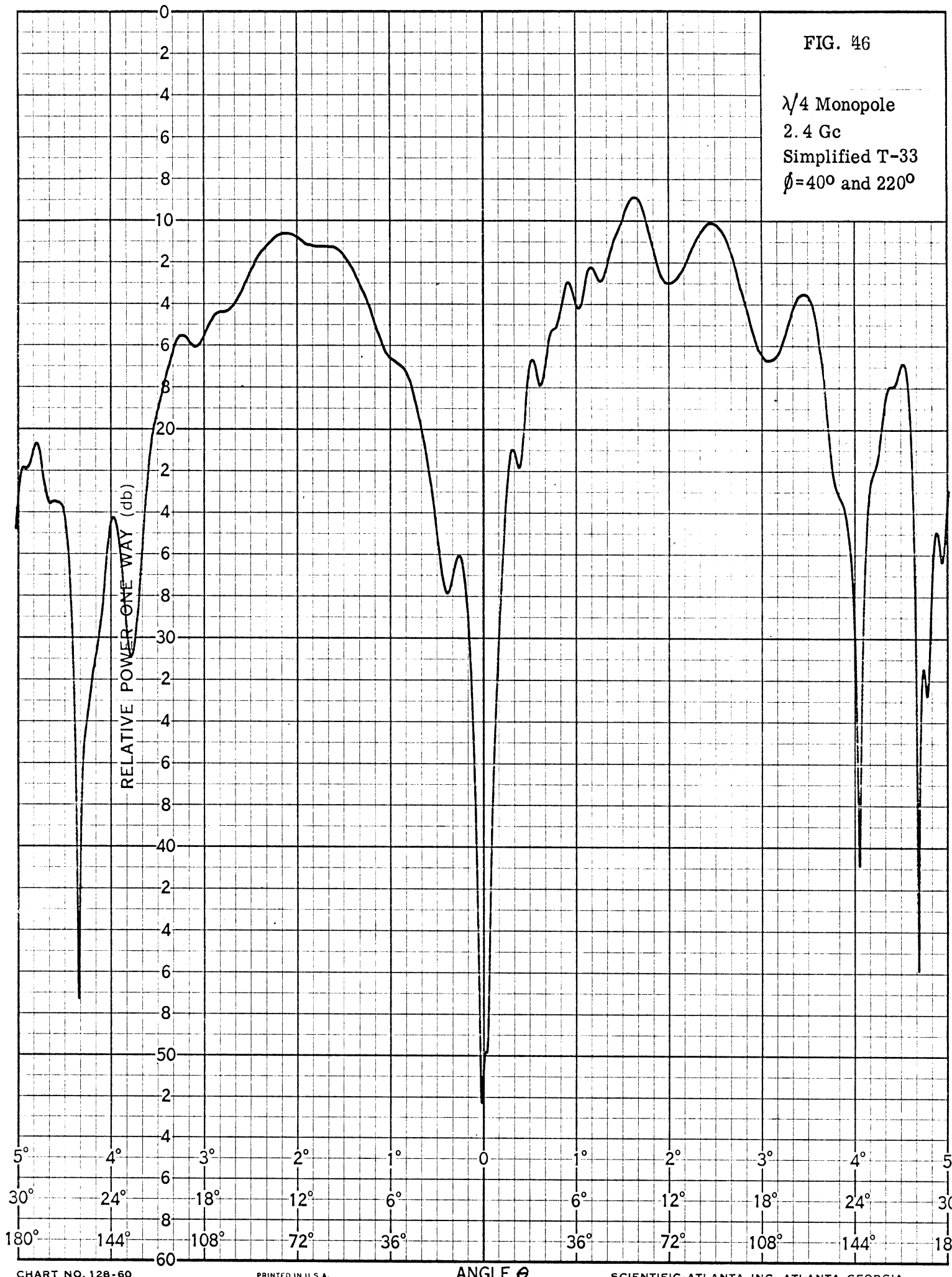
ANGLE ϴ

FIG. 47

λ/4 Monopole
2.4 Gc
Precision T-33
$\phi = 30°$ and $210°$

RELATIVE POWER ONE WAY (db)
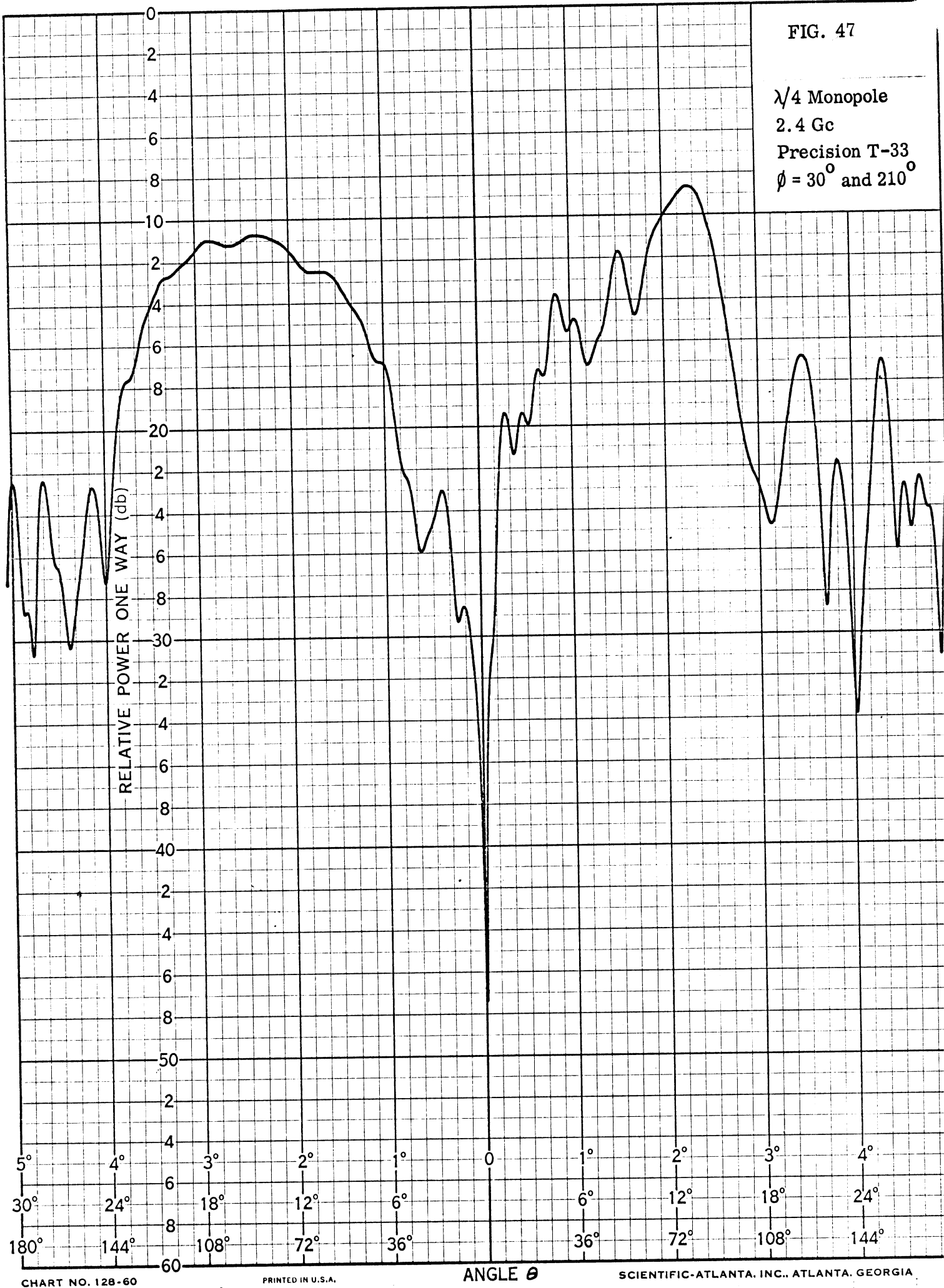
ANGLE θ

FIG. 48

λ/4 Monopole
2.4 Gc
Simplified T-33
∅ = 30° and 210°
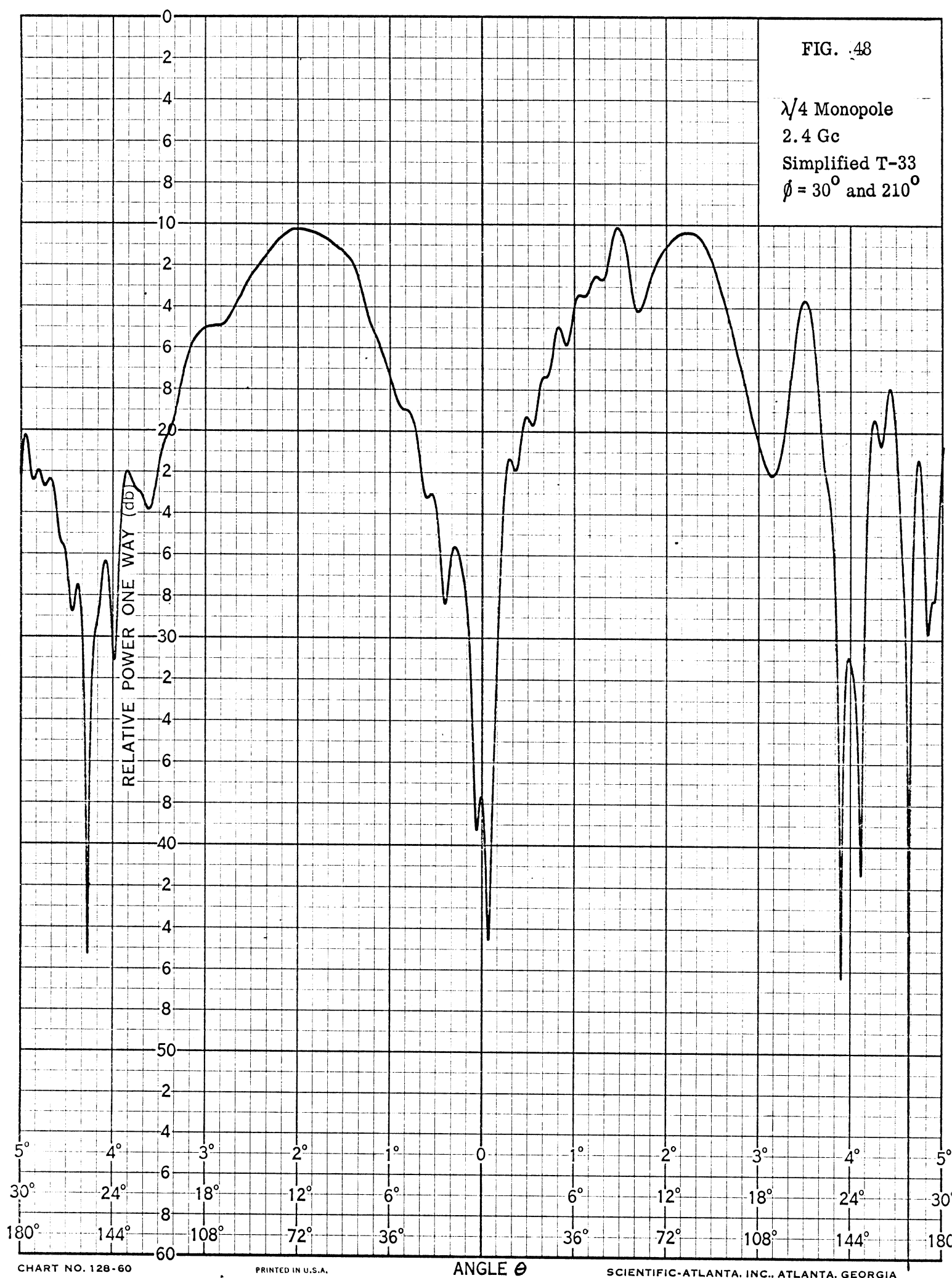
RELATIVE POWER ONE WAY (db)

ANGLE θ

FIG. 49

$\lambda/4$ Monopole
2.4 Gc
Precision T-33
$\phi = 20^{\circ}$ and 200°

RELATIVE POWER ONE WAY (db)

ANGLE θ

CHART NO. 128-60   PRINTED IN U.S.A.   SCIENTIFIC-ATLANTA, INC., ATLANTA, GEORGIA

60
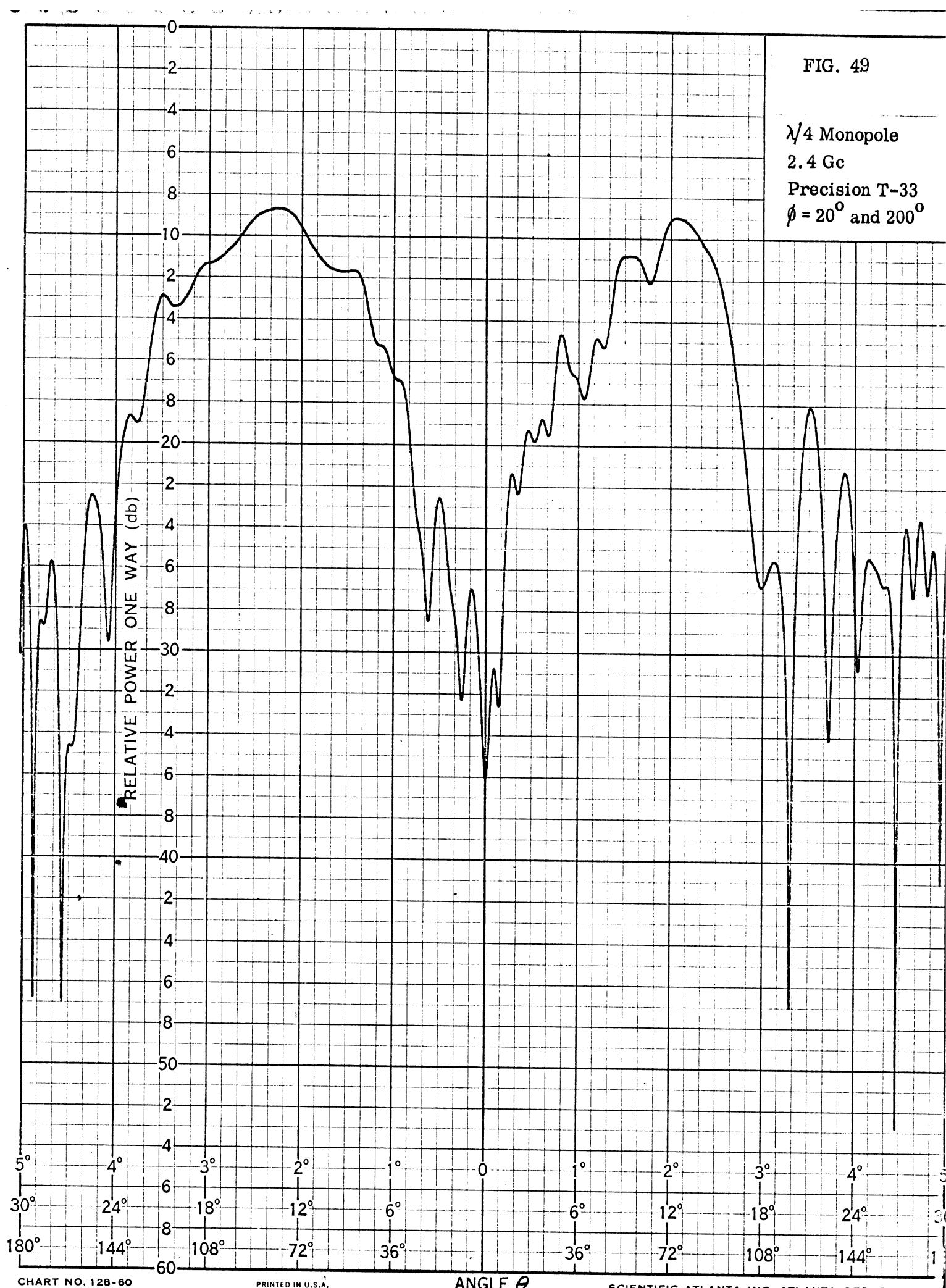
FIG. 50

λ/4 Monopole
2.4 Gc
Simplified T-33
$\phi = 20^{\circ}$ and 200°
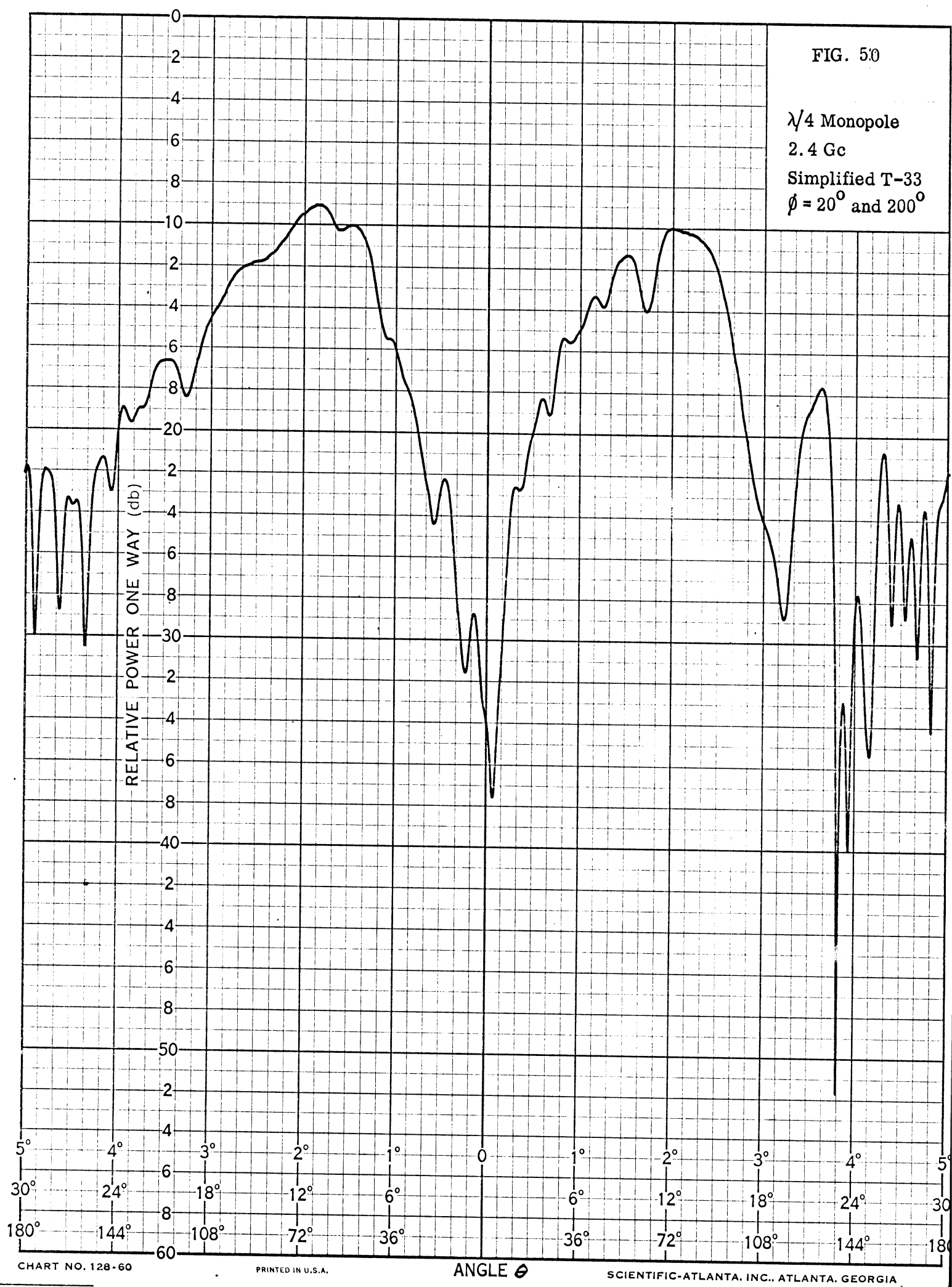
RELATIVE POWER ONE WAY (db)

ANGLE θ

CHART NO. 128-60   PRINTED IN U.S.A.   SCIENTIFIC-ATLANTA, INC., ATLANTA, GEORGIA

61

FIG. 51

λ/4 Monopole
2.4 Gc
Precision T-33
ϕ = 10° and 190°

RELATIVE POWER ONE WAY (db)

ANGLE θ

CHART NO. 128-60   PRINTED IN U.S.A.   SCIENTIFIC-ATLANTA. INC.. ATLANTA. GEORGIA

62

FIG. 52

λ/4 Monopole
2.4 Gc
Simplified T-33
ϕ = 10° and 190°

CHART NO. 128-60   PRINTED IN U.S.A.   ANGLE θ   SCIENTIFIC-ATLANTA. INC.. ATLANTA. GEORGIA

RELATIVE POWER ONE WAY (db)
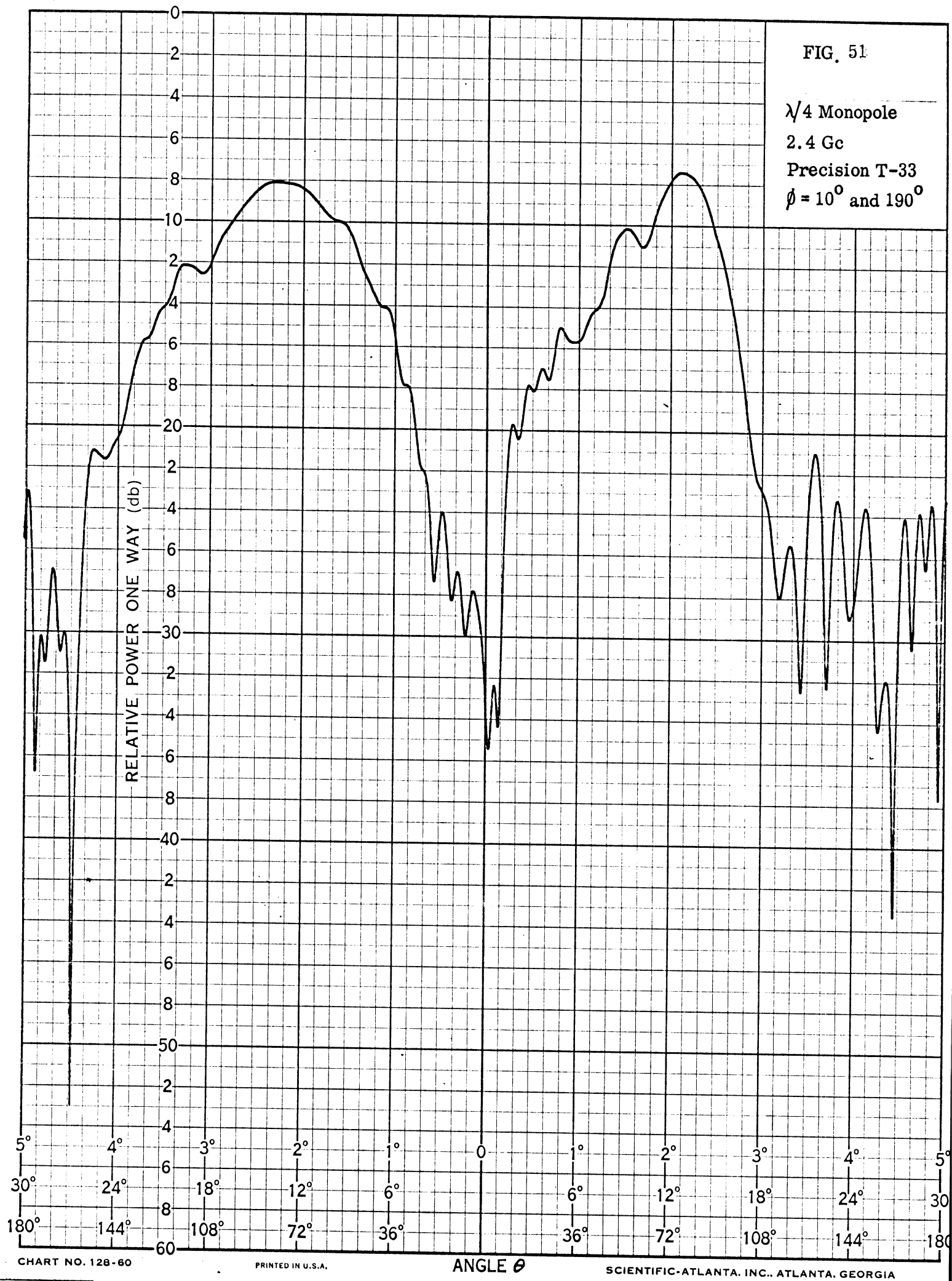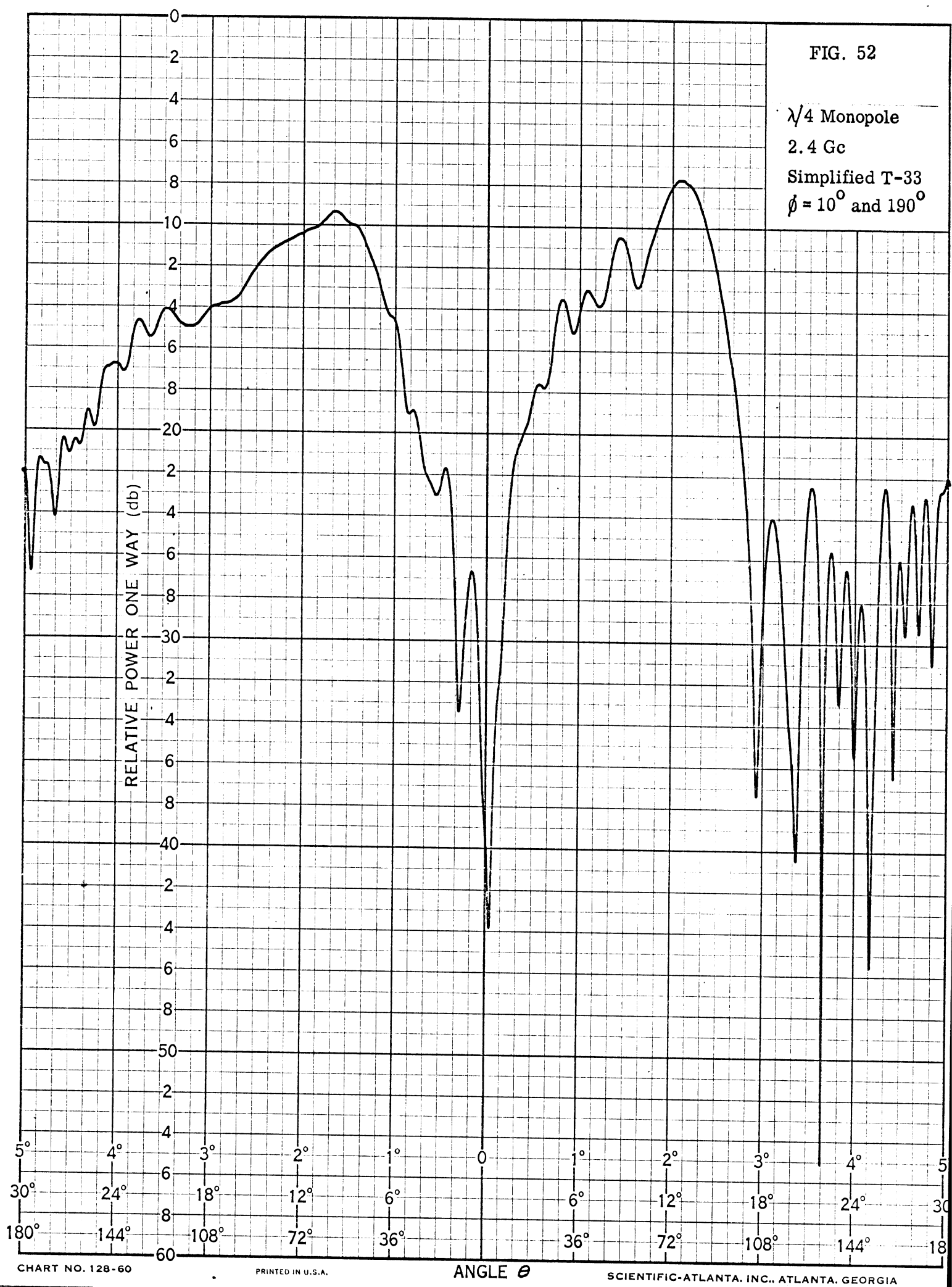
FIG 53

$\lambda/4$ Monopole
2.4 Gc
Precision T-33
Longitudinal Cut
$\phi = 0°$ and $180°$

RELATIVE POWER ONE WAY (db)

ANGLE θ

PRINTED IN U.S.A.

SCIENTIFIC-ATLANTA. INC.. ATLANTA. GEORGIA

FIG. 54

$\lambda/4$ Monopole
2.4 Gc
Simplified T-33
Longitudinal Cut
$\phi = 0°$ and $180°$

RELATIVE POWER ONE WAY (db)

ANGLE θ

CHART NO. 128-60   PRINTED IN U.S.A.   SCIENTIFIC-ATLANTA, INC., ATLANTA, GEORGIA
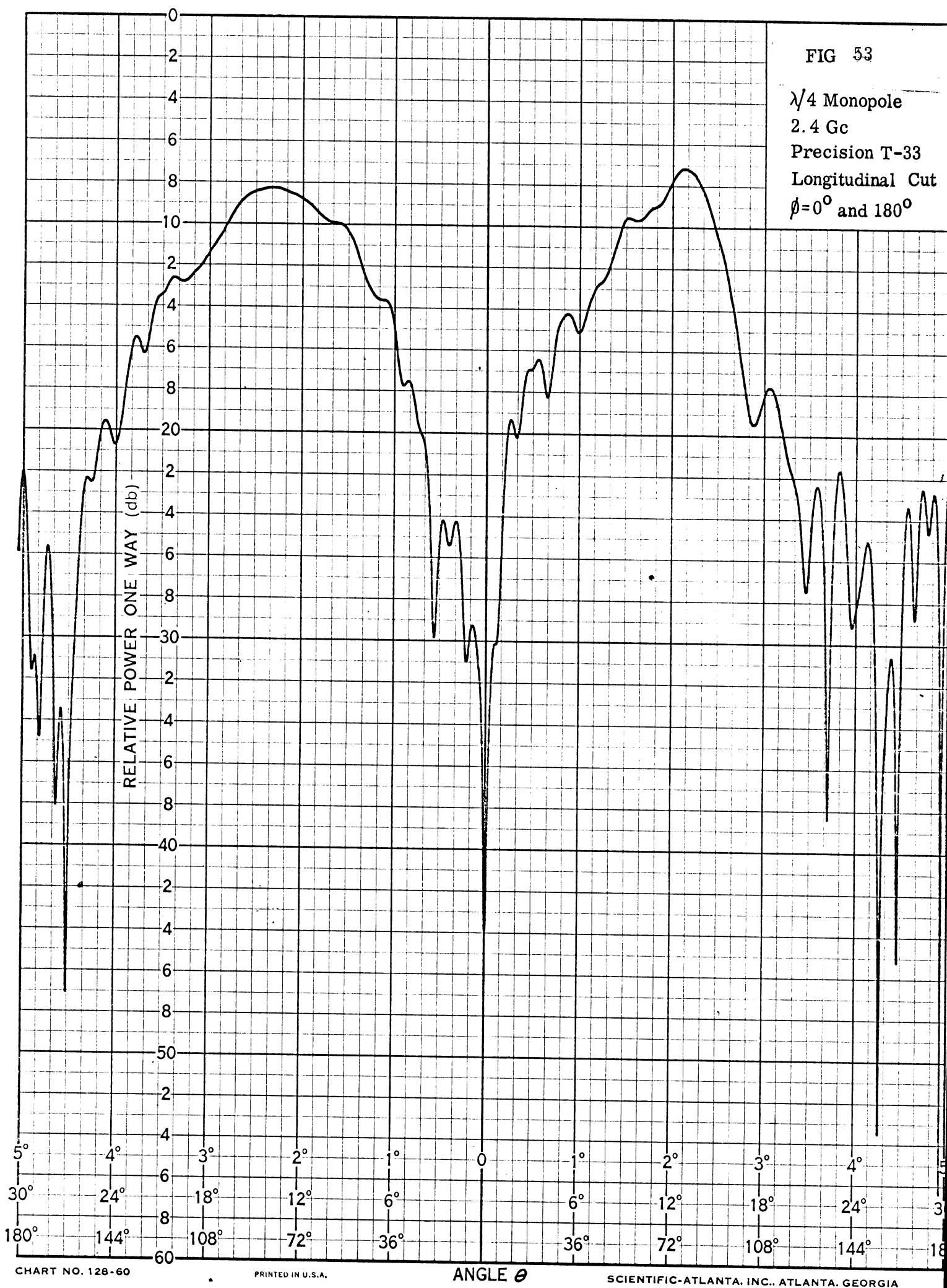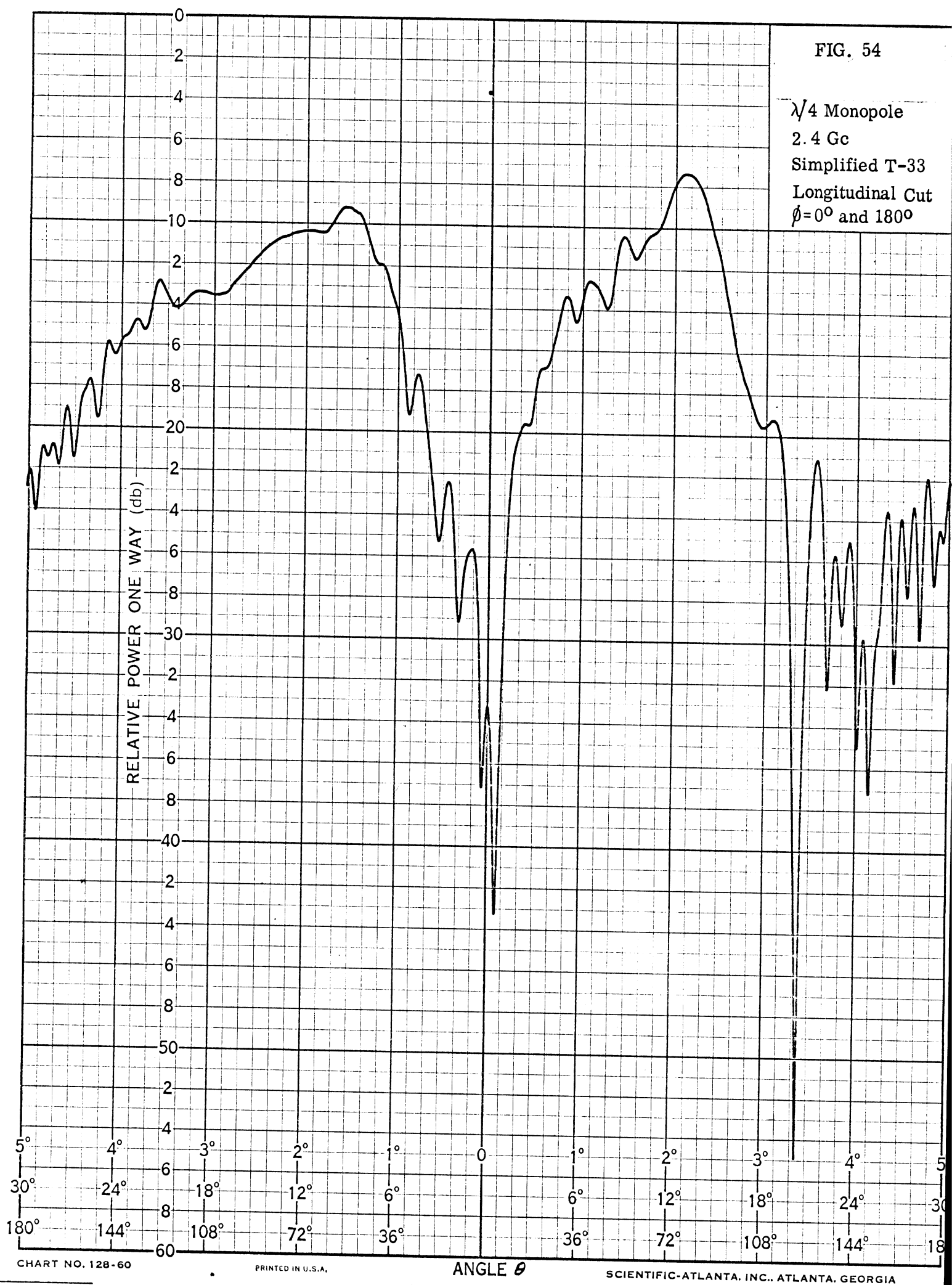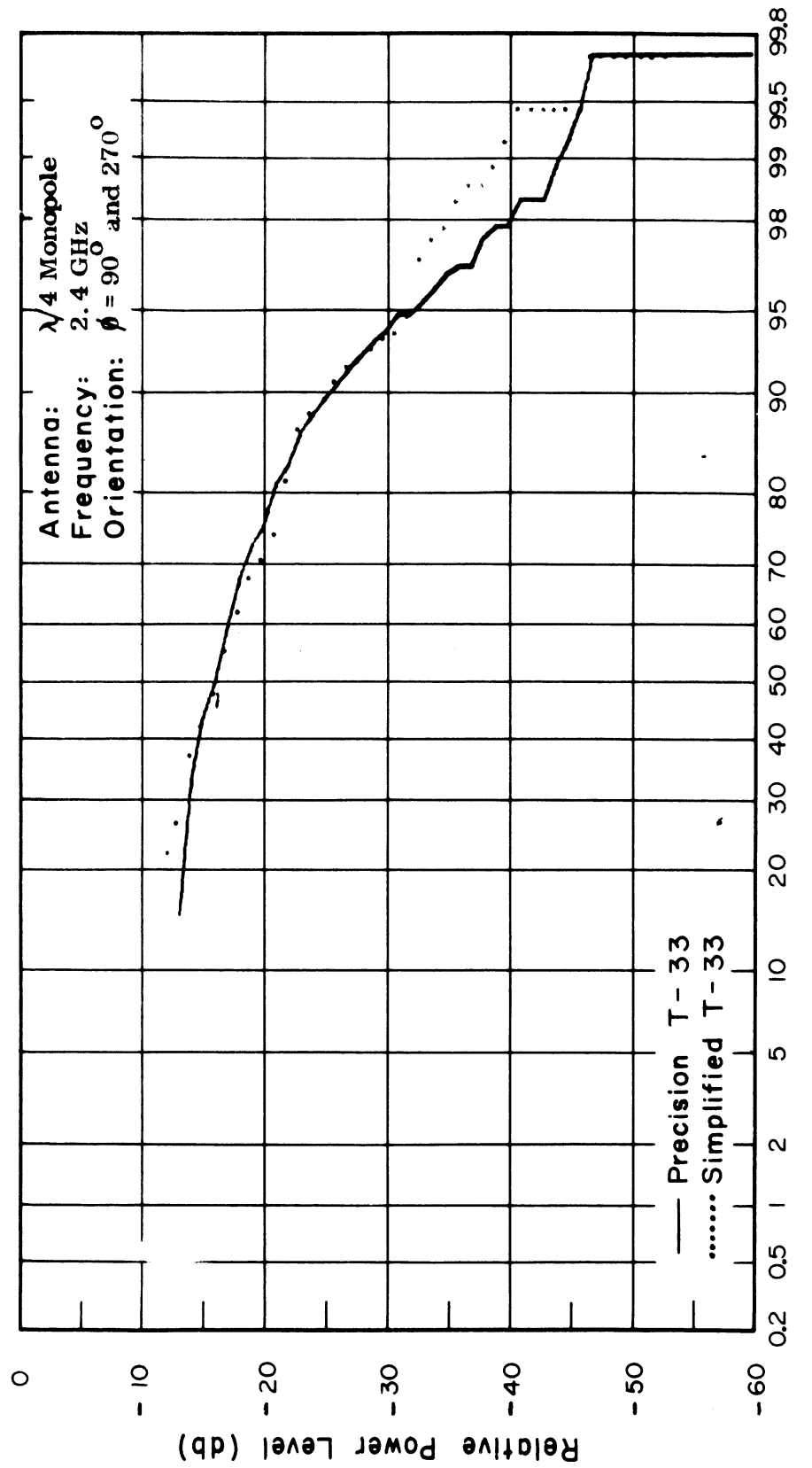
Fig. 55. Cumulative Gain Distributions of Precision and Simplified Models.
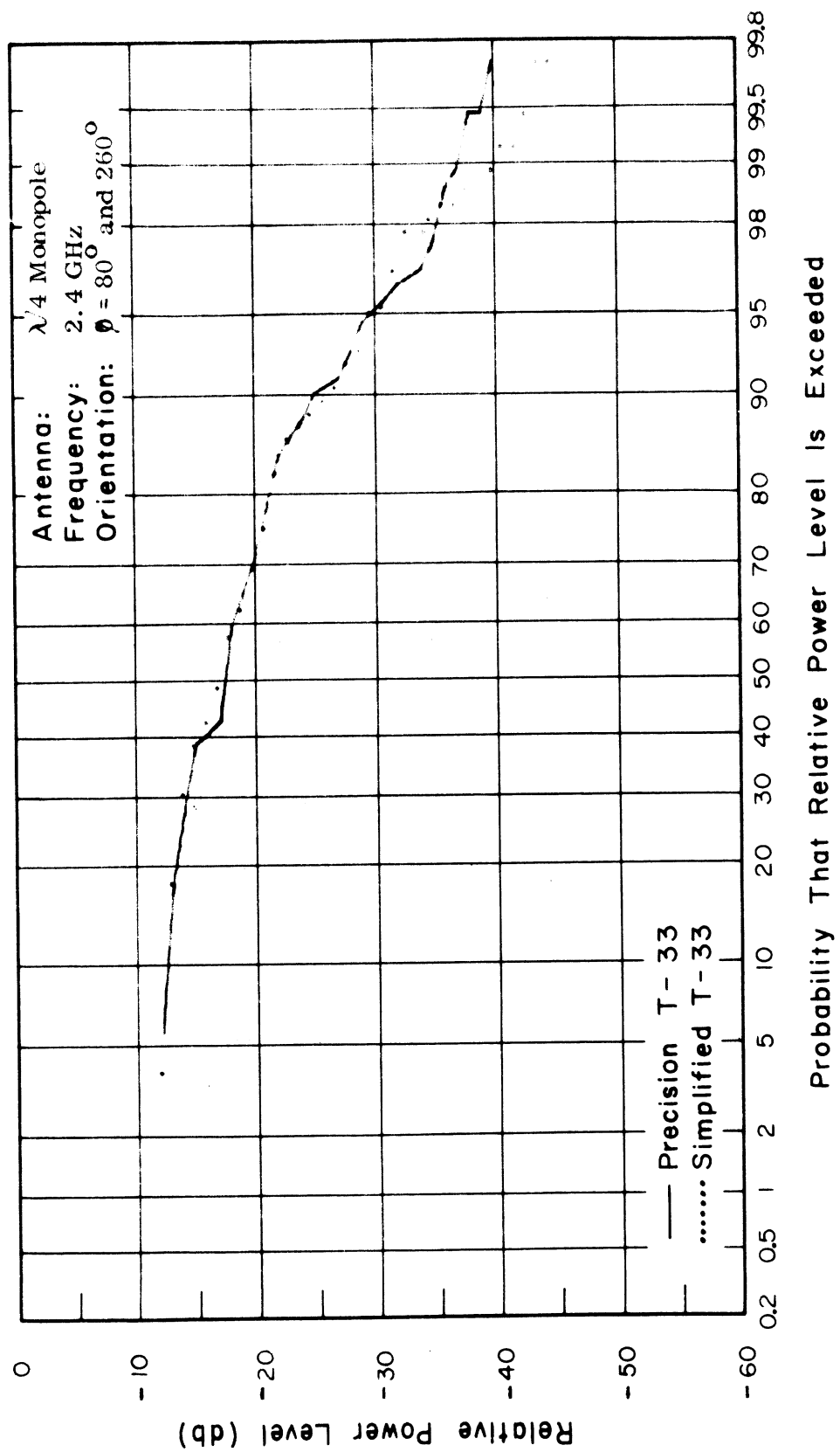
Fig. 56. Cumulative Gain Distributions of Precision and Simplified Models.

67
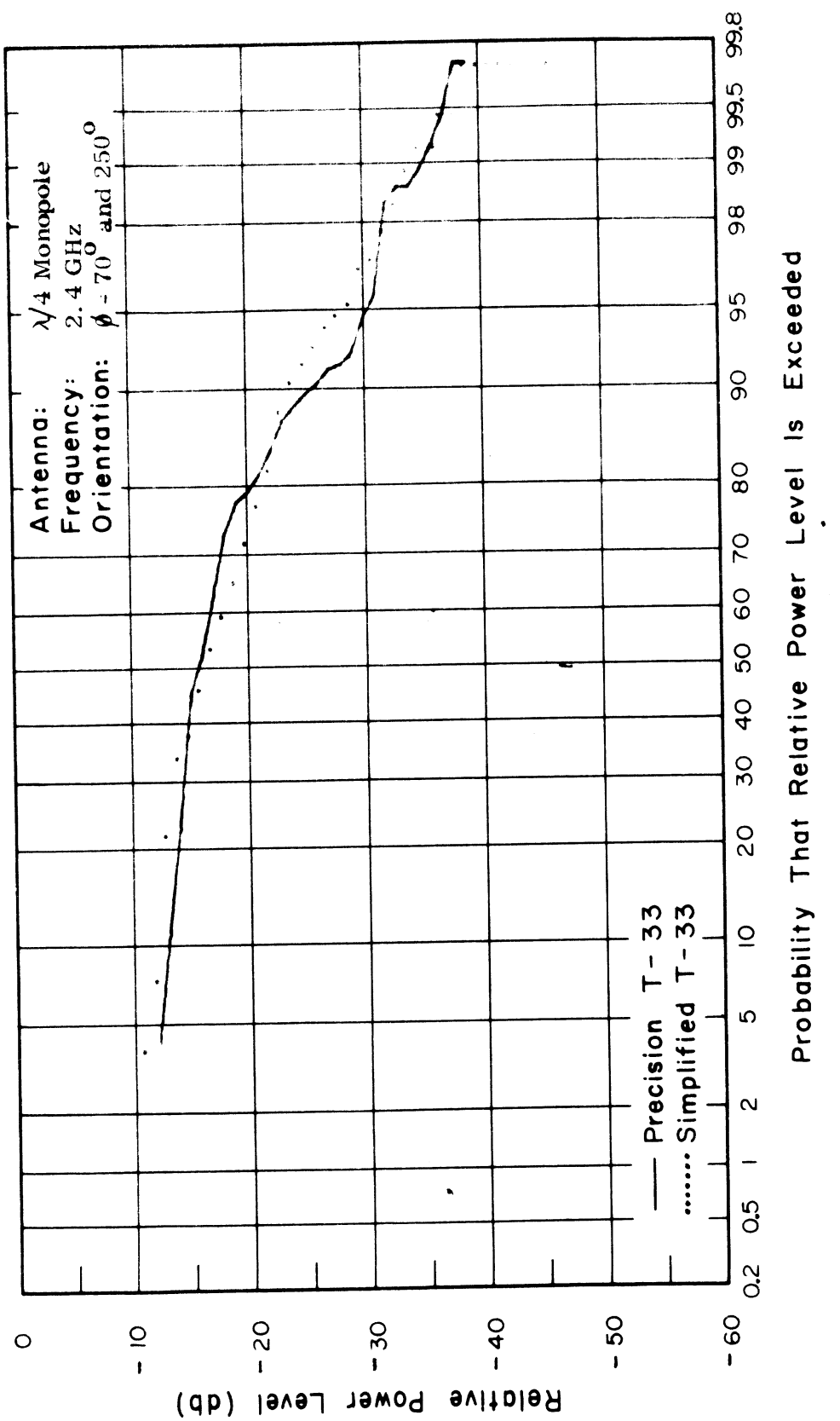
Fig. 57. Cumulative Gain Distributions of Precision and Simplified Models.

68
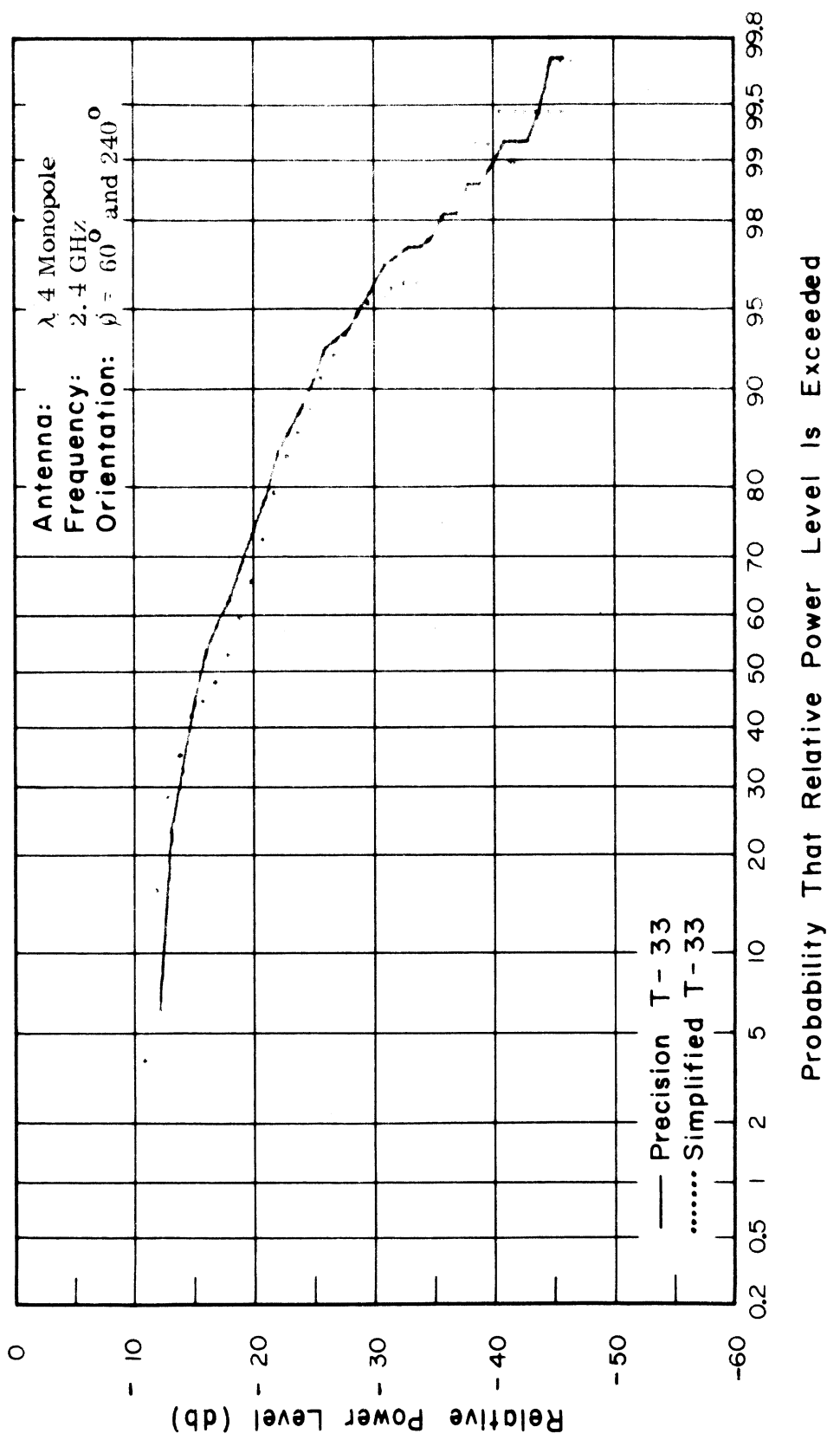
Fig. 58. Cumulative Gain Distributions of Precision and Simplified Models.
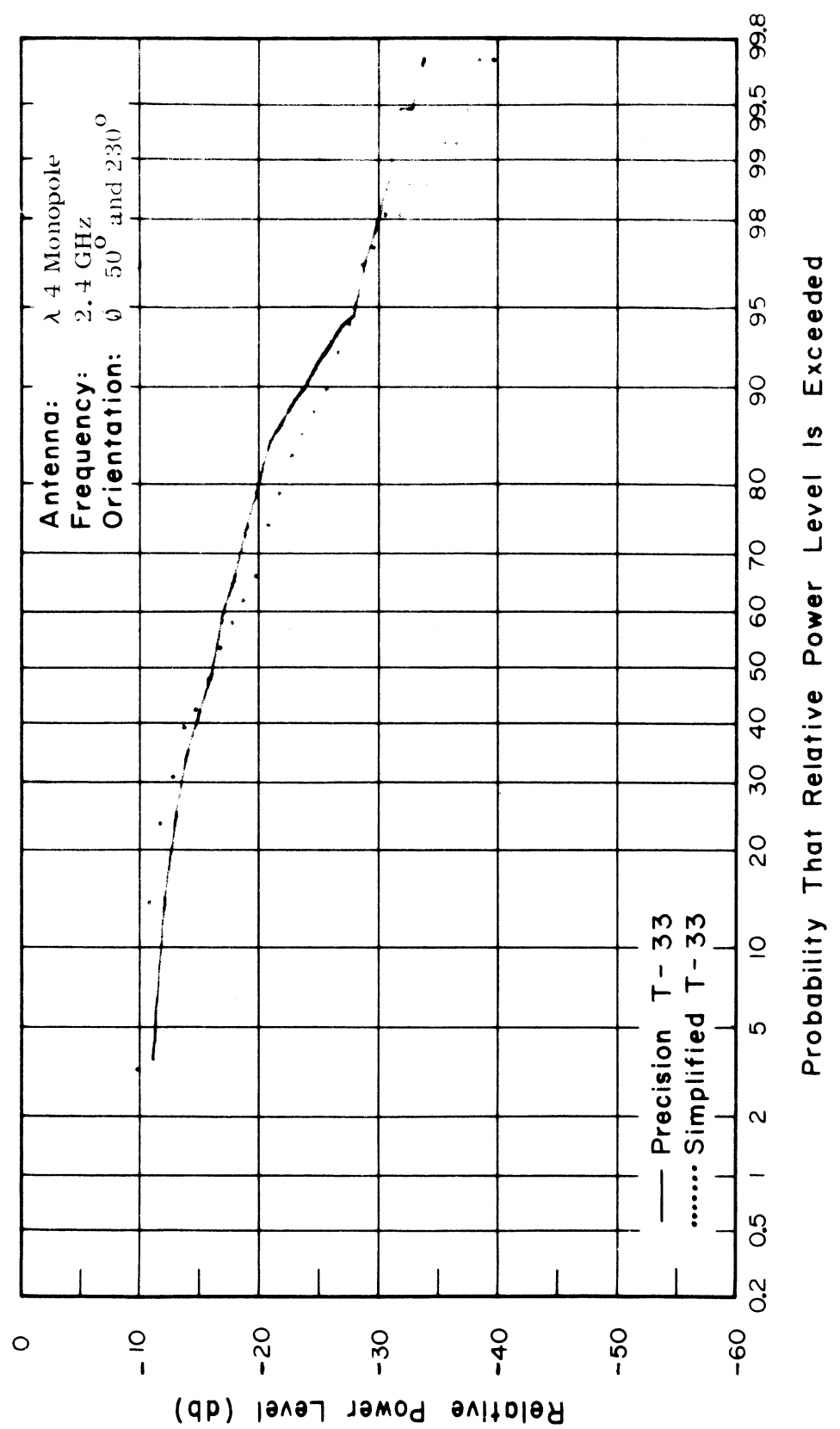
Fig. 59. Cumulative Gain Distributions of Precision and Simplified Models.

Antenna: λ 4 Monopole
Frequency: 2.4 GHz
Orientation: θ 50° and 230°

— Precision T-33
······· Simplified T-33

Probability That Relative Power Level Is Exceeded

Relative Power Level (db)

70
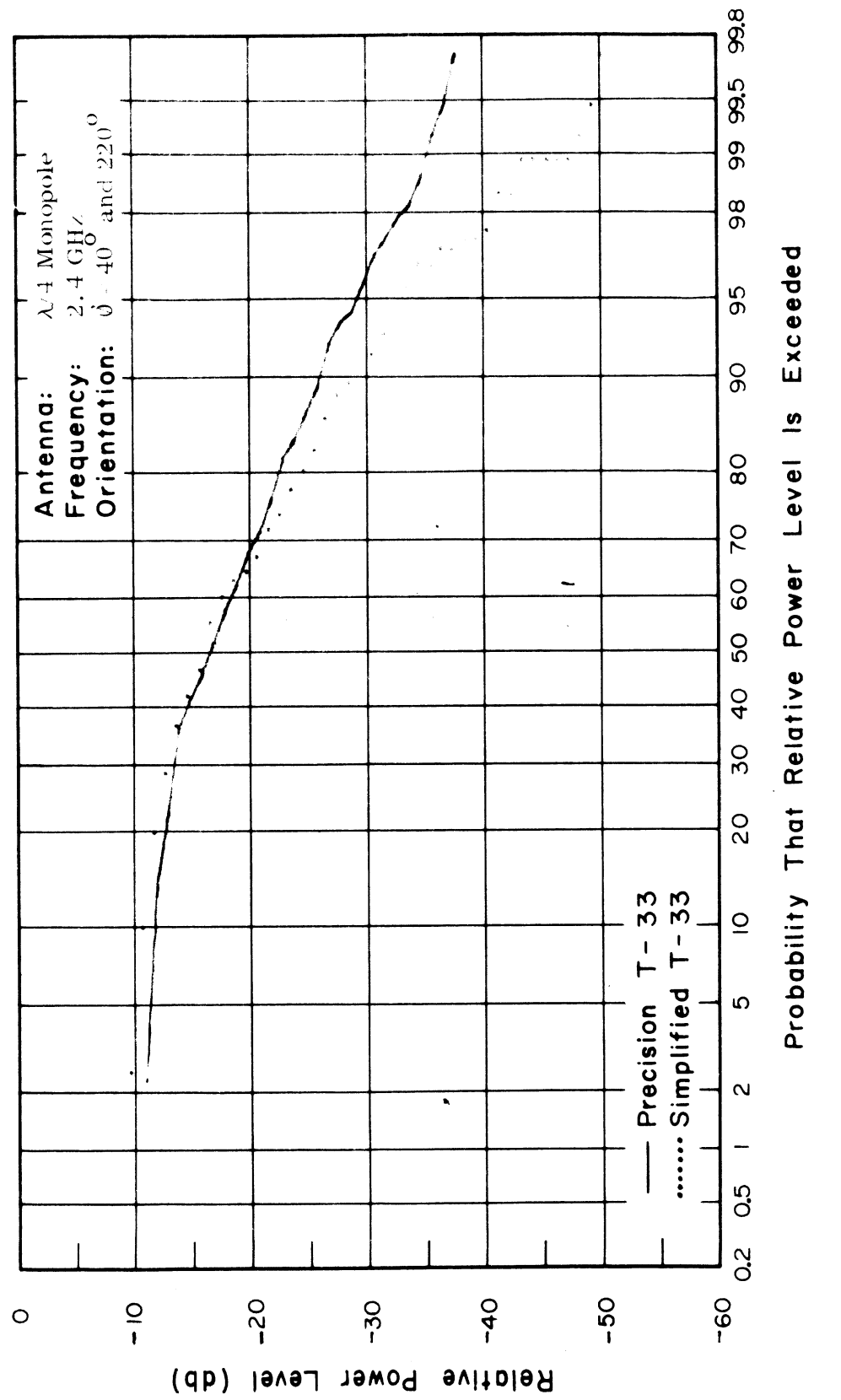
Fig. 60. Cumulative Gain Distributions of Precision and Simplified Models.
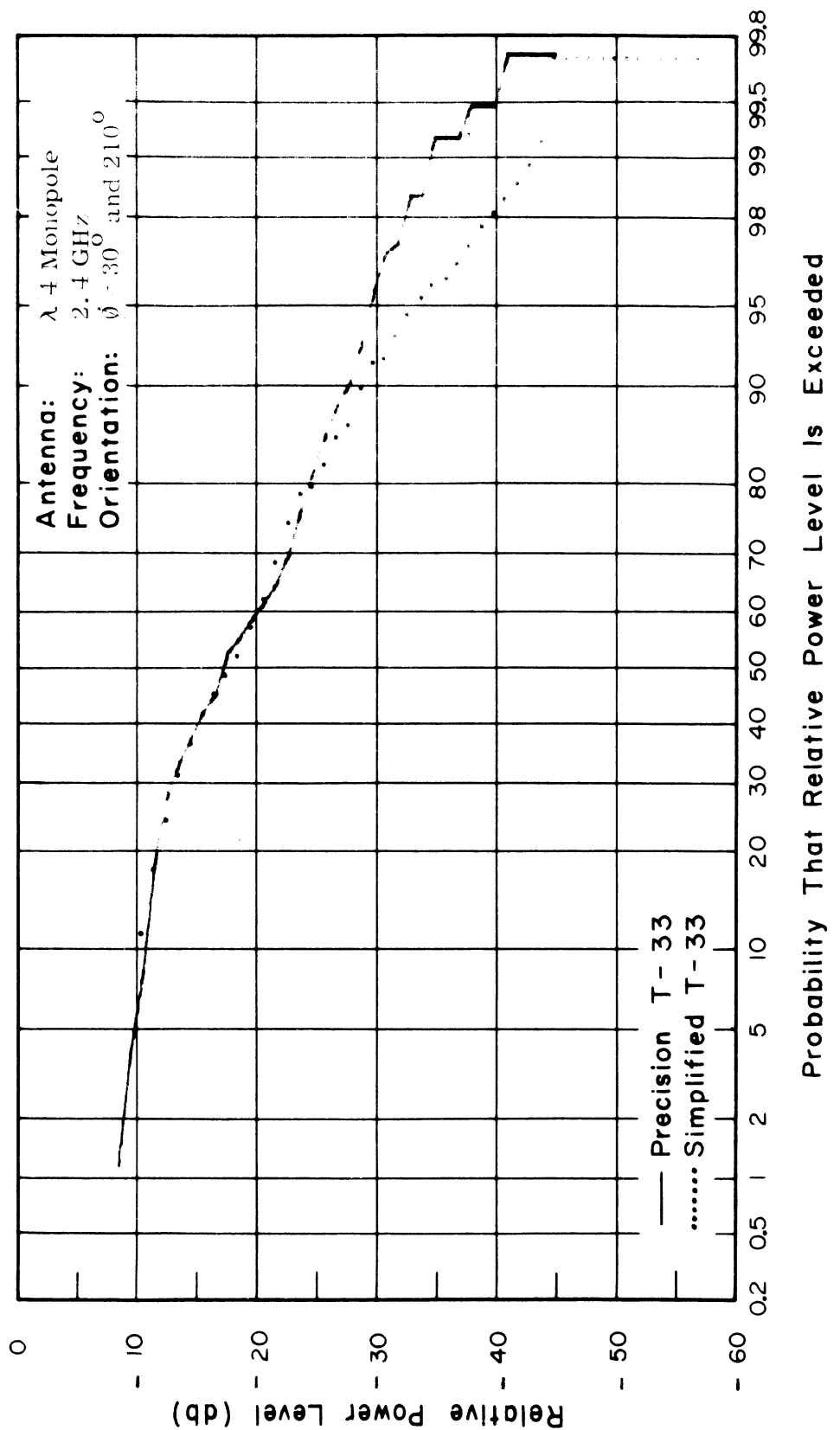
Fig. 61. Cumulative Gain Distributions of Precision and Simplified Models.
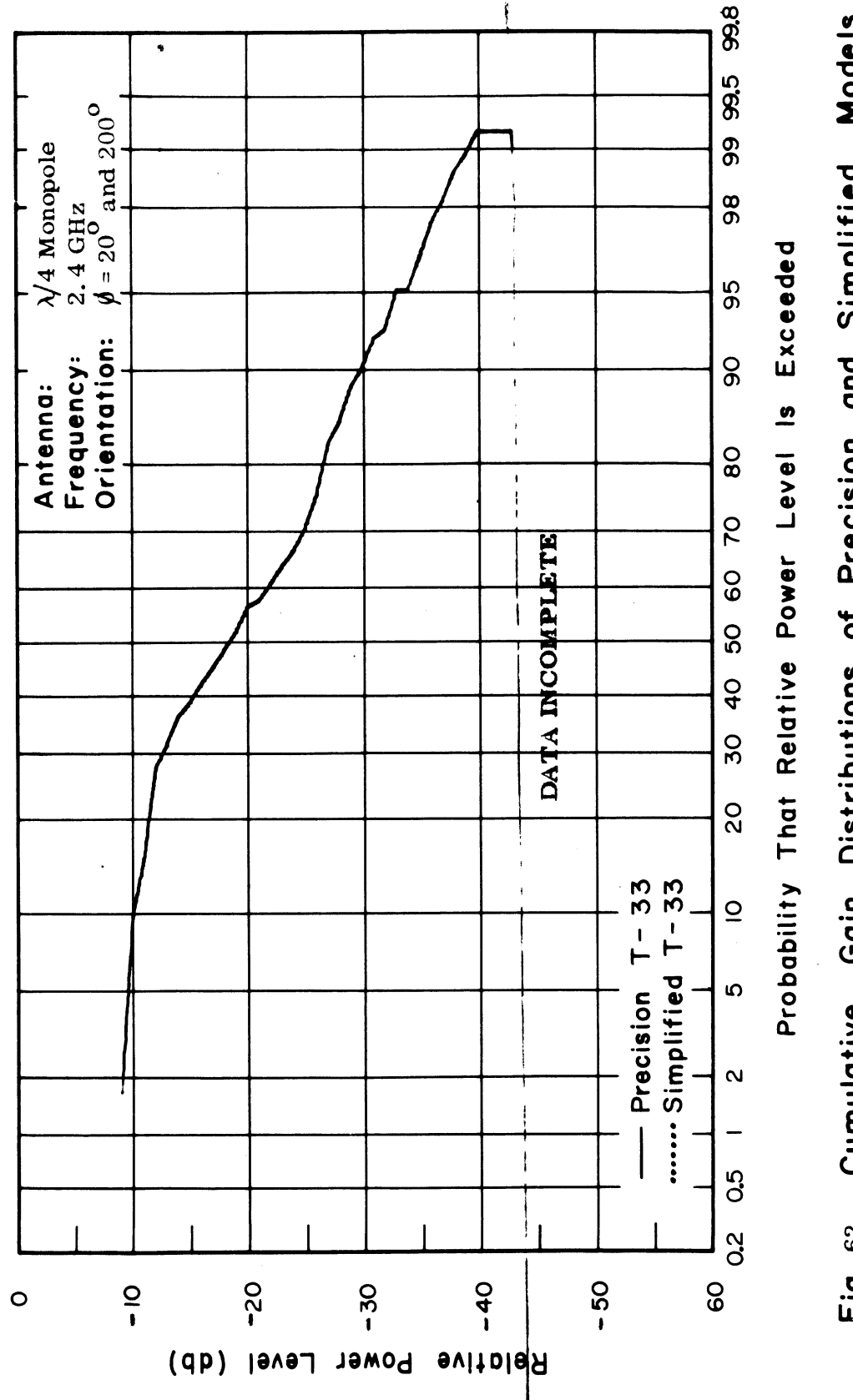
Fig. 62. Cumulative Gain Distributions of Precision and Simplified Models.

73
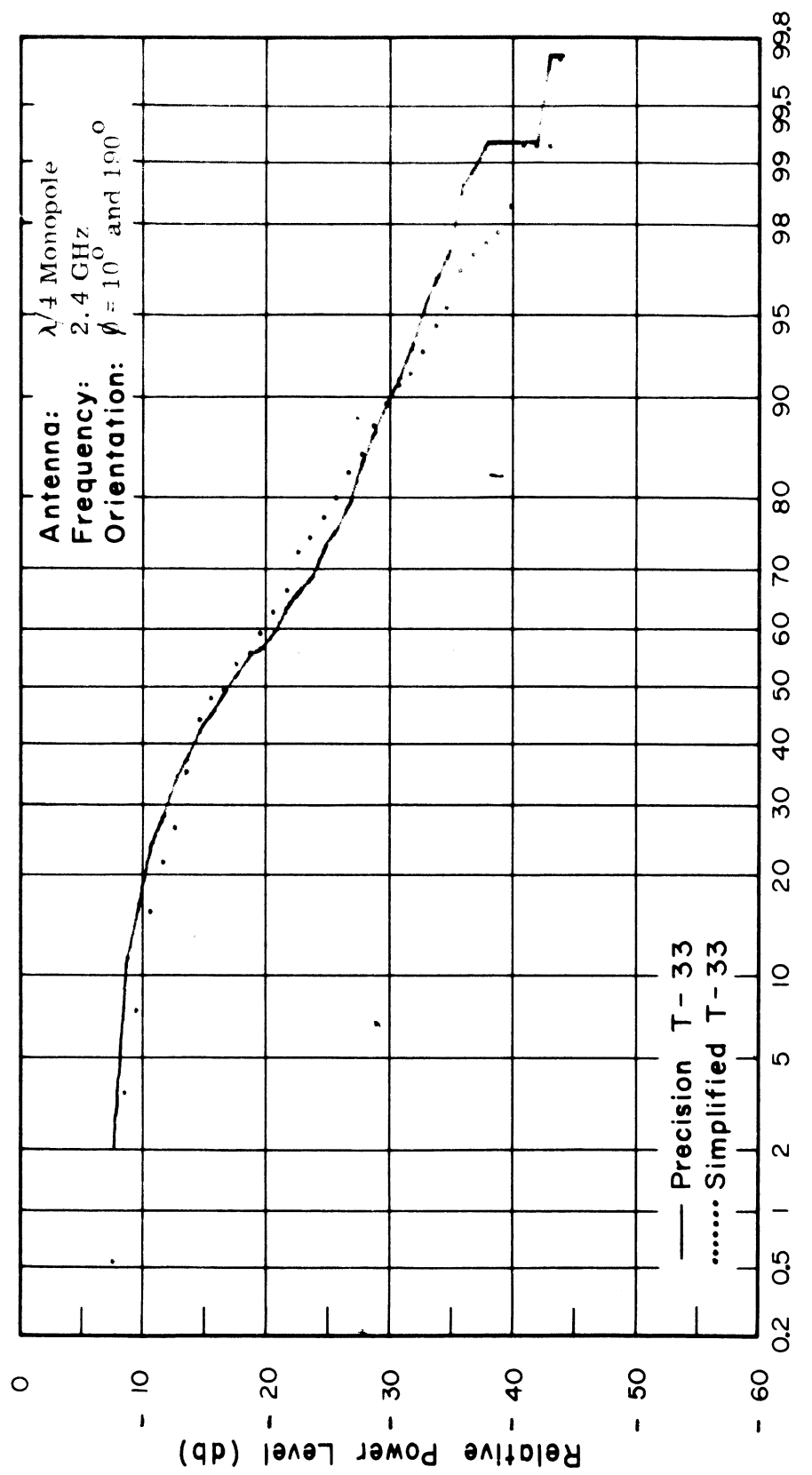
Fig. 63. Cumulative Gain Distributions of Precision and Simplified Models.
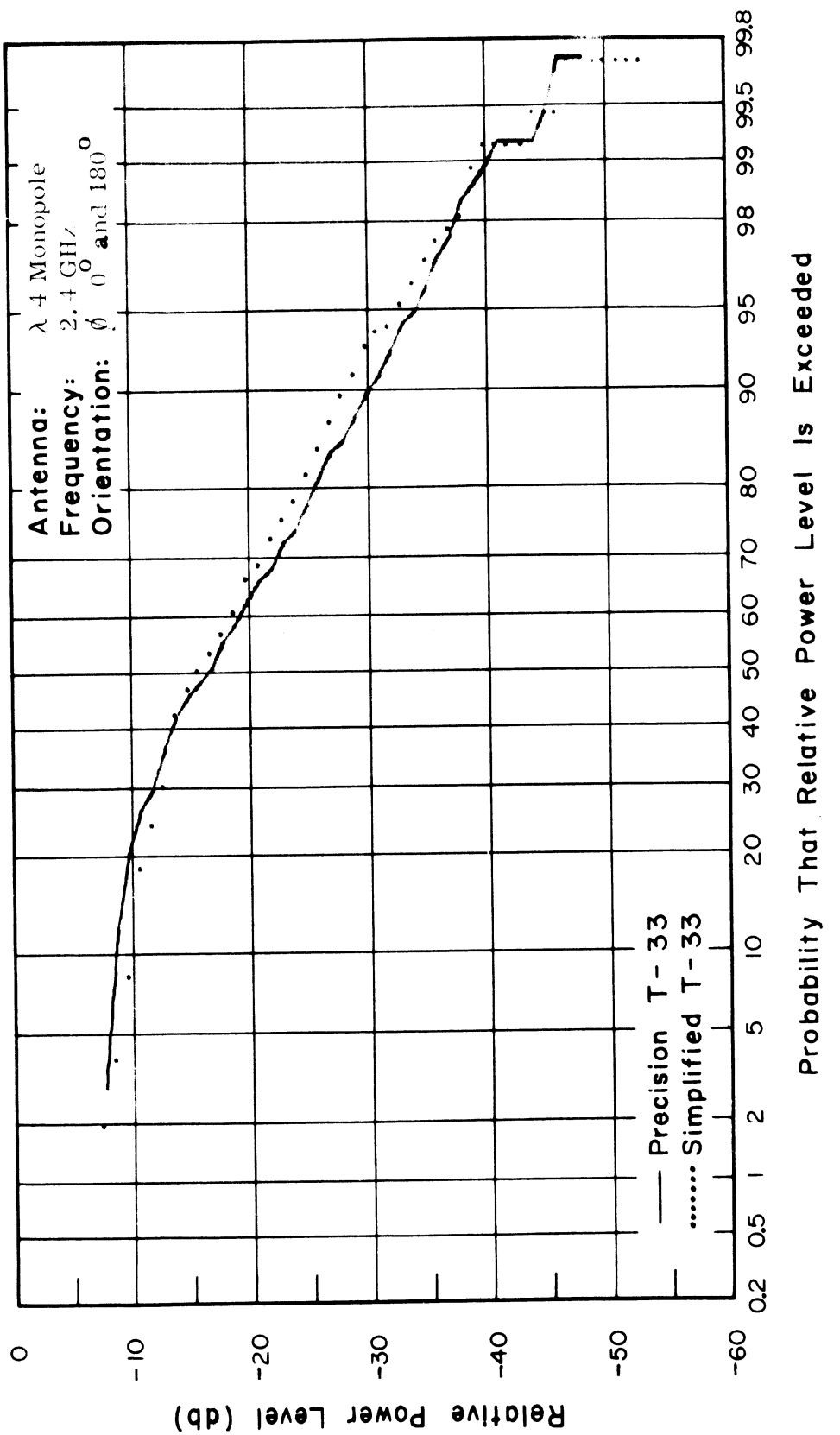
Fig. 64. Cumulative Gain Distributions of Precision and Simplified Models.

75
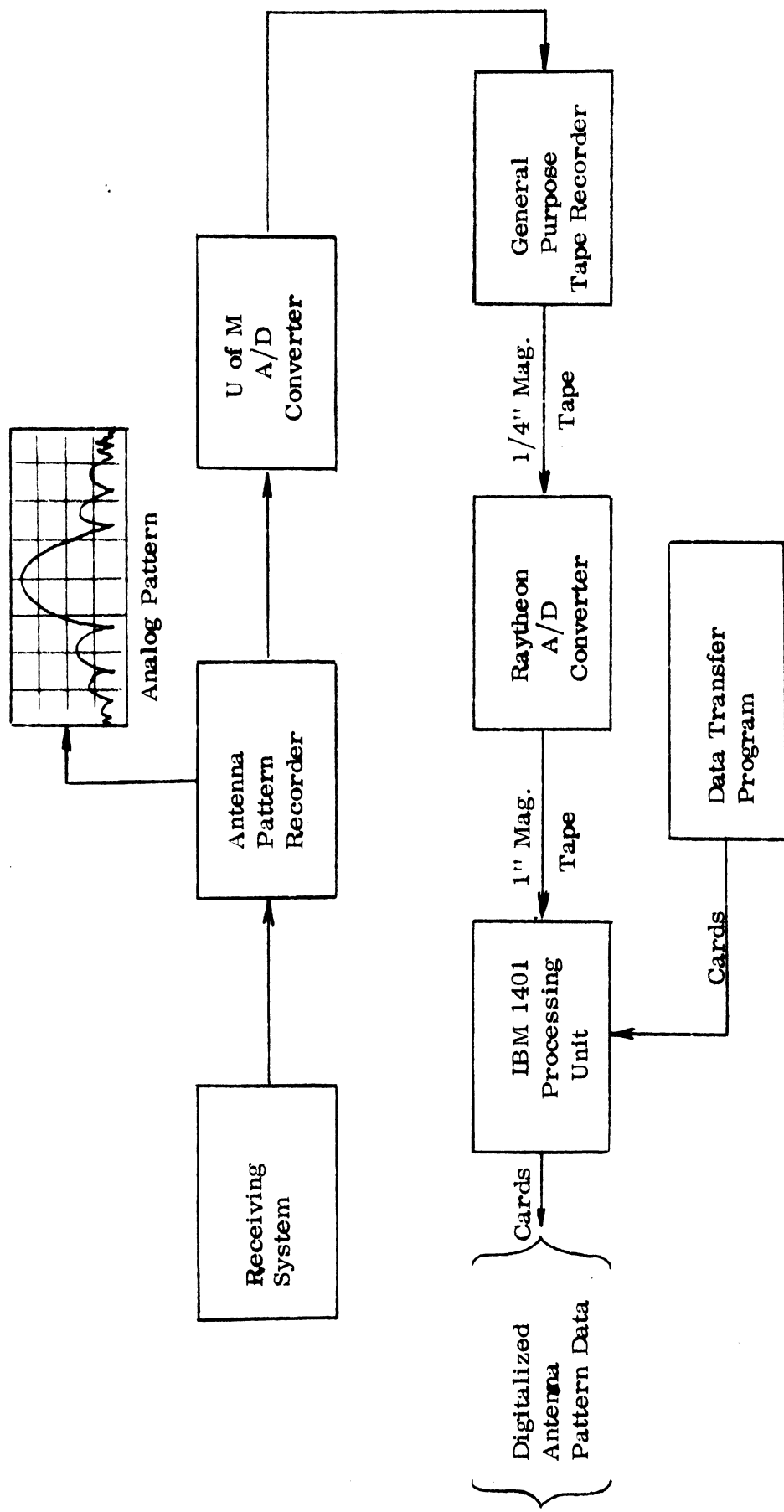
Fig. 65. Automatic Digital Recording System
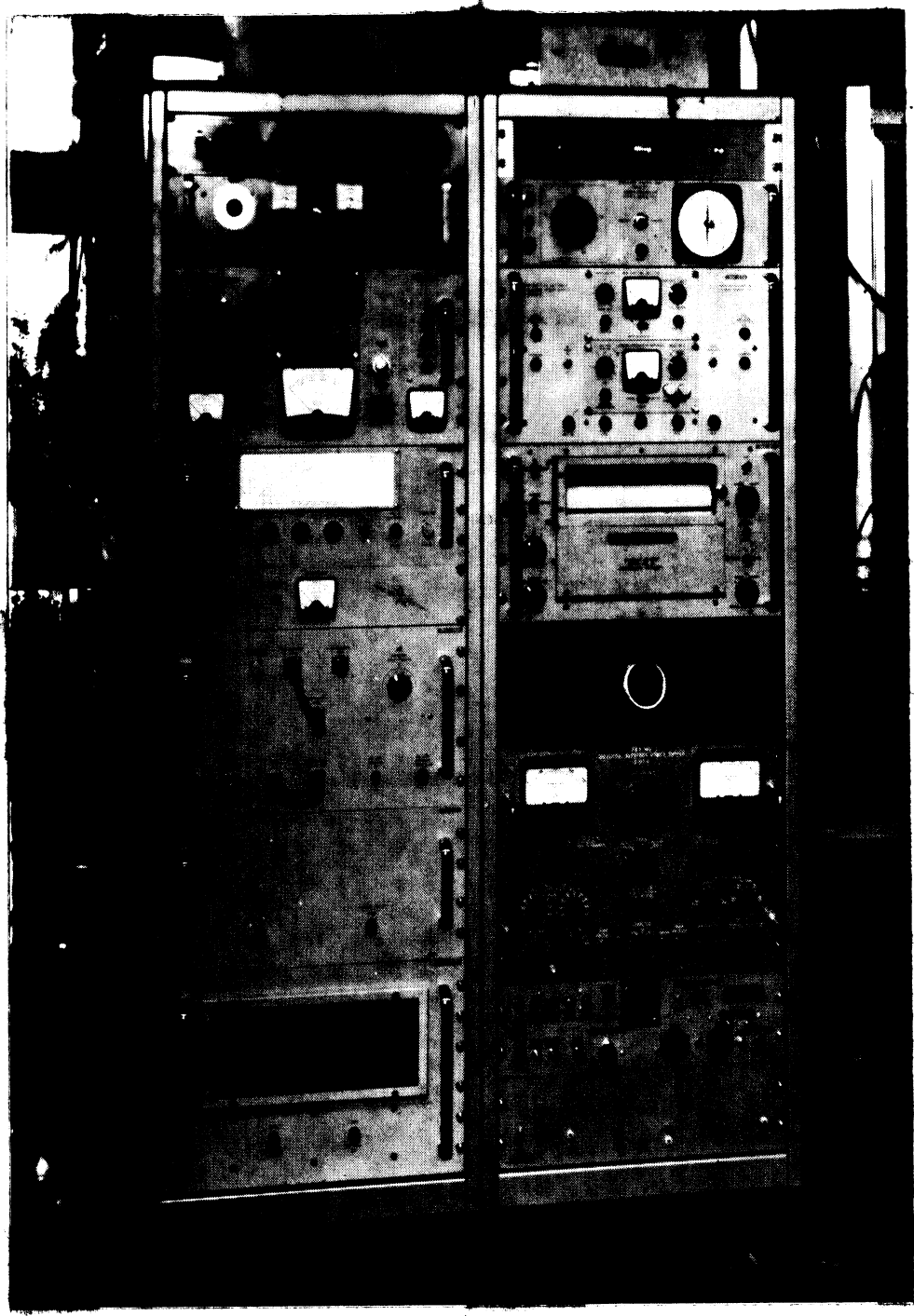
Fig. 66. Wide-Range, High-Gain Receiving System
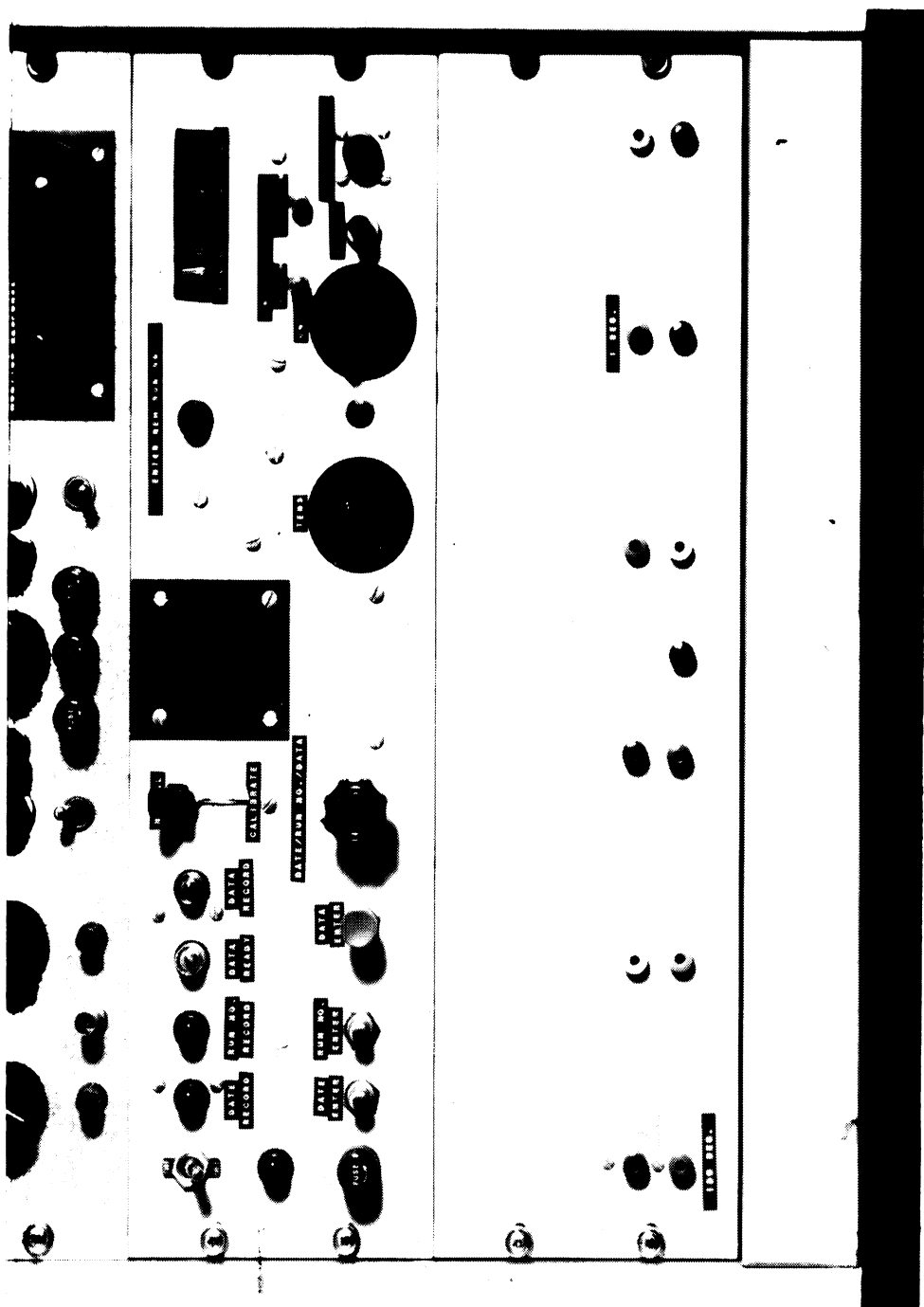
Fig. 67. U of M Analog-to-Digital Converter

Fig. 68. General Purpose Tape Recorder
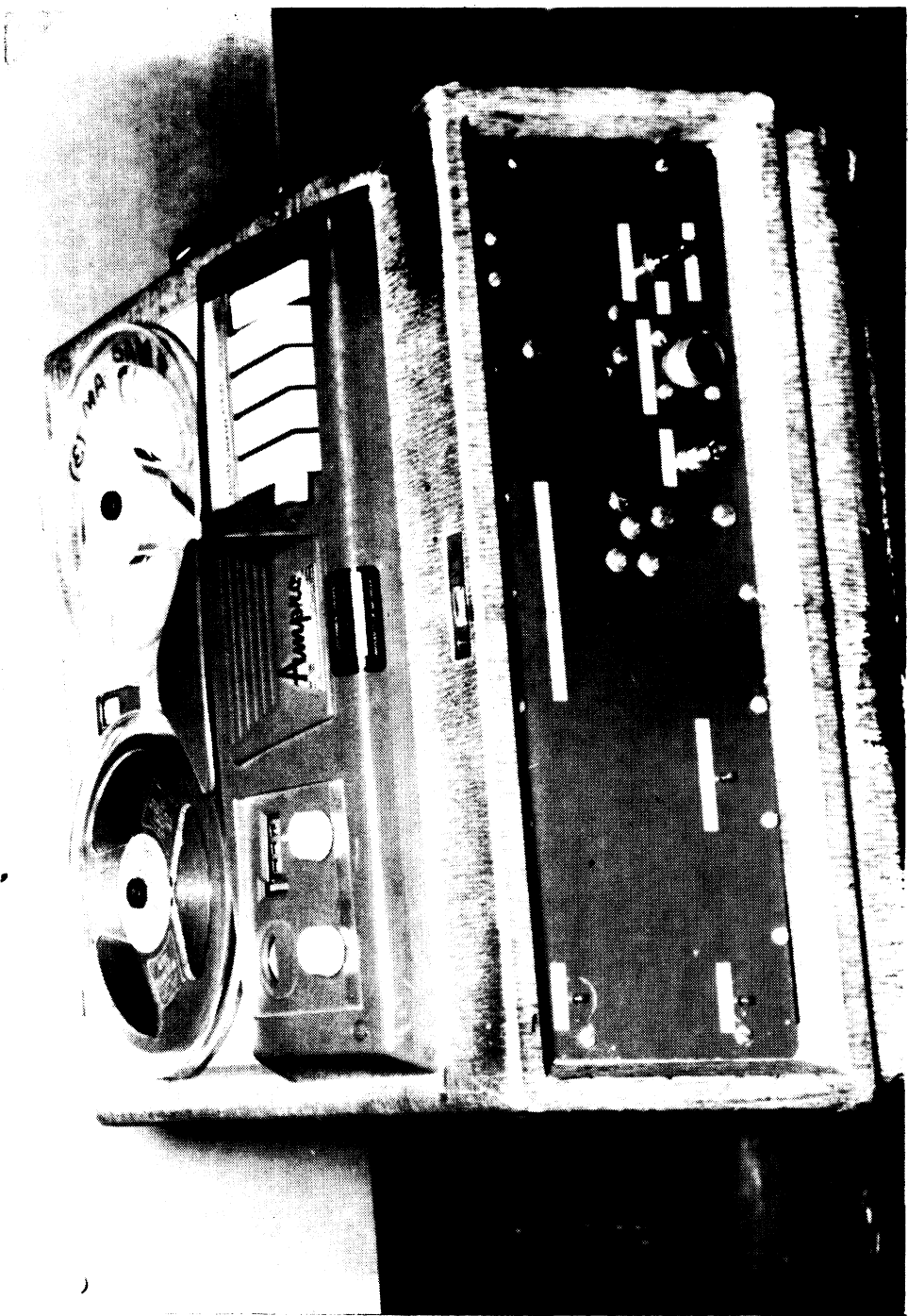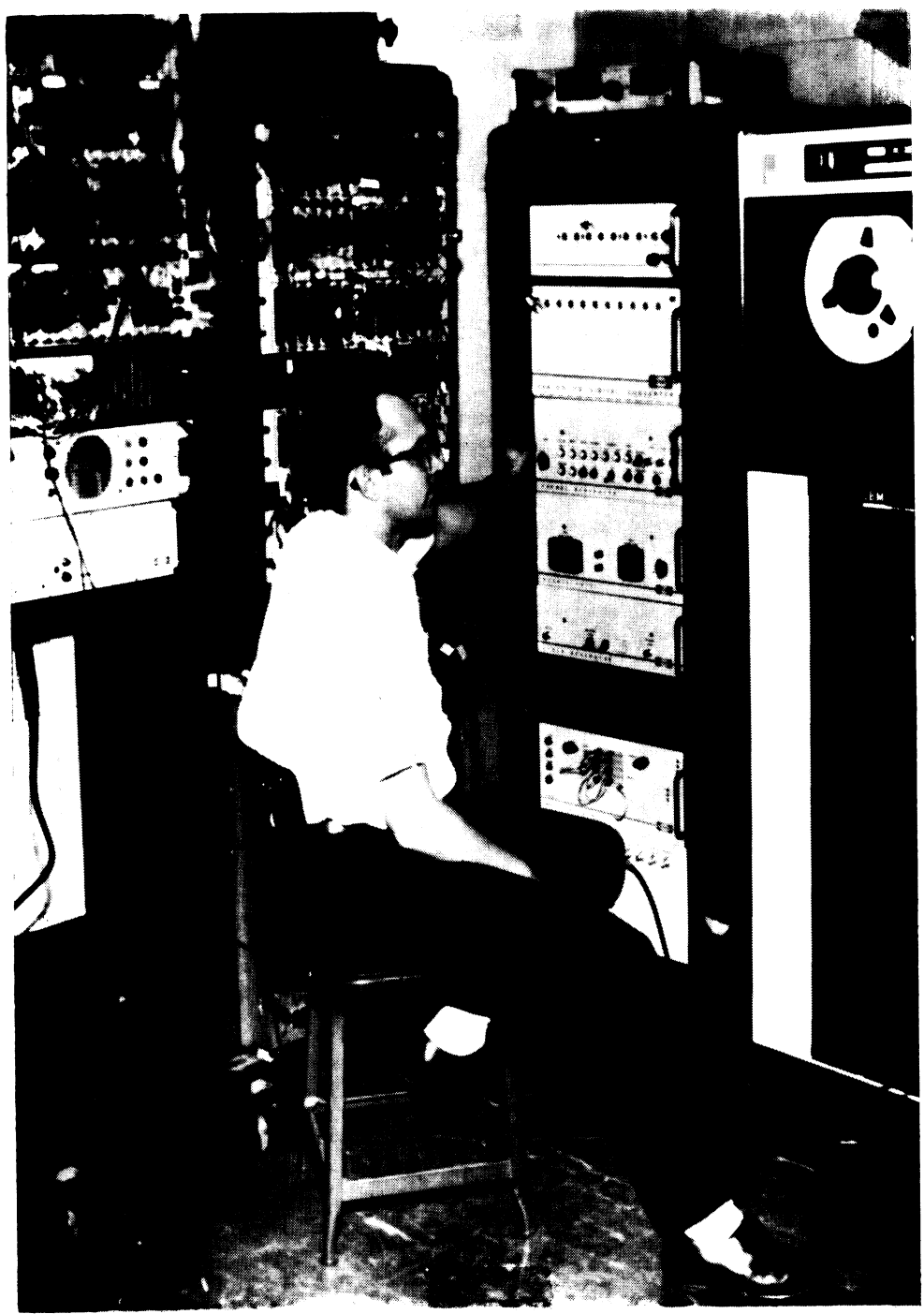
Fig. 69.   Raytheon Analog - Digital Converter
           and Associated Logic Racks (North Campus)

Fig. 70. IBM 1401 Processing Unit and IBM 729 Magnetic Tape Units.
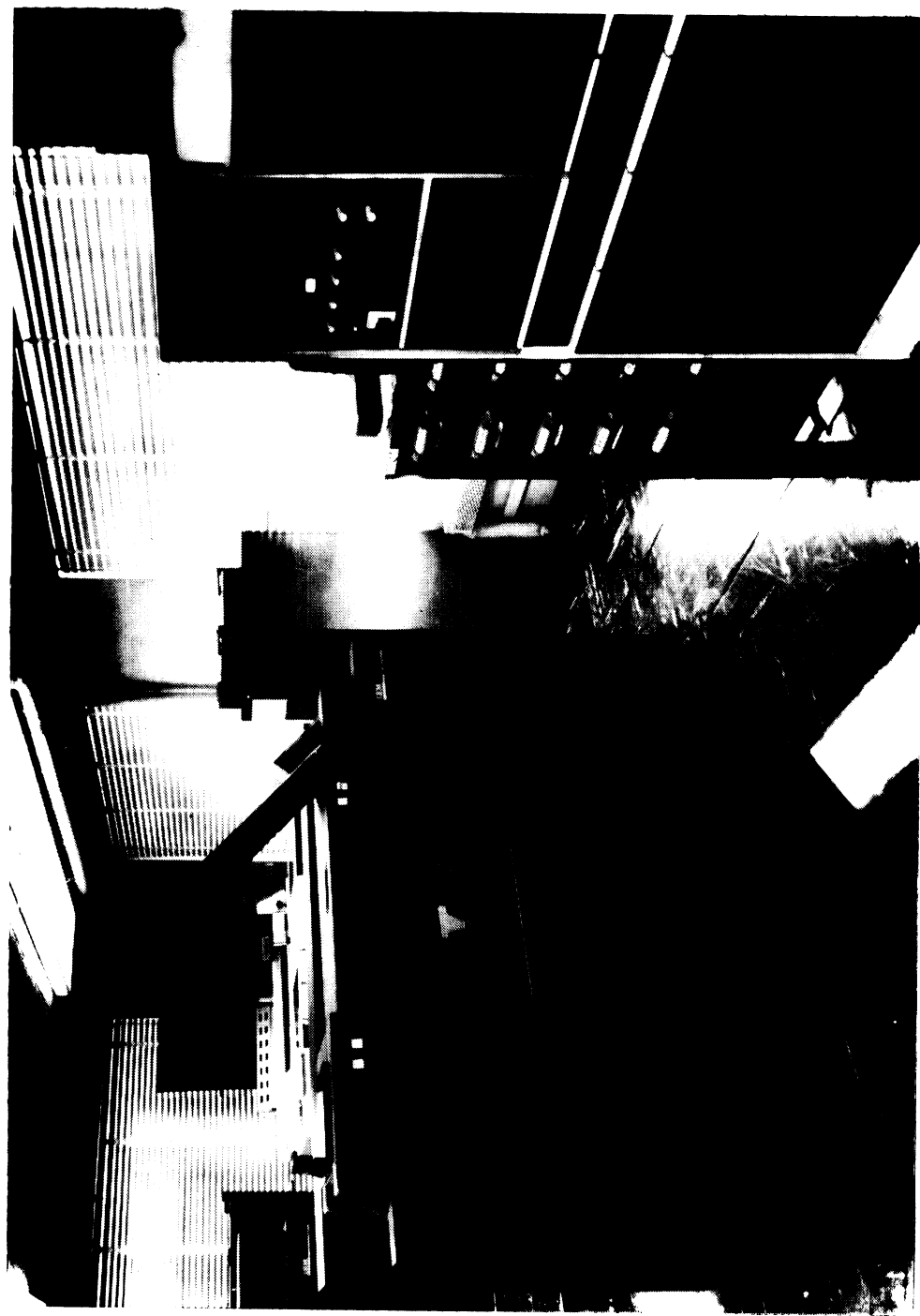
Fig. 71. IBM 1401 Processing Unit and IBM 1402 Card Punch Unit

FIG. 72

λ/4 Monopole - 2.4 Gc
— Typical Analog
Antenna Pattern
⊙ Pattern Data in Digi-
tal Form After Trans-
fer to IBM Cards

RELATIVE POWER ONE WAY

0
2
4
6
8
10
2
4
6
8
20
2
4
6
8
30
2
4
6
8
40
2
4
6
8
50
2
4
6
8
60

4°   3°   2°   1°   0   1°   2°   3°   4°
18°   12°   6°   6°   12°   18°   24°
108°   72°   36°   36°   72°   108°   144°

ANGLE

SCIENTIFIC-ATLANTA, INC., ATLANTA, GEORGIA

83

FIG 73

X-Band Slot – 16.0 Gc
— Typical Analog
   Antenna Pattern
⊙ Pattern Data in Digi-
   tal Form After Trans-
   fer to IBM Cards

RELATIVE POWER ONE WAY (db)

ANGLE
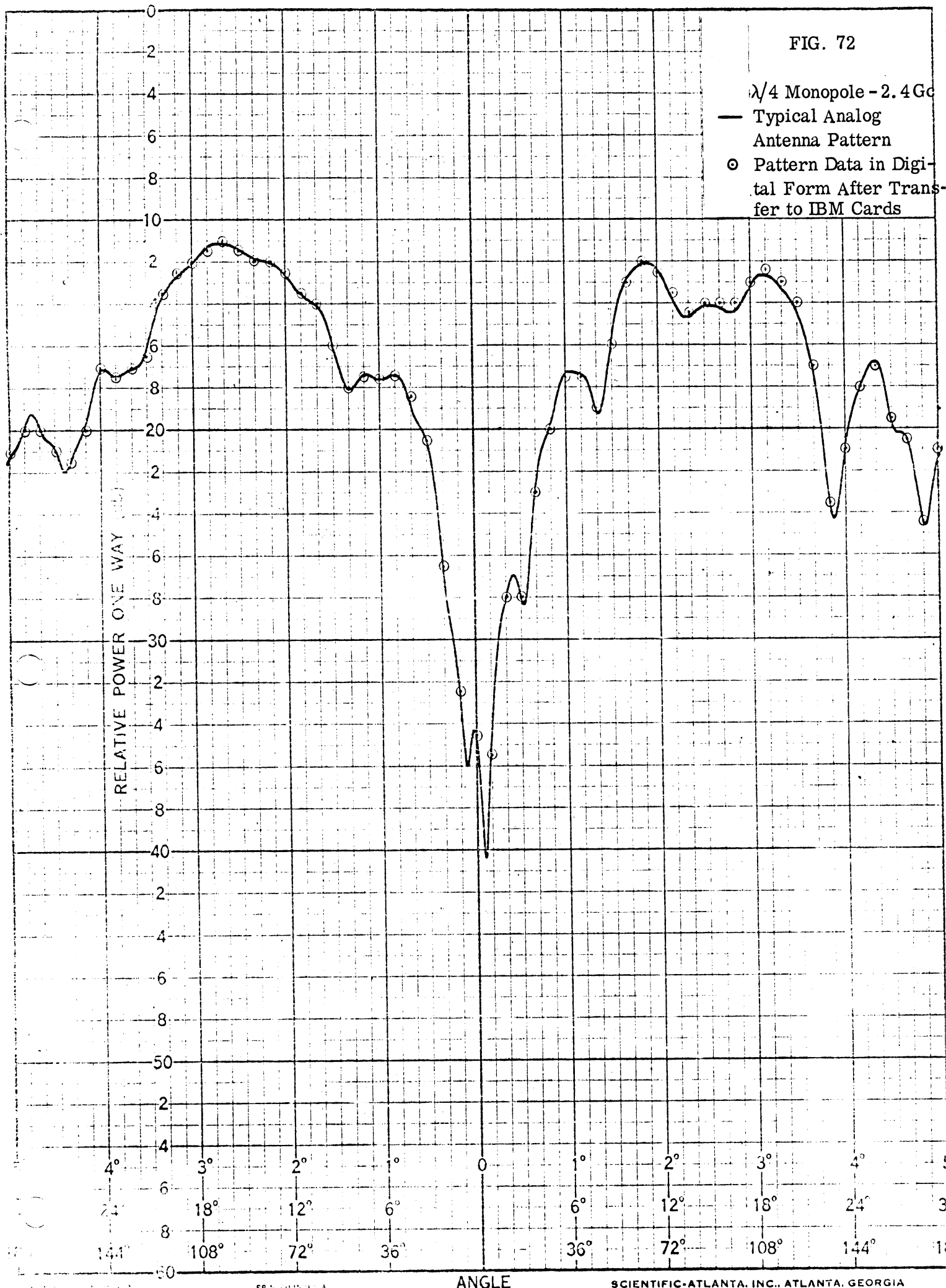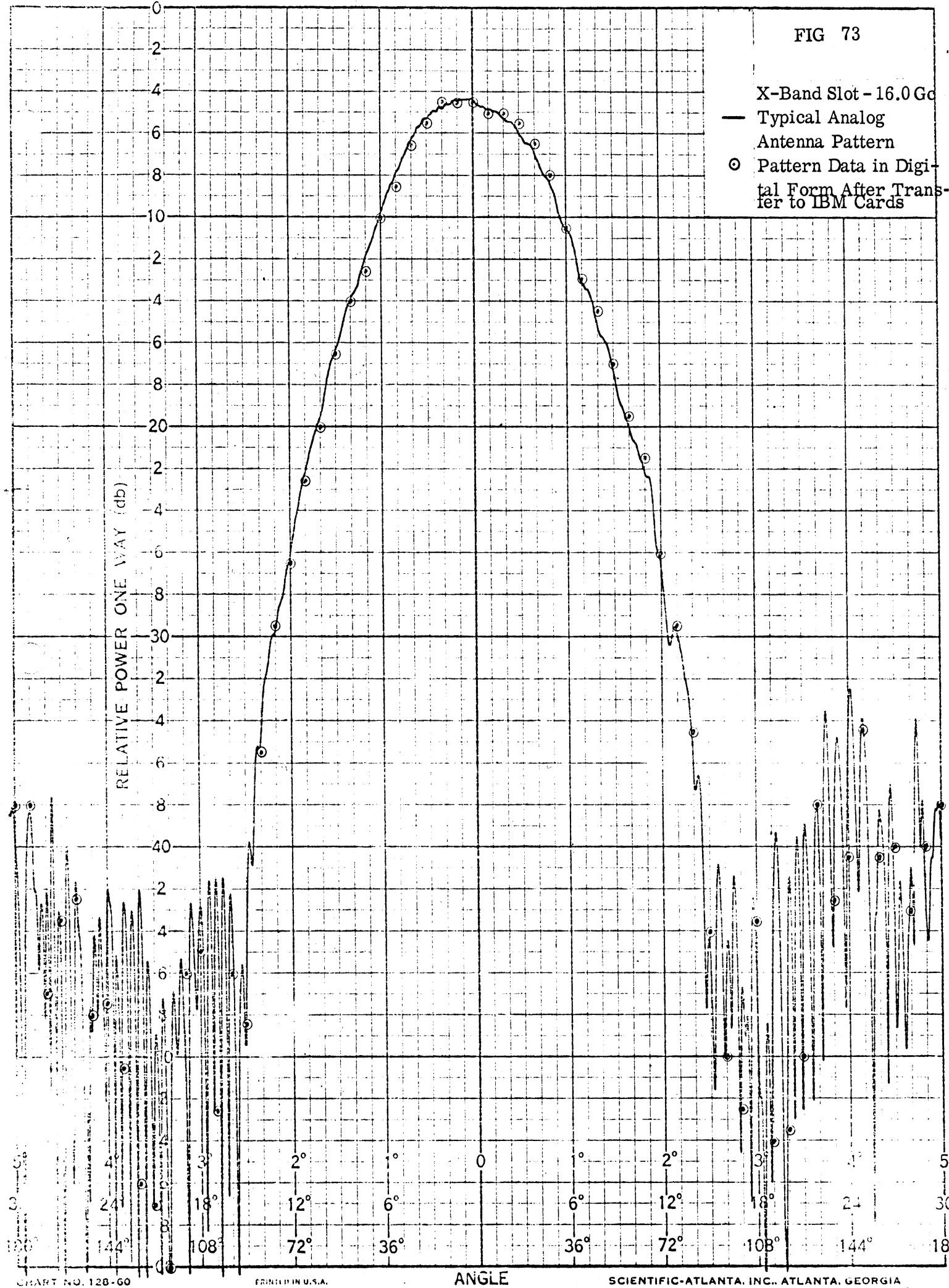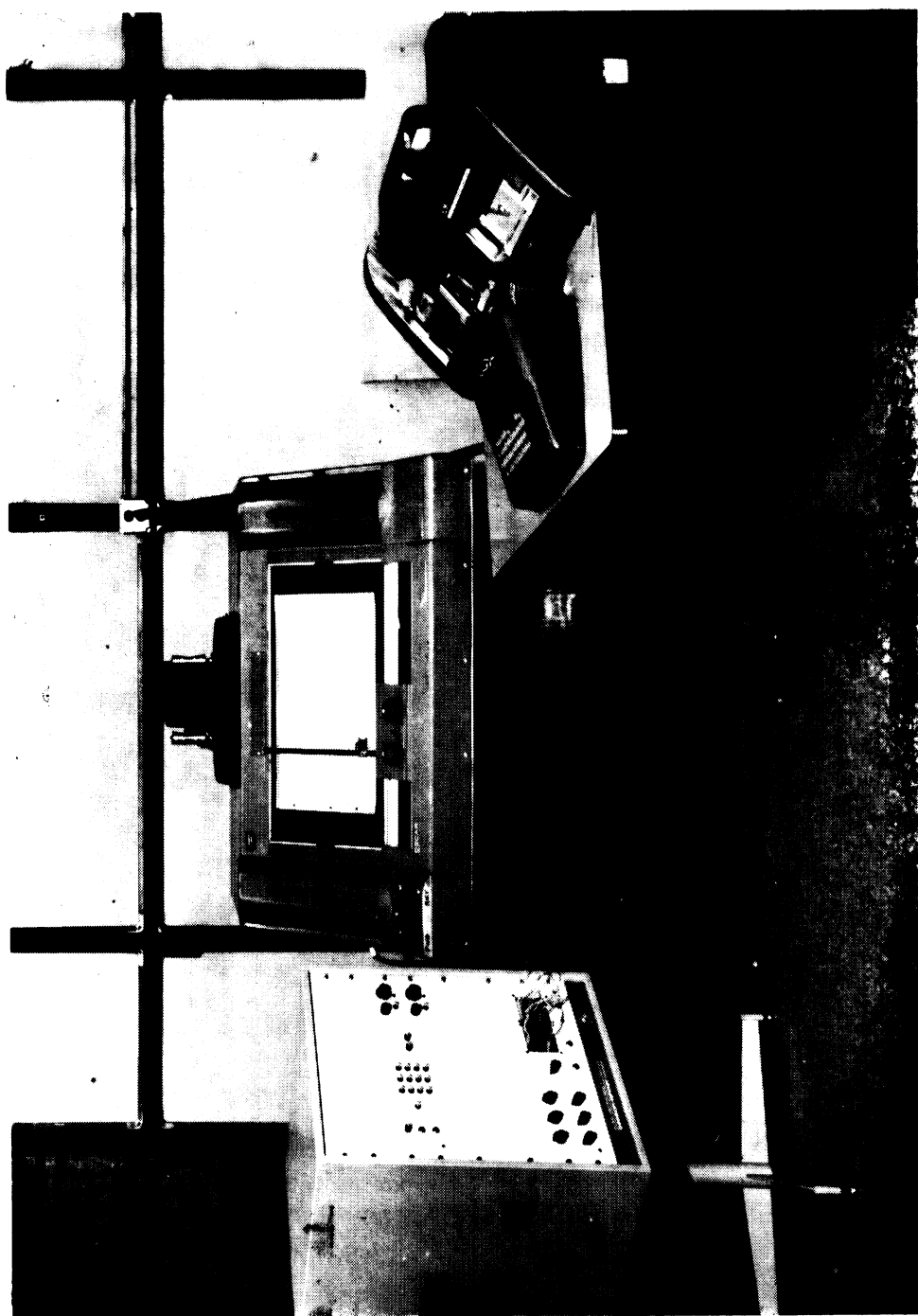
Fig. 74. Semi-Automatic Digital Recording Equipment
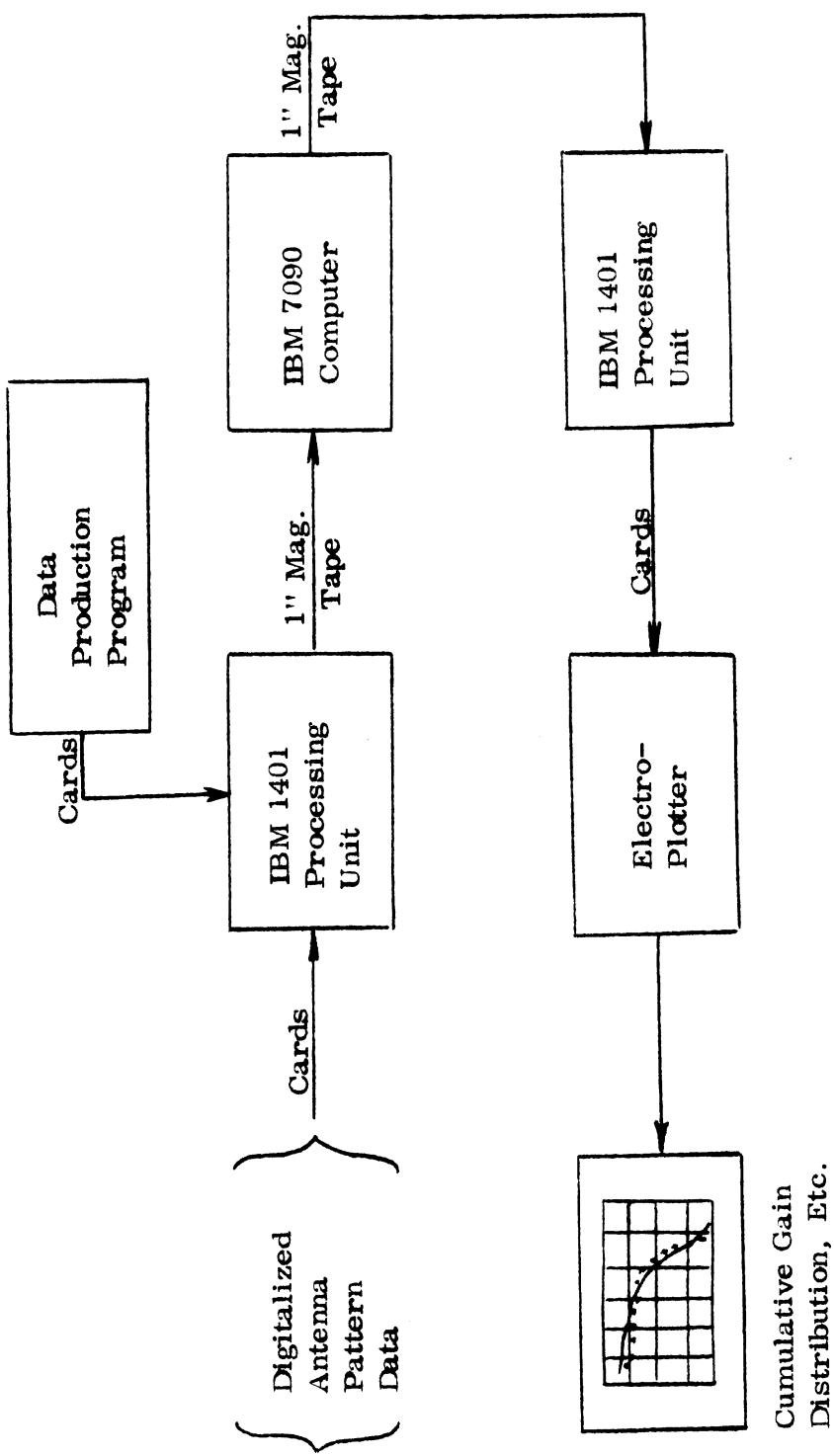
Fig. 75.   Automatic Data Reduction System

Fig. 76. IBM 7090 Digital Computer
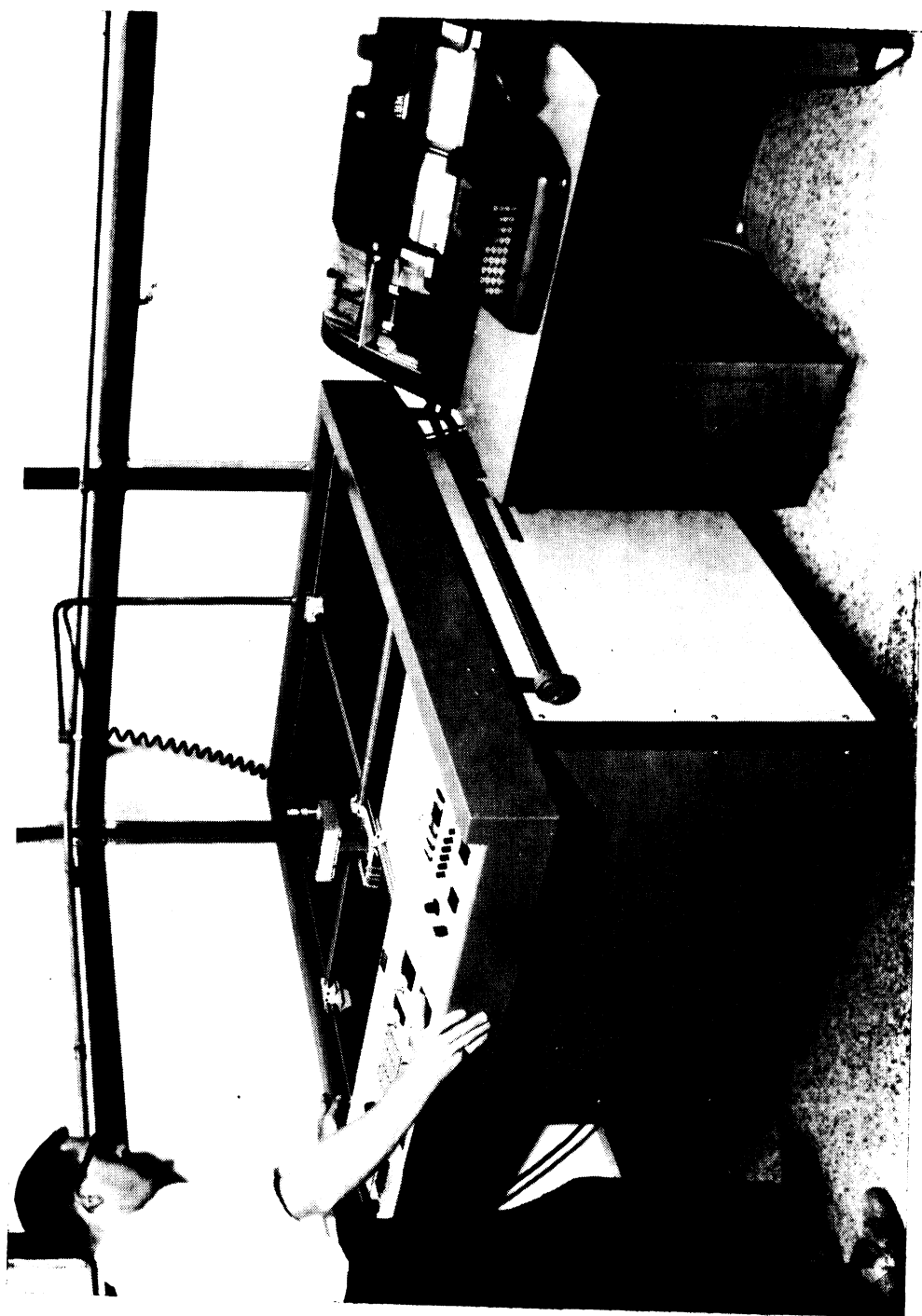
Fig. 77. Benson-Lehner Electroplotter and IBM Card Unit
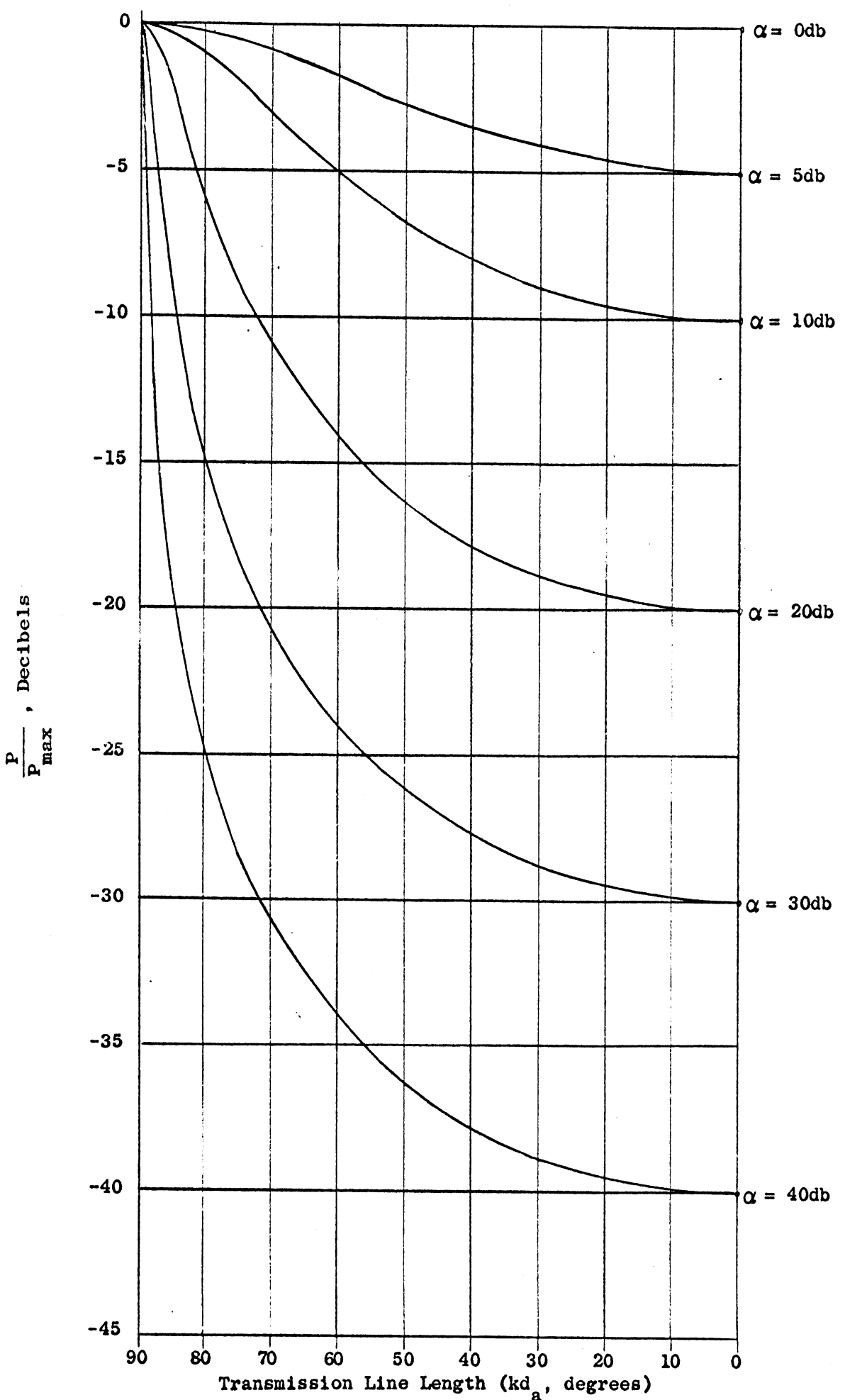
Fig. 78. Power Transfer as a Function of Transmission Line Length

89
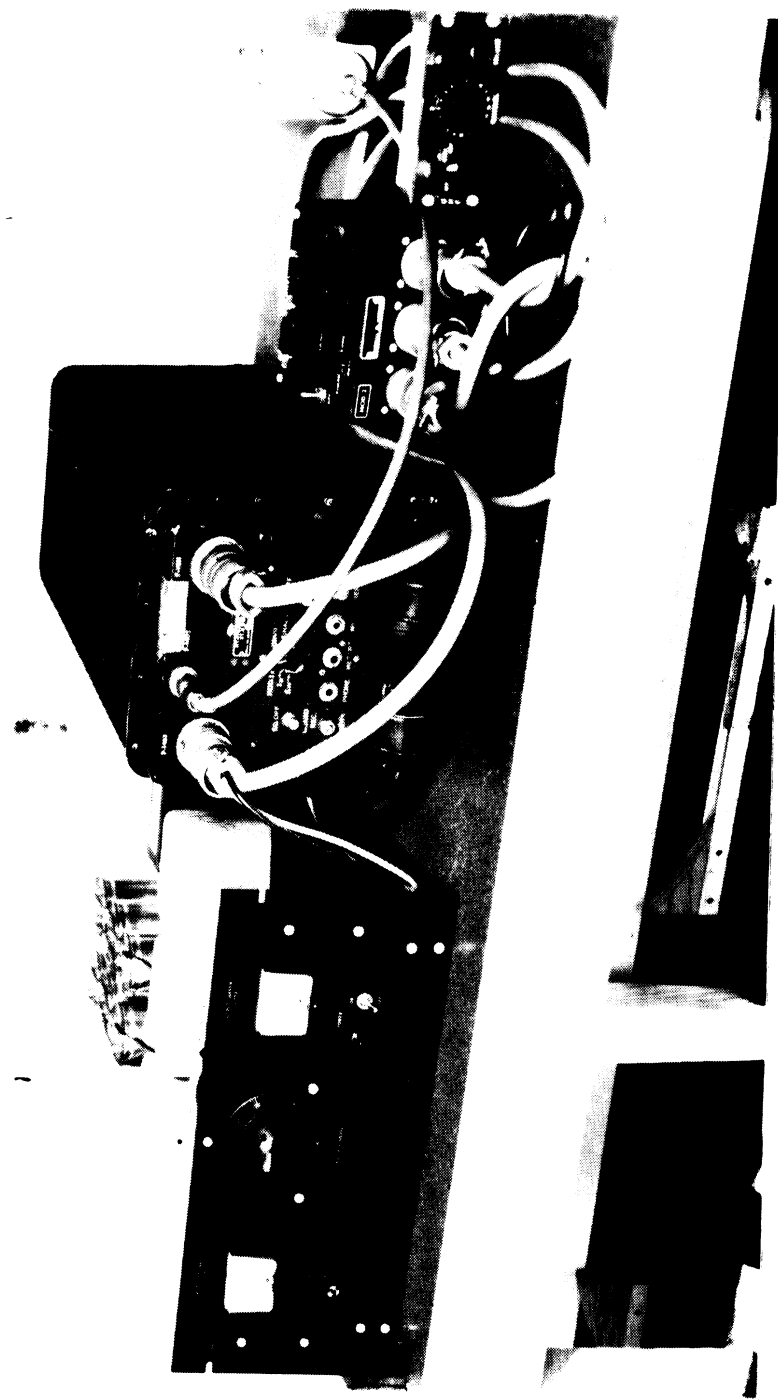
Fig. 79. AN/ARC-27 and Power Supply
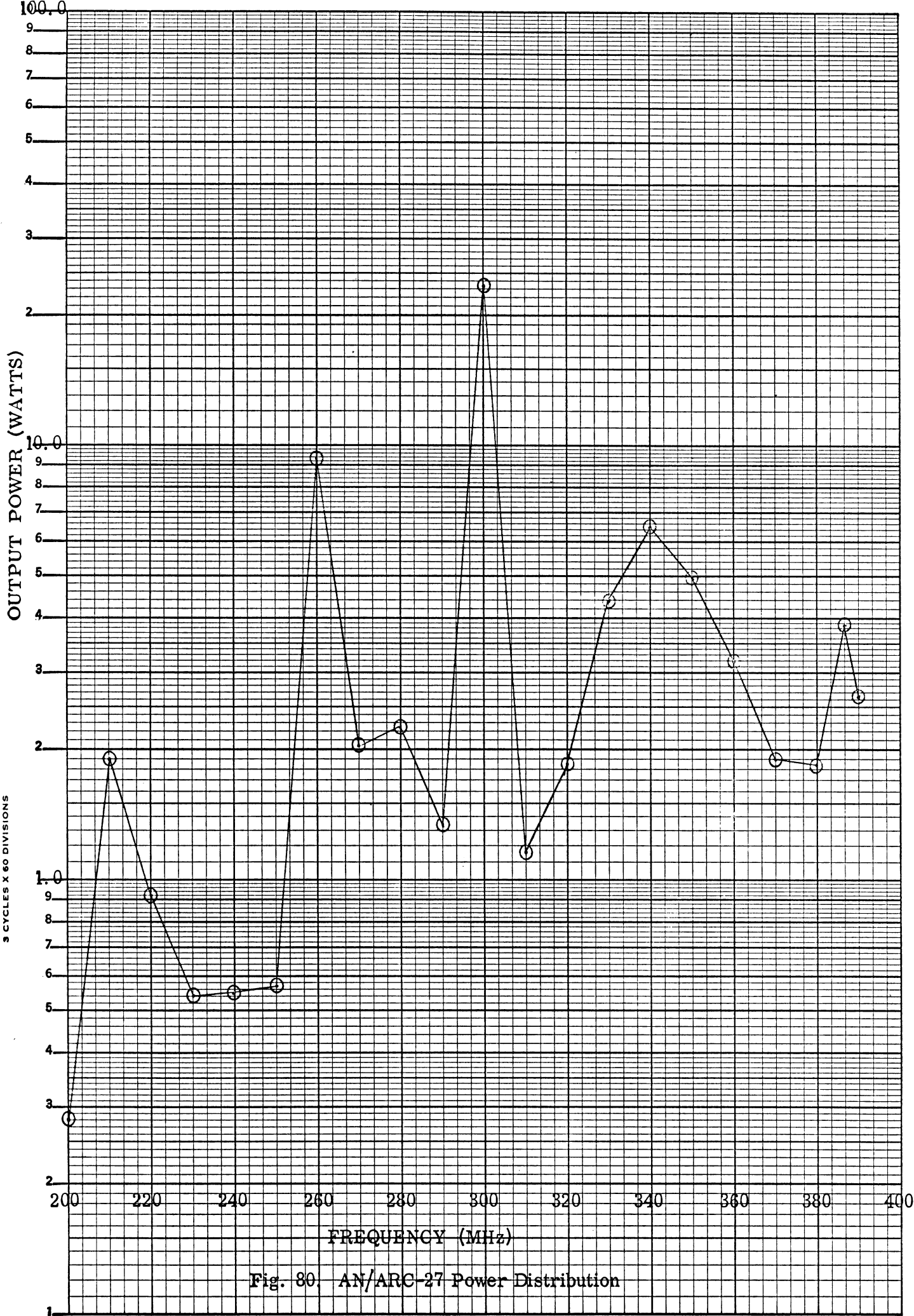
Fig. 80. AN/ARC-27 Power Distribution

The y-axis is labeled OUTPUT POWER (WATTS) with values 1.0, 10.0, 100.0 on a logarithmic scale. The x-axis is labeled FREQUENCY (MHz) ranging from 200 to 400.

| Spectrum Analyzer Dial Reading (MHz)		Origin of Signal
Lower Dial	Upper Dial	
71.0	————	Unknown [+]
77.9	————	Unknown
94.2	350	350
106	372	Unknown
118	396	Unknown
174	508	Unknown
196	553	553
224	609	$609 = 2f_o$
259	678	· Unknown
303	765	$303 = f_o$
375	912	$912 = 3f_o$
398	955	Unknown

Figure 81. AN/ARC-27 Transmitter Spectrum
For a Tuned Frequency, f_o = 300 MHz.

[+]For readings marked 'unknown' either the upper or lower dial
reading may give the correct frequency.

NAME	TITLE	DWG. NO.
	Modified Monopole Antenna (Full Scale)	
SMITH CHART Form 5301-7560-N	GENERAL RADIO COMPANY, WEST CONCORD, MASSACHUSETTS	DATE

IMPEDANCE OR ADMITTANCE COORDINATES

Fig. 82. Impedance Characteristics

(Frequency in MHz)

No. GC 19509
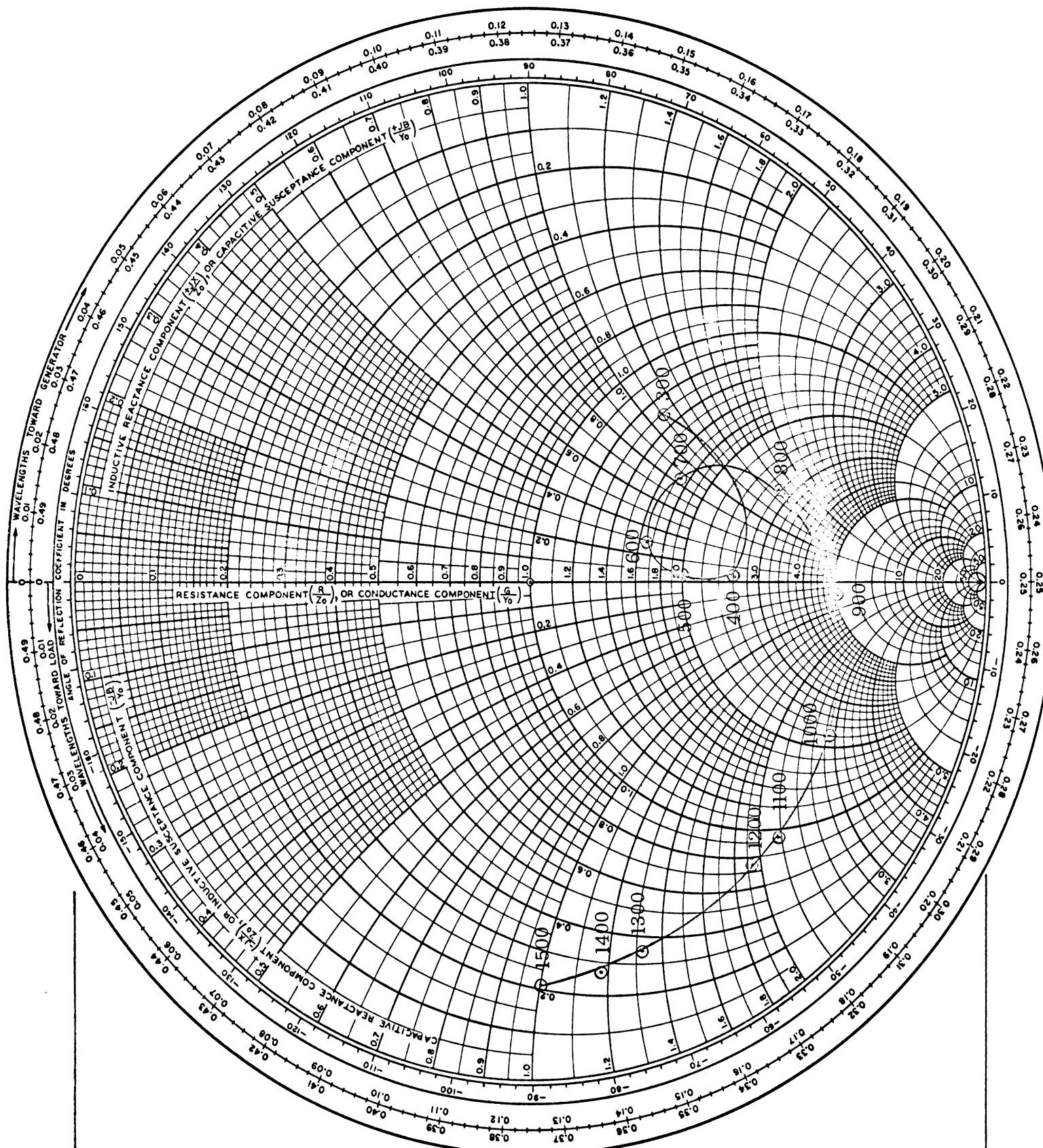
NAME	TITLE		DWG. NO.
		Blade Antenna (AT-256A/ARC)	
SMITH CHART Form 5301-7560-N	GENERAL RADIO COMPANY, WEST CONCORD, MASSACHUSETTS		DATE

IMPEDANCE OR ADMITTANCE COORDINATES

IMPEDANCE OR CAPACITIVE SUSCEPTANCE COMPONENT $\left(\frac{+jB}{Y_0}\right)$

INDUCTIVE REACTANCE COMPONENT $\left(\frac{+jX}{Z_0}\right)$

RESISTANCE COMPONENT $\left(\frac{R}{Z_0}\right)$, OR CONDUCTANCE COMPONENT $\left(\frac{G}{Y_0}\right)$

WAVELENGTHS TOWARD GENERATOR

ANGLE OF REFLECTION COEFFICIENT IN DEGREES

WAVELENGTHS TOWARD LOAD

CAPACITIVE REACTANCE COMPONENT $\left(\frac{-jX}{Z_0}\right)$ OR INDUCTIVE SUSCEPTANCE COMPONENT $\left(\frac{-jB}{Y_0}\right)$

Fig. 83. Impedance Characteristics

(Frequency in MHz)

94

APPENDIX

SIMPLIFICATION OF EQUATION 26

The purpose of this appendix is to show that Equation 26 of 7274-1-T

$$
\frac{P}{P_{max}} = \frac{\left(r_a + \frac{1-\alpha r_a}{\alpha - r_a}\right)^2 (r_a^2 \cos^2 kd_a + \sin^2 kd_a)}{\left[\frac{1-\alpha r_a}{\alpha - r_a}(r_a^2 \cos^2 kd_a + \sin^2 kd_a) + r_a\right]^2 + (1-r_a^2)^2 \sin^2 kd_a \cos^2 kd_a}
\tag{26}
$$

reduces to:

$$
\frac{P}{P_{max}} = \frac{1}{\left(\frac{r_s r_a + 1}{r_s + r_a}\right)^2 \cos^2 kd_a + \sin^2 kd_a}
\tag{27}
$$

To simplify the notation, recall $r_s = \frac{1 - \alpha r_a}{\alpha - r_a}$ (25)

and let $\cos^2 kd_a = x$, $\sin^2 kd_a = 1 - x$ (28)

Substituting 25 and 28 into 26

$$
\frac{P}{P_{max}} = \frac{(r_s + r_a)^2 [r_a^2 x + (1 - x)]}{\left\{r_s [r_a^2 x + (1-x)] + r_a\right\}^2 + (r_a^2 - 1)^2 (1 - x) x}
\tag{29}
$$

$$
= \frac{(r_s + r_a)^2 [(r_a^2 - 1)x + 1}{\left\{r_s [(r_a^2 - 1)x + 1] + r_a\right\}^2 + (r_a^2 - 1)^2 (1 - x) x}
\tag{30}
$$

Consider the denominator of Equation 30

$$
D = \left\{r_s [(r_a^2 - 1)x + 1] + r_a\right\}^2 + (r_a^2 - 1)^2 (1 - x) x
\tag{31}
$$

95

Expanding Equation 31, we obtain

$$D = r_s^2 \left[(r_a^2 - 1)x + 1\right]^2 + 2r_s r_a \left[(r_a^2 - 1)x + 1\right] + r_a^2 + (r_a^2 - 1)^2 (x - x^2) \qquad (32)$$

$$D = \left[(r_a^2 - 1)x + 1\right] \left[r_s^2(r_a^2 - 1)x + r_s^2 + 2r_s r_a + \frac{r_a^2 + (r_a^2 - 1)^2 x - (r_a^2 - 1)^2 x^2}{(r_a^2 - 1)x + 1}\right] \qquad (33)$$

Now consider the fraction which is the last term of Equation 33

$$F = - \frac{(r_a^2 - 1)^2 x^2 - (r_a^2 - 1)^2 x - r_a^2}{(r_a^2 - 1)x + 1} \qquad (34)$$

$$= - \frac{B^2 x^2 - B^2 x - (1 + B)}{Bx + 1} \qquad (35)$$

in which

$$B = (r_a^2 - 1) \qquad (36)$$

By division

$$\begin{array}{r} Bx - (1 + B) \\ Bx + 1 \overline{\smash{\big)}\ B^2 x^2 - B^2 x - (1 - B)} \\ \underline{B^2 x^2 + Bx} \\ - B(1 + B)x - (1 + B) \\ \underline{- B(1 + B)x - (1 + B)} \end{array} \qquad (37)$$

Hence

$$F = - (Bx - 1 - B) \qquad (38)$$

$$= - \left[(r_a^2 - 1)x - 1 - (r_a^2 - 1)\right] \qquad (39)$$

from which the denominator of Equation 30 becomes

$$D = [(r_a^2 - 1)x + 1] [r_s^2(r_a^2 - 1)x + 2r_s^2 + 2r_s r_a - (r_a^2 - 1)x + r_a^2] \quad (40)$$

$$= [(r_a^2 - 1)x + 1] [(r_s^2 - 1)(r_a^2 - 1)x + (r_s + r_a)^2] \quad (41)$$

Using the result of Equation 41, we can rewrite Equation 30

$$\frac{P}{P_{max}} = \frac{(r_s + r_a)^2 [(r_a^2 - 1)x + 1]}{[(r_a^2 - 1)x + 1] [(r_s^2 - 1)(r_a^2 - 1)x + (r_s + r_a)^2]} \quad (42)$$

Equation 42 simplifies to

$$\frac{P}{P_{max}} = \frac{(r_s + r_a)^2}{(r_s^2 - 1)(r_a^2 - 1)x + (r_s + r_a)^2} \quad (43)$$

$$= \frac{(r_s + r_a)^2}{(r_s^2 r_a^2 - r_a^2 - r_s^2 + 1)x + (r_s + r_a)^2} \quad (44)$$

$$= \frac{(r_s + r_a)^2}{\left[(r_s^2 r_a^2 + 2r_s r_a + 1) - (r_a^2 + r_s^2 + 2r_s r_a)\right]x + (r_s + r_a)^2} \quad (45)$$

and finally we have

$$\frac{P}{P_{max}} = \frac{1}{\dfrac{(r_s r_a + 1)^2}{(r_s + r_a)^2} x + 1 - x} \quad (46)$$

97

Since

$$\alpha = \frac{r_s r_a + 1}{r_s + r_a}$$

$$x = \cos^2 kd_a$$

$$1 - x = \sin^2 kd_a$$

$$\frac{P}{P_{max}} = \frac{1}{\alpha^2 \cos^2 kd_a + \sin^2 kd_a} \qquad (47)$$

Equation 46 is the same as Equation 26 with

$$\alpha^2 = \frac{P_{max}}{P_{min}} = \left(\frac{r_s r_a + 1}{r_s + r_a}\right)^2$$

Thus the equivalence of Equations 26 and 27 has been proved.